Acta Biomaterialia 171 (2023) 85–113

Contents lists available at ScienceDirect

Acta Biomaterialia

journal homepage: www.elsevier.com/locate/actbio

Review article

Piezoelectric nanogenerators for self-powered wearable and implantable bioelectronic devices

Kuntal Kumar Das[a], Bikramjit Basu[b], Pralay Maiti[c], Ashutosh Kumar Dubey[a,*]

[a] Department of Ceramic Engineering, Indian Institute of Technology (BHU), Varanasi 221005, India
[b] Materials Research Center, Indian Institute of Science, Bengaluru 560012, India
[c] SMST, Indian Institute of Technology (BHU), Varanasi 221005, India

ARTICLE INFO

Article history:
Received 7 June 2023
Revised 5 August 2023
Accepted 29 August 2023
Available online 4 September 2023

Keywords:
Piezoelectric nanogenerator (PENG)
Piezoelectricity
Energy harvesting
Ceramics
Polymers
Nature-inspired
Composites
Sensors

ABSTRACT

One of the recent innovations in the field of personalized healthcare is the piezoelectric nanogenerators (PENGs) for various clinical applications, including self-powered sensors, drug delivery, tissue regeneration etc. Such innovations are perceived to potentially address some of the unmet clinical needs, e.g., limited life-span of implantable biomedical devices (e.g., pacemaker) and replacement related complications. To this end, the generation of green energy from biomechanical sources for wearable and implantable bioelectronic devices gained considerable attention in the scientific community. In this perspective, this article provides a comprehensive state-of-the-art review on the recent developments in the processing, applications and associated concerns of piezoelectric materials (synthetic/biological) for personalized healthcare applications. In particular, this review briefly discusses the concepts of piezoelectric energy harvesting, piezoelectric materials (ceramics, polymers, nature-inspired), and the various applications of piezoelectric nanogenerators, such as, self-powered sensors, self-powered pacemakers, deep brain stimulators etc. Important distinction has been made in terms of the potential clinical applications of PENGs, either as wearable or implantable bioelectronic devices. While discussing the potential applications as implantable devices, the biocompatibility of the several hybrid devices using large animal models is summarized. This review closes with the futuristic vision of integrating data science approaches in developmental pipeline of PENGs as well as clinical translation of the next generation PENGs.

Statement of significance

Piezoelectric nanogenerators (PENGs) hold great promise for transforming personalized healthcare through self-powered sensors, drug delivery systems, and tissue regeneration. The limited battery life of implantable devices like pacemakers presents a significant challenge, leading to complications from repititive surgeries. To address such a critical issue, researchers are focusing on generating green energy from biomechanical sources to power wearable and implantable bioelectronic devices. This comprehensive review critically examines the latest advancements in synthetic and nature-inspired piezoelectric materials for PENGs in personalized healthcare. Moreover, it discusses the potential of piezoelectric materials and data science approaches to enhance the efficiency and reliability of personalized healthcare devices for clinical applications.

1. Introduction

Energy harvesting is the solution to the renewable energy sources. From the clinical application perspective, the harvesting of biomechanical energy endogenously, i.e., human body movements can be utilized to operate various wearable and implantable bioelectronic devices [1,2]. In synchronization with the Internet of things (IoT), bioelectronic devices are poised to contribute significantly to the healthcare sector. These devices are conventionally operated by the commercially available electrochemical batteries. However, these batteries have limited lifetime and therefore, recharging and replacement after specific durations become essential [3,4]. In case of implantable biomedical devices, such battery replacement requires repetitive surgeries, which often results in post-operative complications such as bleeding, inflammation, infection etc. [5,6]. On the other side, these electrochemical bat-

* Corresponding author.
E-mail address: akdubey.cer@iitbhu.ac.in (A.K. Dubey).

https://doi.org/10.1016/j.actbio.2023.08.057
1742-7061/

teries increase the size and weight of bioelectronic devices, which puts a restriction on their miniaturization. In this context, the miniaturization of these devices is relevant so that they can be run via energy, harvested from different biomechanical energy sources. In some of the recent studies, it has been reported that biomechanical energy can be harvested from a number of *in vivo* sources such as, heart (beating), blood circulation, lung motions (during respiration), and various human daily life activities etc. [5,7–9]. The biomechanical energy can be converted into electrical form to run battery-less devices. Such an arrangement can avoid the above-mentioned battery-related clinical complications. Towards this end, a number of energy conversion mechanisms have been explored such as piezoelectric, triboelectric, electromagnetic, magnetoelastic etc. [10–13]. Recently, piezoelectric nanogenerators (PENGs) based devices have harvested substantial interest due to their reasonably higher and reversible electro-mechanical response. PENGs have a number of applications in various wearable and implantable bioelectronics, such as self-powered sensors, self-powered pacemakers, deep brain stimulators, drug delivery, tissue regeneration etc. [14–21]. PENGs respond to even minor strains, and can produce enough power to run such electronic devices. In addition, PENGs can be manufactured in relatively smaller dimensions and structures [22,23].

The wearable and implantable bioelectronic devices, centered around piezoelectric energy harvesting, can be used for the treatment of arrhythmia using battery-less self-powered pacemaker [6,15]. Heart-beat vibrations can be converted to useful electrical energy by piezoelectric materials to run the pacemaker circuit and this process can regulate the disordered heart beat frequency. The neural disorders such as epilepsy, tremor, parkinson's disease etc. can be treated by providing electrical stimulations to the specific regions of the brain using piezoelectric nanogenerators (deep brain stimulators) [16]. These PENGs can potentially replace the commercially available neural stimulators, which uses hazardous chemical batteries. Importantly, PENGs can provide green energy, *in vivo*. PENGs have the potential to serve as drug delivery systems by utilizing their piezoelectric properties. When the PENG device experiences mechanical pressure, it generates electrical potentials that can be used for controlling the release of drugs at the targeted sites, minimizing the side effects, associated with conventional drug delivery methods. Furthermore, PENGs can be integrated with other bioelectronic devices such as, biosensors to provide real-time monitoring and feedback on the drug release process, making them a promising platform for next-generation drug delivery systems [19]. The piezoelectric nanogenerators (PENGs) demonstrated the promising potential towards the treatment of various tissue defects (localized tissue regeneration), including hard tissues, cardiovascular system, neural system etc. [20,21]. The PENGs have potentiality to monitor physical health by the use of self-powered sensors (blood pressure measurement, strain measurement etc. [Fig. 1] [14,17]. The successful clinical translation of such a novel approach can potentially revolutionize the field of medicine.

Piezoelectric ceramics and polymers are used to develop PENGs by virtue of their capabilities for piezoelectric energy harvesting, electro-mechanical coupling factor, piezoelectric strain coefficient, and other relevant dielectric properties. Perovskite piezoceramics such as, $BaTiO_3$, (K, Na) NbO_3 etc. exhibits excellent piezoelectric properties [24,25]. Piezoelectric polymers such as, PVDF, co-polymer of PVDF exhibit moderate piezoelectric characteristics with well-defined flexibility, stretchability as well as biocompatibility [26]. Alongside, some of the nature-inspired piezoelectric materials such as cellulose, collagen etc. can be used to develop cost effective PENGs for biomedical applications. (e.g., self-powered sensors, pacemakers, drug delivery systems).

PENGs can be used for wearable devices without any direct interface with cells, blood, proteins etc. However, PENGs can also be used for implantable biomedical devices and in those kinds of targeted clinical applications, PENGs need to have clinically acceptable biocompatibility in terms of its interactions with the living system.

The article provides a state-of-the-art review on the recent advancements of PENGs in the field of wearable and implantable bioelectronic devices. The science behind piezoelectricity and working fundamentals of PENGs for energy harvesting has been discussed. Further, the types of PENGs, based on various inorganic, organic and nature-inspired piezoelectric materials along with their potentiality towards *in vivo* piezoelectric energy harvesting have been critically reviewed. In addition, the widespread bioelectronic applications of PENGs, i.e., self-powered sensors, self-powered pacemakers, deep brain stimulators, tissue regeneration, and drug delivery have been extensively discussed.

2. Fundamentals and working principles of PENGs

The phenomenon of piezoelectricity represents linear electromechanical coupling [27]. Piezoelectric materials undergo deformation when exposed to external mechanical forces to generate electric field. Such conversion of mechanical stress into electric field is known as the direct piezoelectric effect [Fig. 2 (a)]. The converse mechanism, electric field induced mechanical strain is referred as the converse piezoelectric effect [Fig. 2 (b)] [28,29]. Piezoelectricity is present in materials with non-centrosymmetric crystal structure. Among 32 crystal classes, 21 of them shows non-centrosymmetricity and consequently, piezoelectricity [30]. In inorganic materials, piezoelectricity arises due to asymmetric charge distributions in crystals, which deform under mechanical stress [27]. The piezoelectric property of inorganic materials is temperature dependent and disappears at Curie temperature. At the Curie temperature, the crystal structure takes the form of a higher symmetry phase, which diminishes its piezoelectric property [31]. In case of organic materials, piezoelectricity arises due to reorientation of permanent molecular dipoles by application of mechanical stress, which produces a net polarization [32]. The electromechanical conversion behavior of such materials serves as the potential tool in piezoelectric energy harvesting applications.

Piezoelectric energy harvesting is more commonly governed by two different modes of operation, i.e., d_{31} and d_{33}, where 'd' refers to the piezoelectric strain coefficient [Fig. 2 ((c),(d))]. The first and second numbers indicate the orientation, in which electric field is generated and the direction of the applied force, respectively. When a piezoelectric material undergoes shear stress, another mode i.e., d_{15} defines piezoelectric coefficient. In general, PENGs uses compressive and bending motions as well as vibrations for harvesting biomechanical energy [33,34].

Piezoelectric materials possess an exceptional ability to transform the applied mechanical energy to electrical energy. The mechanical stimulation prompts the creation of non-coincident positive and negative charges, which results in the formation of dipole. Such characteristic makes piezoelectric materials highly valuable for diverse biomedical applications, particularly as energy harvesters [35–37].

The piezoceramic energy harvesting inorganic materials normally possess wurtzite or perovskite type crystal structures. Perovskite structure based piezoceramics show higher piezoelectric strain coefficient (d_{33}/d_{31}) than wurtzite-based structures [38,39]. The intrinsic brittleness property of piezoceramics does not allow them to undergo large mechanical deformations. On the other hand, piezopolymers have very good flexibility and they can withstand large strains without failure. In contrast, piezopolymers do not exhibit high piezoelectric strain coefficients and electromechanical coupling factors [40]. The piezoelectric composite materials, containing both ceramics and polymers exhibit good mechan-

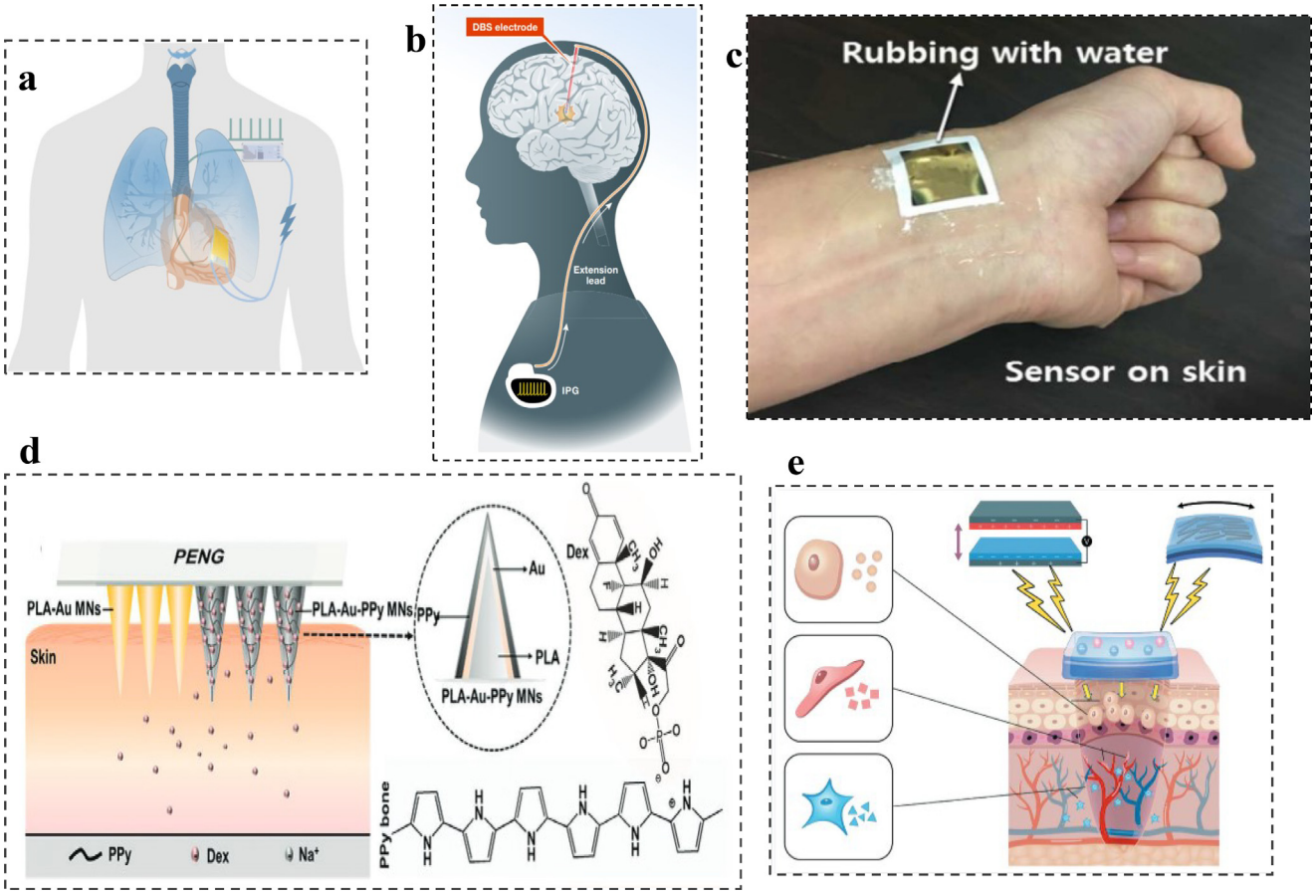

Fig. 1. Piezoelectric nanogenerators (PENGs) represent a new class of biomedical devices with many promising clinical applications. (a) Self-powered pacemaker. [Open access] [15]. (b) Deep brain stimulator. [Open access] [16]. (c) Piezoelectric sensor. Reproduced with permission from [17]. Copyright 2016, American Chemical Society. (d) Drug delivery. Reproduced with permission from [19]. Copyright 2021, John Wiley and Sons. (e) Wound healing. [Open access] [20]. [IPG-Internal Pulse Generator, PLA-Polylactic acid, Au-Gold, PPy: Polypyrrole, MN: Microneedles, Dex: Dexamethasone].

ical flexibility and excellent electrical properties [41,42]. Overall, piezoelectric composites are the potential prospective candidates for energy harvesting applications. Currently, there has been notable advancement in the development of PENGs intended for diverse applications in wearable and implantable bioelectronics.

3. PENGs based on nanostructures (nanotubes, nanorods and nanowires)

The inorganic nanotubes based PENGs have gained remarkable attention due to outstanding piezoelectric properties. Stassi et al. [43] developed a piezoelectric PENG using ZnO nanotubes which was incorporated in 100 nm porous polycarbonate membrane, generated a voltage and current outputs of 1.15 V and 100 µA, respectively. The developed PENG device produced a power density of 287.5 mW/cm^3. Similarly, Lee et al. [44] developed aligned diphenylalanine nanotubes and further, peptide-based PENG was fabricated. Meniscus driven self-assembly process was used to produce horizontally aligned diphenylalanine nanotubes with unidirectional polarization [Fig. 3 (a)]. The developed PENG produced a voltage and current of 2.8 V and 37.4 nA, respectively, under the influence of an impact force of 42 N [Fig. 3 ((b), (d))]. The device produced a power of 8.2 nW, which could power the LCD panels. Lee et al. [45] developed perovskite $PbTiO_3$ aligned nanotubes for piezoelectric energy harvesting [Fig. 3 (e)]. The devices were planted in open grassy field to extract energy from natural bending motions in synchronous with the environment [Fig. 3 (f)]. The PENG device produced a voltage and current density of 620 mV and 1 nA/cm^2, respectively, under periodic concave and convex bending [Fig. 3 (g)]. In a study by Almohammed et al. [46], a PENG device, based on graphene oxide/ diphenylalanine peptide nanotubes, revealed the potentiality of horizontally aligned diphenylalanine peptide nanotubes as suitable piezoelectric material, used in energy harvesting applications. The PENG device produced a good voltage and current of 6 V and 60 nA, respectively, by mechanical bending. Jung et al. [47] developed PZT nanotubes-based PENG for energy harvesting applications. The PZT nanotubes were synthesized using template-assisted method. The nanotubes were enclosed within polydimethylsiloxane (PDMS) and Pt/Ti coated polyamide films were used as electrodes. The device, as represented by Fig. 3 (h), produced the voltage and current of 1.52 V and 54.5 nA, respectively, during bending [Fig. 3 (i), (j)]. The developed energy harvester generates a power output of 37 nW/cm^2.

The inorganic nanorods based PENGs are found to exhibit remarkable piezoelectric energy harvesting capability. Rukeishi et al. [48] developed ZnO nanorods with diameter and length of (57±11) nm and (3.9±0.8) nm, respectively, by chemical vapour deposition [see Fig. 4 (a), (b)]. Fig. 4 (c) shows the variation of voltage with various mechanical stresses. The maximum voltage, developed by the PENG device was 0.7 V. Zhang et al. [49] developed patterned textile of ZnO nanorods arrays and further integrated them into a PENG. The nanorod arrays of ZnO were sandwiched between silver electrodes in form of silver coated fabric. The developed PENG device generates a maximum voltage of 4 V [Fig. 4 (d)] and current of 20 nA, under palm clapping. The ZnO nanorods based nanogen-

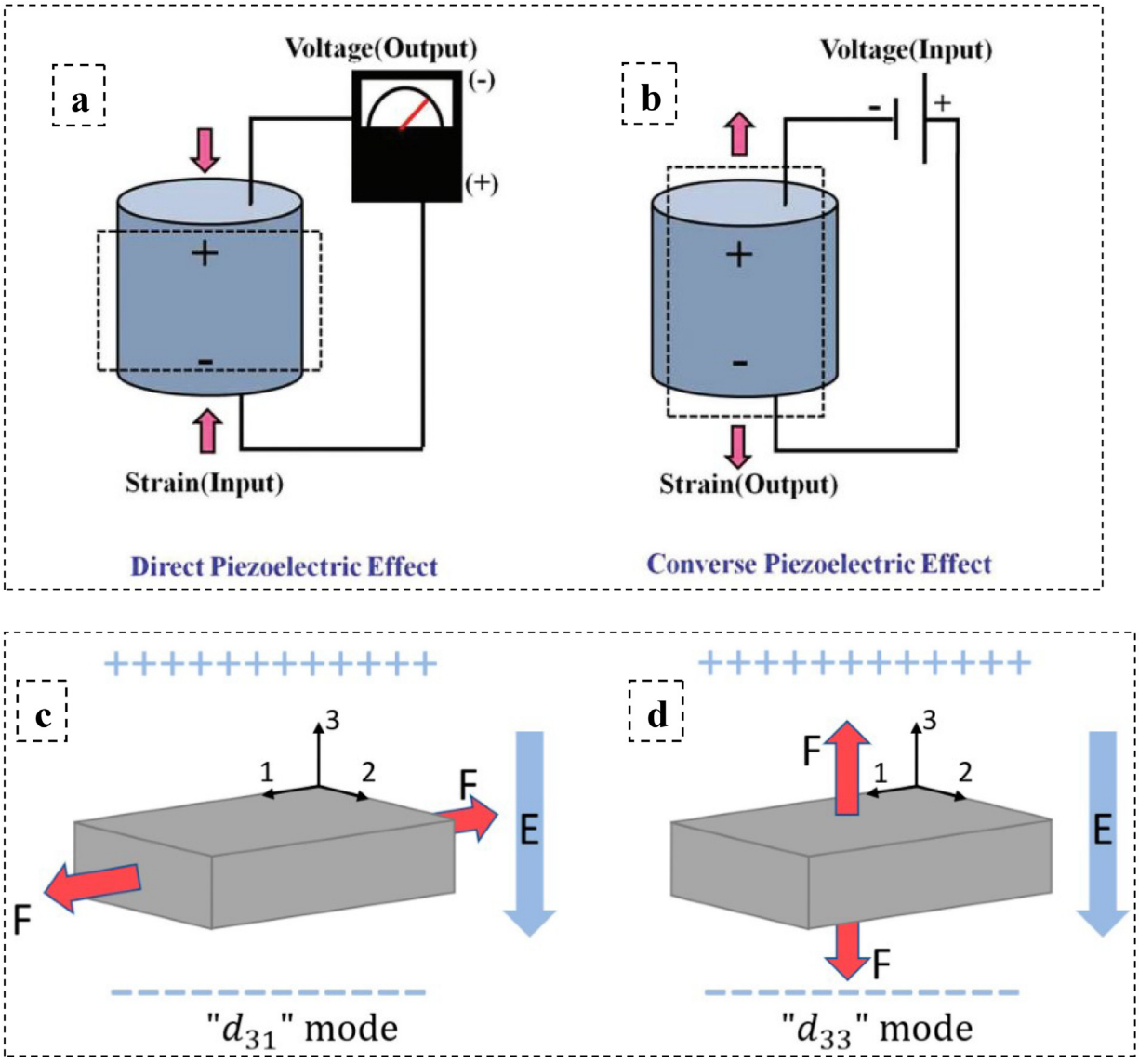

Fig. 2. Working mechanisms of piezoelectric energy harvesting. Different modes of piezoelectricity. (a) Direct piezoelectric effect and (b) Converse piezoelectric effect. Reproduced with permission from [29]. Copyright 2019, John Wiley and Sons. (c) d_{31} mode and (d) d_{33} mode. [Open access] [33].

erator is found to be suitable to power microelectronic devices. It powered up a display unit under palm pressing, as shown in [Fig. 4 (e)] and lightened up several LEDs under foot pressing [Fig. 4 (f)]. Deng et al. [50] reported the growth of ZnO nanorods on kapton film through hydrothermal method. The nanorods grew in the radial direction on the surface of the substrate, i.e., kapton film. The developed PENG had a tuning fork shaped beam containing ZnO nanorods, as illustrated in [Fig. 4 (g)]. The maximum output voltage and current produced by the nanogenerator was 160 mV and 11 nA, respectively [Fig. 4 (h), (i)]. The device produced the maximum power of 0.92 μW/cm^3 under a load resistance of 9 MΩ.

Nanowires-based 1D nanostructures produce considerable influence on the output electrical characteristics of PENG devices to run low powered bioelectronics. Moorthy et al. [51] created a PENG device based on single nanowire of 0.65 Pb ($Mg_{1/3}Nb_{2/3}$) O_3-0.35 $PbTiO_3$ (PMN-PT) [Fig. 5 (a)]. PMN-PT nanowires were developed using hydrothermal processing route. A single PMN-PT nanowire of length 5 μm, was further integrated into a PENG device and V-I characteristics were measured [Fig. 5 (b)]. The device generates a voltage and current of 9 mV and 1.5 nA, respectively, under bending and unbending [Fig. 5 (c) (i), (ii)]. In a different study [52], zinc pthalocyanine (ZnPc) nanorods [Fig. 5 (d)] were used to develop a PENG device [see Fig. 5 (e)]. The ZnPc nanorods were grown on aluminium substrate as the bottom electrode. ZnPc was deposited on aluminium foil utilizing physical vapor deposition technique. Fluorine doped tin oxide (FTO) acted as the top electrode. The developed nanogenerator produced a voltage of 0.968 mV [Fig. 5 (f)]. Similarly, a PENG device was developed with film thickness of 100 nm which produced a voltage output of 0.524 mV. Wasim et al. [53] synthesized ZnO nanorod arrays for piezoelectric energy harvesting applications [Fig. 5 (g)]. ZnO nanorod arrays were grown on both sides of etched Al rod substrate using chemical bath deposition. A diagrammatic representation of the operational process of ZnO nanorods based energy harvester is shown in Fig. 5 (h). It was observed that the voltage produced on the top side of the device under cyclic force varies from 0.59 to 0.62 mV [Fig. 5 (i)]. However, on the bottom side, the voltage varies from 0.52 to 0.55 mV.

The piezoelectric characteristics of nanostructured substrates, used in PENGs, are significantly influenced by their orientation and disorder. For example, the alignments of nanotubes, like ZnO nanotubes, diphenylalanine nanotubes and $PbTiO_3$ nanotubes enhance their ability to produce electric charges, when exposed to

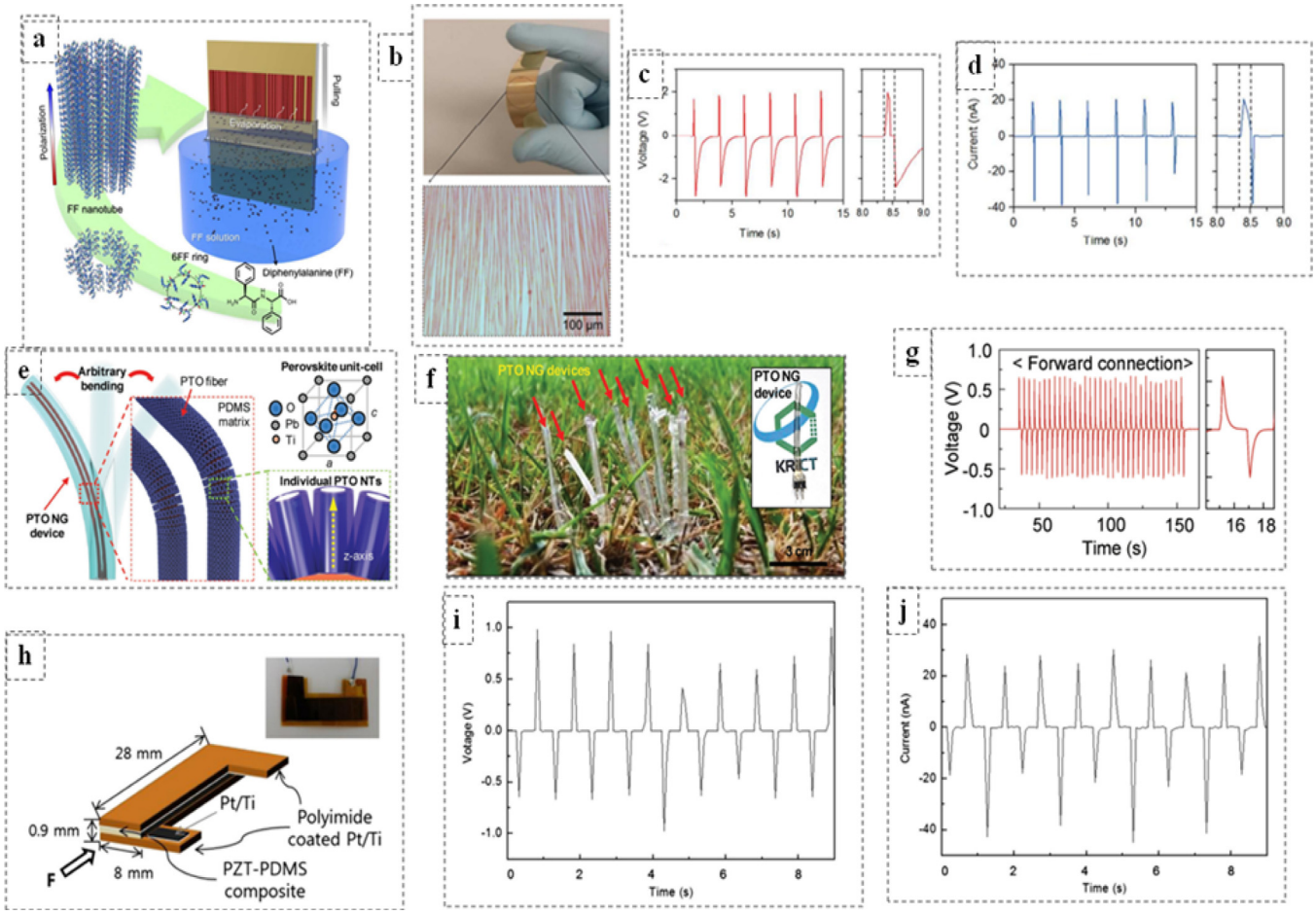

Fig. 3. The innovation in biomaterial synthesis allows development of new PENGs. (a) Schematics showing fabrication process of peptide nanotube array with unidirectional polarization via meniscus mediated self-assembly. (b) Photograph of the nanotube array-based PENG on flexible substrate along with optical microscopic image. (c) Voltage response of the peptide nanotube array-based PENG. (d) Current response of the peptide nanotube array-based PENG. Reproduced with permission from [44]. Copyright 2018, American Chemical Society. (e) $PbTiO_3$ nanotube array-based PENG on PDMS matrix executing bending motion. (f) PENG devices in the field, inset image shows the PENG device structure. (g) Voltage response of the PENG device. Reproduced with permission from [45]. Copyright 2017, John Wiley and Sons. (h) PZT-PDMS PENG device illustration. (i) Voltage output of the PZT-PDMS based PENG. (j) Current output of the PZT-PDMS based PENG. Reproduced with permission from [47]. Copyright 2013, Elsevier.

mechanical pressure along tube-axis. On the other hand, the introduction of structural imperfections, like defects and impurities restrict their effectiveness in converting mechanical energy into electrical energy. Similarly, the alignments of nanorods (such as ZnO, Zinc Phthalocyanine, PMN-PT) along the rod or wire-axis maximize their piezoelectric response. On contrary, the presence of disordered structures, like surface roughness and grain boundaries reduce their overall efficiency. Therefore, it is important to carefully control the orientation of nanostructures and minimize structural irregularities in order to optimize the piezoelectric performance of PENGs [43–53].

4. PENGs based on piezoelectric materials

4.1. Piezoceramics based PENGs

The pioneer piezoelectric ceramic perovskite, $BaTiO_3$ (BT), uncovered in 1947, gained remarkable attention over years due to its multifunctional potentials [54]. Shuai et al. [55] reported the development of BT ceramic nanoparticles that enhanced the electroactive β-phase of polyvinylidene fluoride from 46 % to 59 % and produced a voltage increment by 356 %. Karaki et al. [56] fabricated dense BT ceramics with high piezoelectric strain coefficient and electromechanical coupling factor of 490 pC/N and 42%, respectively. BT nanoparticles are incorporated in polymer matrix [e.g., polyvinylidene fluoride (PVDF), polydimethylsiloxane (PDMS)] to develop PENGs with reasonable piezoelectric properties and mechanical flexibility for energy harvesting applications [57,58]. Lin et al. [58] developed BT nanotubes, based stretchable and flexible PENG. BT nanotubes were produced by hydrothermal method and PDMS-BT composite based PENG was developed. The PENG produces a voltage and current of 5.5 V and 50 nA, respectively, with a current density of 350 nA/cm^2. Similarly, Park et al. [59] developed BT thin film of thickness 300 nm, which was deposited on Pt/Ti/SiO_2/(100)Si substrate, using RF magnetron sputtering. The fabricated PENG contained metal-insulator-metal (MIM) structure, which is further connected to interdigital electrodes [Fig. 6 (a)]. The initial undeformed and bending states of PENGs are represented as Fig. 6 (b) [(i), (ii)] and Fig. 6 (b) [(iii), (iv)], respectively. During bending, PENG develops charges at each MIM structure, which flows through the electrodes and during unbending, the charge flow is reverted back. The BT based nanogenerator produces a voltage of upto 1.0 V, under bending [Fig. 6 (c)]. The current and power densities, produced by the PENG was 0.19 μA/cm^2 and ~7 mW/cm^3, respectively. A lead-free PENG, based on BT/polydimethylsiloxane (PDMS)/Carbon(C), was developed by Luo et al. [60]. The PENG with 3.2% C-doping produces a voltage output of approximately 7.43 V, under periodic motions of a vibrator. The maximum power, produced by the PENG was 7.92 μW, under a load resistance of 2 MΩ. It was also revealed

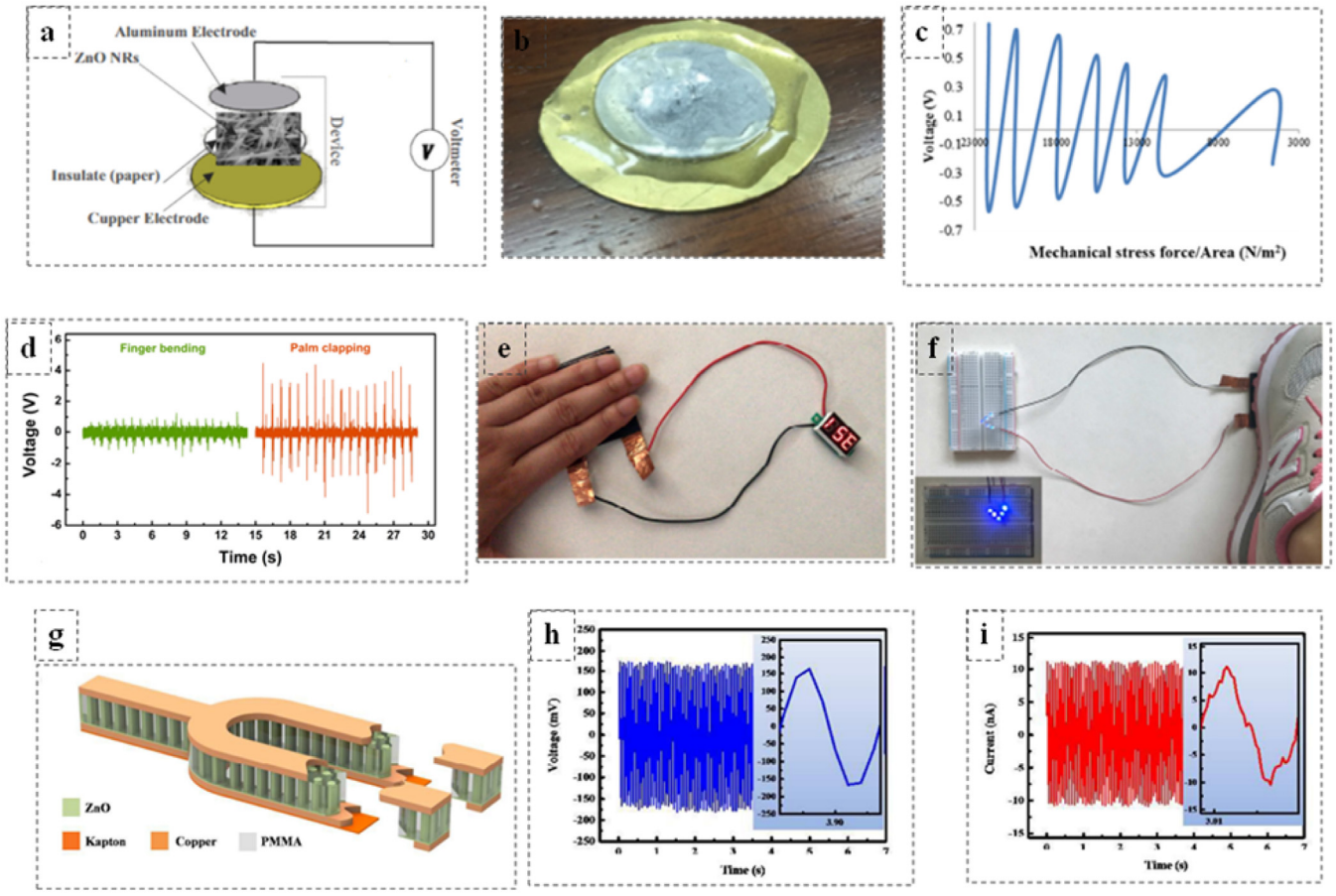

Fig. 4. Many oxide based biomaterials like ZnO in nanorod format are used in PENG devices. (a) ZnO nanorods based PENG device. (b) Appearance of PENG device. (c) Variation of voltage of ZnO nanorods based PENG under compressive mechanical stresses. Reproduced with permission from [48]. Copyright 2019, Elsevier. (d) Voltage response of the ZnO nanorods array-based PENG under finger bending and palm clapping. (e) ZnO nanorods array-based PENG powering display screen under palm pressing. (f) ZnO nanorods array-based PENG lighting up several LEDs under foot stepping. Reproduced with permission from [49]. Copyright 2019, Elsevier. (g) Tuning fork shaped PENG based on ZnO nanorods. (h) Voltage response of the tuning fork-based PENG. (i) Current response of tuning fork-based PENG. Reproduced with permission from [50]. Copyright 2018, Royal Society of Chemistry.

that PENG with C-doping produces 143% more voltage output as compared to that without C-doping. Likewise, BT nanowires-based PENG was developed by Parl et al. [61], that produces a voltage output and short circuit current of 7.0 V and 0.16 μA, respectively, under periodic bending and unbending. In a different study, BT based nanotubes array on Ti-mesh substrate were compressed with polydimethylsiloxane layer and was further assembled in-between two indium tin oxide (ITO) coated polyethylene terephthalate (PET) electrodes to develop a PENG device [62]. The PENG produces voltage and current outputs of 10.6 V and 1.1 μA, respectively, under repetitive bending and release.

Considering the environmental aspects, lead-free ceramics gained notable attention due to their non-toxic behaviour, without compromising piezoelectric and dielectric constant values. Towards this end, potassium sodium niobate (KNN) based lead-free perovskite ceramics got remarkable attention in recent years. KNN based ceramics display good piezoelectric (∼ 100-400 pC/N) and electromechanical constant (0.36) values [63,64]. The piezoelectric constant values of KNN are often increased by adding dopants. Kim et al. [65] improved the d_{33} value (204 pC/N) of KNN by adding 0.03 mol% of (Bi, Na) TiO_3 (BNT) with maximum open circuit voltage output and power density of 10.8 V and 24.6 nW/cm^2, respectively, subjected to a mechanical force of 650 N with a frequency of 1 Hz. Wang et al. [66] developed a PDMS based PENG with KNN nanorods. The PENG produces an open circuit voltage in several tens of mV. Similarly, Huan et al. [67] reported that a pure KNN based device produces an open circuit voltage and short circuit current of 3.5 V and 0.3 μA, respectively, under a mechanical stress of 0.1 MPa. A study was performed to understand the influence of KNN nanorods on PVDF-KNN based PENG [68]. It has been reported that 10% KNN nanorods within PVDF composite film showed dielectric constant (ε) value of ∼23 and produced energy density of 0.053 J/cm^3, when poled at 164 kV/cm. The PENG produces an open circuit voltage and short circuit current of 3.4 V and 0.1 μA, respectively, by applying repetitive compressive force.

Further, KNN ceramics are structurally/compositionally modified to enhance the piezoelectric behaviour of the PENG. Jeong et al. [69] dispersed Li-doped KNN (KNLN) along with Cu nanorods in PDMS matrix to develop a PENG, as shown in Fig. 6 (d). Fig. 6 (e) demonstrates the power generation mechanism in the PENG. During bending of the PENG device, the current flows from top to bottom side of electrodes due to accumulation of positive charges on the top side of electrode which reverses during unbending. The PENG device produces a voltage and current outputs of 12 V and 1.2 μA, respectively [Fig. 6 (f)]. KNN nanorod arrays were grown on $SrTiO_3$ substrates along (110) orientation by hydrothermal method [70]. Both, vertically and laterally integrated nanogenerator devices based on PMMA coated KNN nanorod arrays were developed which were further packaged with PDMS. The nanogenerator devices generates a maximum voltage of 10 V, under finger tapping. The power, produced by the vertically integrated KNN nanorod arrays based PENG was 2.25 nW and laterally in-

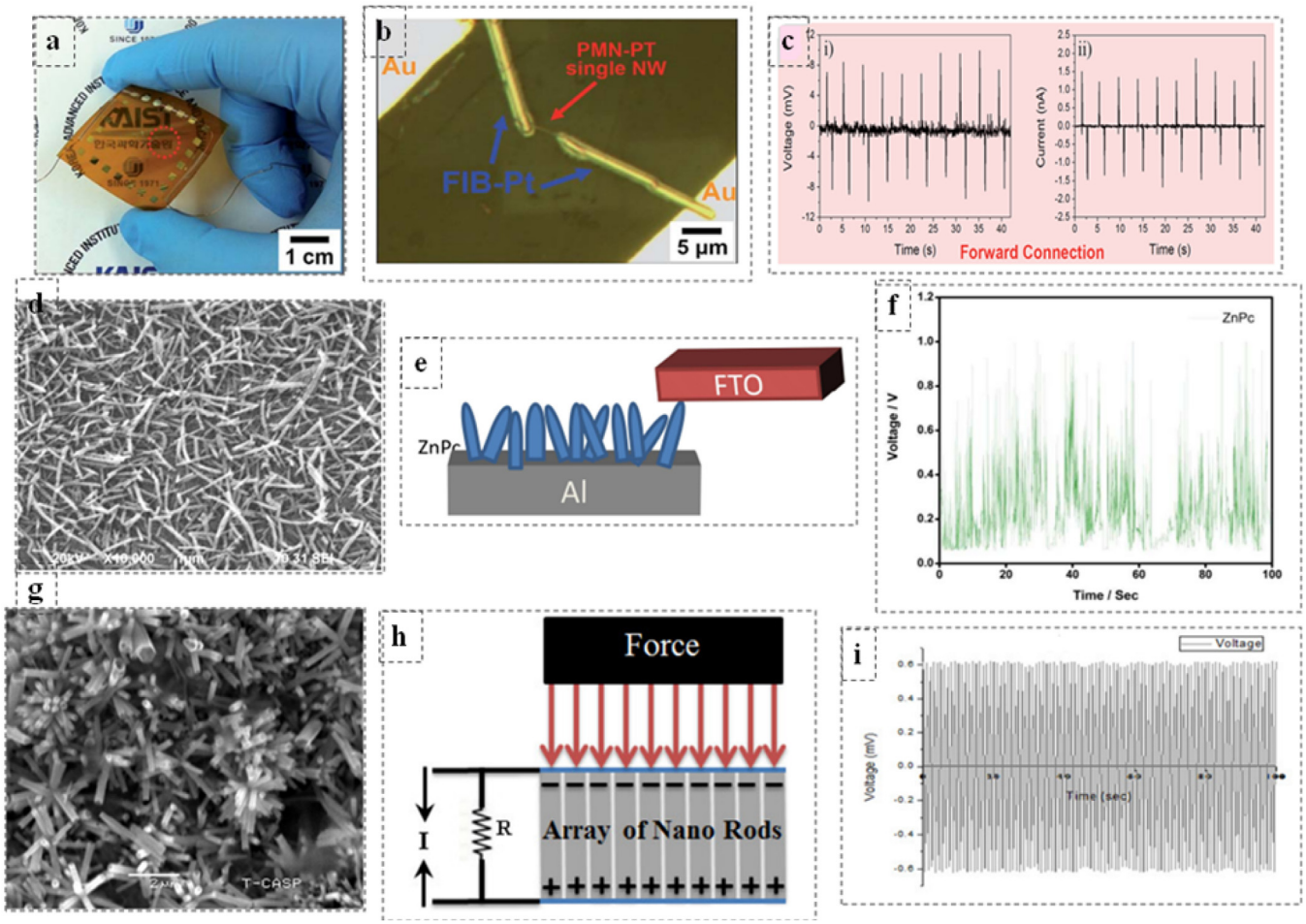

Fig. 5. Conventional piezoelectric materials, like PMN-PT or newer materials like Zinc Phathalocynine (ZnPc) or ZnO nanorods in combination are used in PENG devices. (a) PMN-PT single nanowire-based PENG device. (b) PMN-PT nanowire, connected to Au electrodes using fused ion beam technique. (c) Voltage and current response of the single PMN-PT nanowire-based PENG [Open access] [51]. (d) SEM micrograph of 300 nm thick ZnPc nanorods. (e) ZnPc nanorods based PENG device with FTO electrode. (f) Voltage response of ZnPc nanorods based PENG device. Reproduced with permission from [52]. Copyright 2020, Elsevier. (g) Topside view of SEM micrograph of ZnO nanorods. (h) Schematics demonstrating working mechanism of ZnO nanorods based PENG. (i) Voltage response of the ZnO nanorods based PENG device. [Open access] [53].

tegrated KNN nanorod arrays based PENG produces the power of 0.36 nW, at load resistance of 10 MΩ. Zhang et al. [71] developed 0.915 $(Na_{0.5}K_{0.5})(Nb_{0.94}Sb_{0.06})O_3$-0.045 $LiTaO_3$-0.04 $BaZrO_3$ (NKNS-LT-BZ) nanoparticles. The KNN composition with a textured structure is located at the polymorphic phase boundary (PPB) region, where both rhombohedral and tetragonal phases coexist. This unique phase boundary region contributes to the excellent piezoelectric properties. The presence of multiple phases induces higher strain in the crystal structures, leading to enhanced charge separation and improved piezoelectric performance. Overall, the coexistence of multiple phases in the PPB region is beneficial for the evolution of piezoelectric properties in KNN.

Along with NKNS-LT-BZ nanoparticles and PVDF, a PENG was developed, which produced an open circuit voltage output and short circuit current output of 18 V and 2.6 μA, respectively, under cyclic compressive force of 50 N at a frequency of 1 Hz. The enhancement in piezoelectric properties was attributed to the unique crystal structure of KNN-BNZ-AS-Fe nanoparticles [72].

As far as the superior piezoelectric properties are concerned, lead zirconate titanate (PZT) shows enhanced piezoelectric properties around 50/50 composition near morphotropic phase boundary (MPB) region [73]. At MPB, rhombohedral to tetragonal phase transition occurs for PZT. Due to its excellent piezoelectric properties, PZT is used for developing PENGs. Wu et al. [74] developed parallelly placed PZT nanowires-based textile. These aligned nanowires were transferred into polyethylene terephthalate (PET) film and covered with PDMS, followed by electroding to develop a PENG. The PENG produces a voltage and current outputs of 6 V and 45 nA, respectively, under periodic bending and unbending. Similarly, laterally aligned single-crystal PZT nanowires were synthesized to develop PENGs [75]. Laterally aligned PZT nanowires along with interdigitated Pt/Ti electrodes and PDMS films were used in such devices. The nanogenerator produced a voltage and power density of 10 V and 0.27 μW/cm^2, respectively, under a pressure of 70 kPa. Along with PZT nanowires, PZT nanorods are also used in many studies to develop flexible high performance PENGs. Jin et al. [76] developed PZT nanorod arrays on Ti substrate using hydrothermal treatment in presence of polymer surfactant. The nanorod arrays comprise an initial layer of PZT film and tetragonal single crystalline nanorods along (001) orientation. The PZT nanorods exhibited a high piezoelectric strain coefficient of 1600 pm/V. The PENG based on PZT nanorod arrays produced an open circuit voltage of 3.3 V, when the device was compressed under a load of 10 N at 10 Hz frequency. The PENG generates a power output of 3.16 μW/cm^2 at a load resistance of 1 MΩ. In addition, when the PENG device was subjected to finger tapping motions, the voltage generated by the device has increased to 10 V with the power output of 5.92 μW/cm^2.

The synergistic interactions of ferroelectricity and piezoelectricity improves the electrical properties of PZT based PENG [77]. For

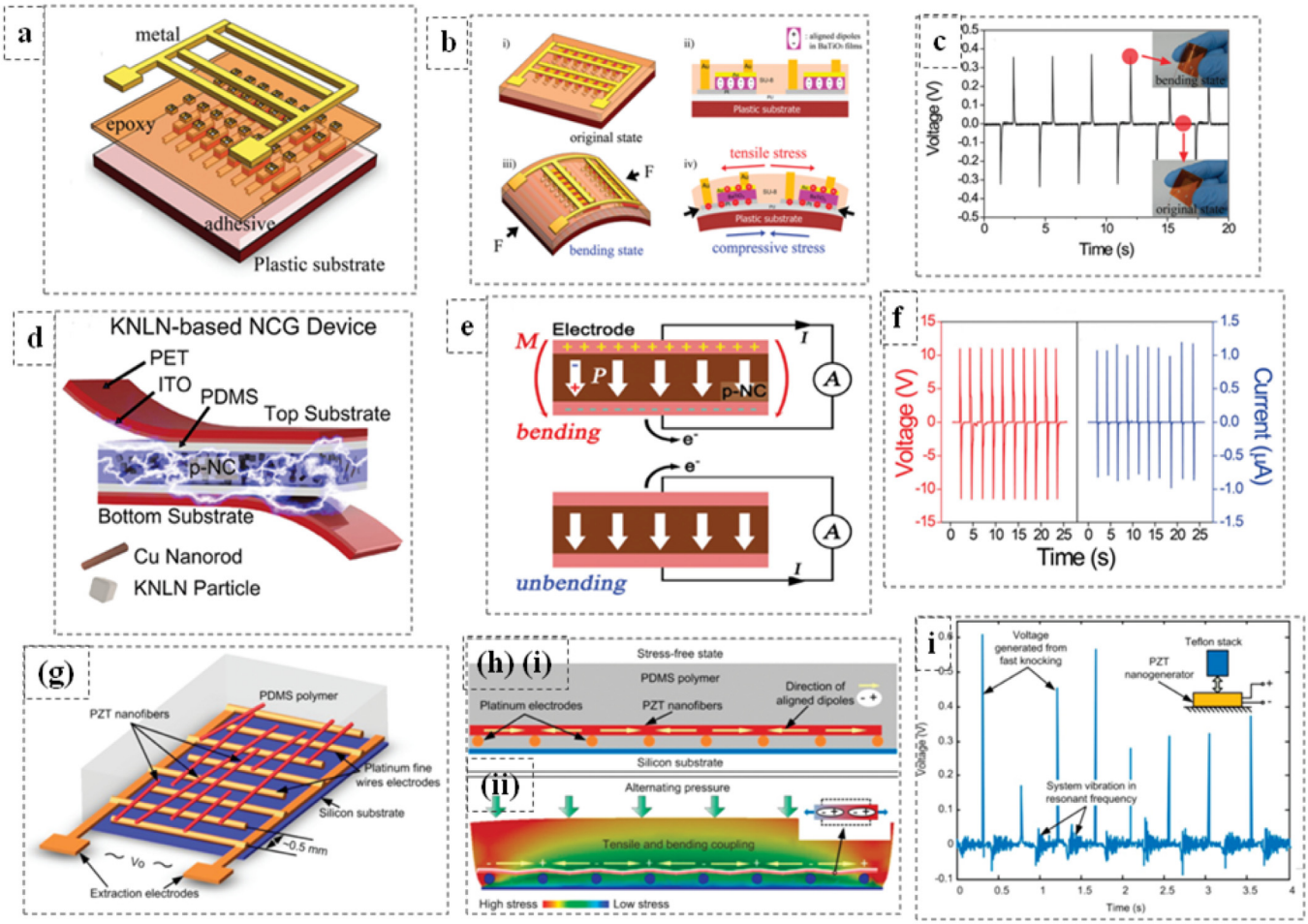

Fig. 6. Piezoelectric energy harvesting based on inorganic piezoelectric materials (piezoceramics). (a) An illustration of fabrication of $BaTiO_3$ (BT) based PENG. (b) Schematic of power generation in BT based PENG during unbending and bending state. (c) Open circuit voltage generated in BT-PENG during unbending and bending state. Reproduced with permission from [59]. Copyright 2010, American Chemical Society. (d) An illustration of Li-doped KNN (KNLN) based PENG. (e) Schematic illustration of power generation during bending and unbending in KNLN based PENG. (f) Open circuit voltage and short circuit current generation of KNLN based PENG during unbending and bending in forward connection. Reproduced with permission from [69]. Copyright 2014, John Wiley and Sons. (g) Schematic of PZT based PENG. (h) (i) Schematic representing cross-section of PZT nanofibers within PENG, (ii) Power generation mechanism of PENG nanofibers aligned in longitudinal direction. (i) Open circuit voltage generation within PZT based PENG, under teflon stack induced force. Reproduced with permission from [80]. Copyright 2010, American Chemical Society.

example, PDMS/PZT flexible porous PENG generates a high open circuit voltage output and short circuit current of 29 V and 116 nA, respectively, under compressive force of 30 N. A high performance composite thin film-based PENG was developed by Lee et al. [78]. The composite thin films had amine-functionalized PZT nanoparticles (PZT-NH_2) along with thermoplastic triblock copolymer that was grafted with maleic anhydride. Such device architecture generated a high open circuit voltage and short circuit current of 65 V and 1.6 μA, respectively, by bending to a displacement of 10 mm under a strain rate of 6 cm/s. The device underwent through 5000 bending cycles within 700 s, establishing good electromechanical flexibility. Qi et al. [79] developed PZT nanoribbons-based PENG device that produces the voltage and current of 0.25 V and 40 nA, respectively, under tapping frequency of 2.3 Hz. Some of the studies used PZT nanofibers to develop PENG devices. Chen et al. [80] developed PZT nanofibers of diameter of about 60 nm and length of 500 μm. These nanofibers were aligned along interdigited electrodes of Pt wires, which was then packaged within a soft PDMS polymer on Si substrate, as represented in Fig. 6 (g). The power generation mechanism, from longitudinally aligned PZT nanofibers is illustrated in [Fig. 6 (h) ((i), (ii))]. The developed PENG produces a voltage and power of 1.63 V and 0.03 μW, respectively [Fig. 6 (i)]. Similarly, Gu et al. [81] developed vertically aligned PZT nanowire arrays. The nanowires arrays were generated using electrospun nanofibers. The developed PENG produced a very high voltage output of 209 V and current density of 23.5 $\mu A/cm^2$, under a compressive force.

From the above discussion, it can be concluded that electromechanical converter PZT ceramic can be used in different forms, such as nanowires, nanorods, nanoribbons, and nanofibers, to develop high performance flexible nanogenerators. Apart from this, there are some relaxor ferroelectrics based on PZT ceramic system, which are potentially used by researchers to develop high performance PENGs [e.g., lead magnesium niobate-lead titanate (PMN-PT), lead zinc niobate-lead titanate (PZN-PT)] [82–84]. Thin films based on PMN-PT ($Pb(Mn, Nb)O_3$-$PbTiO_3$) exhibit superior piezoelectric strain coefficient and voltage constant than those of PZT [85]. Chen et al. [86] reported that the single-crystalline PMN-PT nanobelt arrays-based PENG could generate an open circuit voltage and short circuit current of 6 V and 102 μA, respectively, at a strain agitation of 0.2% under periodic stretching and compression. Moreover, these nanobelt arrays exhibited extremely high piezoelectric strain coefficient of 677 pm/V. A PMN-PT/PVDF based PENG was developed by Li et al. [87]. 0.7 $Pb(Mg_{1/3}Nb_{2/3})O_3$-0.3 $PbTiO_3$(0.7PMN-0.3PT) (PMN-PT) nanorods were synthesized using hydrothermal route. The composite was developed by dispersing

these nanorods into PVDF matrix and further integrated into a PENG device. The device produces a maximum open circuit voltage output and current of 10.3 V and 46 nA, respectively.

Wurtzite structure based inorganic ceramic, ZnO, has been reported to display piezoelectric behavior and found to be a potential material for developing PENG devices for various bioelectronic applications [88]. Banna et al. [89] developed ZnO nanorods based flexible PENG on carbon paper and such PENG developed a maximum voltage and current output of 6.8 V and 1.45 μA, respectively, under compressive stress. It was revealed that with an increase in the molar concentration (10-70 mM) of ZnO nanorods, the voltage and current outputs are increased from 3.6 to 6.8 V and 0.79 to 1.45 μA, respectively. In another work, ZnO nanoparticles were dispersed in PDMS matrix to develop PENG, which generates a voltage and power of 20 V and 20 μW, respectively, on finger tapping [90].

The dopants are often introduced into ZnO structure to improve the piezoelectric properties towards energy harvesting applications. Hsu et al. [91] developed nano-inspired 2.3% sulphur-doped ZnO based PENG on PET substrate. The PENG produces a voltage and current outputs of $\sim$ 0.646 V and $\sim$ 4.32 $\times$ 10^{-8} A, respectively, in dark, under a loading of 500 g/cm^2, i.e., environmental vibrations. Under UV light illumination, the PENG generates a voltage and current of $\sim$ 0.689 V and 5.73 $\times$ 10^{-8} A, respectively, under similar loading. The maximum current was obtained in the frequency range of 30-100 Hz. Similarly, Sinha et al. [92] developed 5 mol.% yittrium (Y)-doped ZnO based PENG, which exhibited an open circuit voltage output of 20 V under gentle finger tapping motions. Nour et al. [93] carried out comparative analysis on energy harvesting abilities of ZnO nanorods and 9% Ag-doped ZnO nanorods. Pure ZnO nanorods based PENG generated a voltage of 7 mV and Ag-doped ZnO nanorods generated a voltage output of 2 mV. Lee et al. [94] studied the solution processed Ag-doped ZnO nanowires for nanogenerator applications. The ZnO nanowires were grown on flexible polyester. The PENG generates a power output of 0.5 μW, which is 2.9 times higher than power, generated by undoped ZnO nanowires-based PENG. Similarly, Zhu et al. [95] suggested that 1% Fe-doped ZnO nanoarrays produce more voltage output as compared to undoped ZnO nanoarrays. Similarly, there are several other dopants which enhances the piezoelectric response and consequently, the voltage output of ZnO and thereby, increasing the power generation capability of PENGs, e.g., V, Ga, Cl, and Li-doped ZnO generate voltages of 32, 1.1, 9.45, and 2 V, respectively [96–99]. Some of the studies used cost-effective routes for developing PENG devices for energy harvesting applications. Batra et al. [100] reported that 5 mol. % Nd-doped ZnO nanorods based PENG generates an open circuit voltage of $\sim$ 31 V under finger tapping motions which provides an approximate force of 0.3 N; whereas, undoped ZnO nanorods based PENG generates $\sim$ 2 V.

Wurtzite structure-based alumnium nitride (AlN) exhibits moderate piezoelectric coefficient. Thin films and nanostructures, based on AlN are used for developing PENG devices [101,102]. Algieri et al. [103] developed flexible biocompatible AlN thin film on polyimide substrate by direct sputtering. The fabricated PENG device was patterned using cost-effective microfabrication techniques. The AlN thin film exhibited piezoelectric strain coefficient of 4.93 $\pm$ 0.09 pm/V. The PENG device generates a voltage and current outputs of $\sim$ 1.4 V and 1.6 μA, respectively, under periodic compressive deformations. The device could able to produce power output of 1.57 μW, under optimum resistive load.

4.2. Piezopolymers based PENGs

Polymers have intrinsic flexible property which is desired for wearable and implantable bioelectronic applications. The piezoelectric polymers are used to develop flexible high performance PENGs.

PVDF along with its co-polymer P(VDF-TrFE) are highly explored piezoelectric polymers to develop PENG devices [104,105]. Thakur et al. [106] developed PVDF-ZnO nanoparticles based PENG device, which generated a voltage and current of $\sim$ 24.5 V and 1.7 μA, respectively. The device produces a power density of $\sim$ 32.5 mW/cm^3. Similarly, Dutta et al. [107] developed PVDF based nanocomposite films, wherein silica coated NiO nanoparticles were incorporated in polymer matrix to enhance β-phase [Fig. 7 (a)]. The developed PENG generated maximum voltage output of 53 V [Fig. 7 (b)]. The current and power densities produced by the PENG was $\sim$ 0.3 μA/cm^2 and 685 W/m^3, respectively. Gaur et al. [108] incorporated $BaTiO_3$ (BT) nanoparticles in PVDF matrix to induce strong piezoelectric character and developed a nanocomposite film by solvent casting technique. 10 wt% BT based nanocomposite film was poled under a field of 300 kV/cm for 1 h. The developed PENG generates an open circuit voltage and power density of 78 V and 120 μW/cm^2, respectively, under finger tapping.

Electrospinning of PVDF based fibers have been extensively studied for developing PENGs due to formation of high β-phase fraction. The degree of alignment of dipoles is found to be in proportionate with the magnitude of applied field [109–113].

The co-polymer of PVDF is found to be suitable for developing PENG devices for biomedical applications due to its flexibility, stability, and biocompatibility [114,115]. Gui et al. [116] reported the potentiality of P(VDF-TrFE) nanofibers with interdigital electrodes of Au for developing PENG device. The interdigital electrodes were used to collect the charges during application of force. The P(VDF-TrFE)-based PENG produces a voltage output and peak current of 5 V and 1.2 μA, respectively. To enhance the piezoelectric behavior of the polymer, a conductive filler such as, reduced graphene oxide (RGO) is commonly used. This is because the conductive nature of graphene creates percolating paths that facilitate charge transportation within the polymer, thereby improving its overall piezoelectric performance. Habibur et al. [117] incorporated 0.1% RGO in P(VDF-TrFE) matrix. The unpoled PENG generates a maximum voltage and peak current of 2.4 V and 0.8 μA, respectively. Another conductive filler, MgO, was incorporated in polymer matrix to enhance piezoelectricity. In addition, such MgO nanofillers increases the breakdown strength and improve the electrical properties [118,119]. In a study reported by Singh et al. [120], MgO nanoparticles were incorporated in P(VDF-TrFE) matrix, which increased the piezoelectric, ferroelectric as well as mechanical properties of the nanocomposite film. The fabricated PENG device showed good energy harvesting performance while executing bending motion with a voltage output of 2 V (two times higher than the voltage, produced from pure P(VDF-TrFE) film) [Fig. 7 (c)].

Zhou et al. [22] harnessed the advantages of 3D printing to fabricate a highly stretchable kirigami PENG using $BaTiO_3$ nanoparticles, a Poly(vinylidene fluoride-co-trifluoroethylene) matrix, and silver flakes-based electrodes. The PENG showcased a modified T-joint-cut kirigami structure, surpassing limitations of traditional designs and enabling high stretchability to over 300% strain. This highlights the potential of 3D printing in developing flexible and wearable bioelectronic systems.

Poly (L-Lactic acid) (PLLA) is another piezoelectric polymer, reported for developing PENG devices. Zhu et al. [121] developed PLLA electrospun nanofibers-based PENG device, which generated a voltage output of 0.55 V from joint deformation and current of 230 pA. Smith et al. [122] suggested the potential use of PLLA nanowires as nanogenerators with characteristic shear piezoelectricity, a phenomenon where a material generates an electric potential in response to shear mechanical stress or shear deformation.

Polyacrylonitrile (PAN) is piezoelectric polymer and is used to develop PENGs for low power bioelectronics. Cai et al. [123] developed PAN thin film-based PENG device for energy harvesting

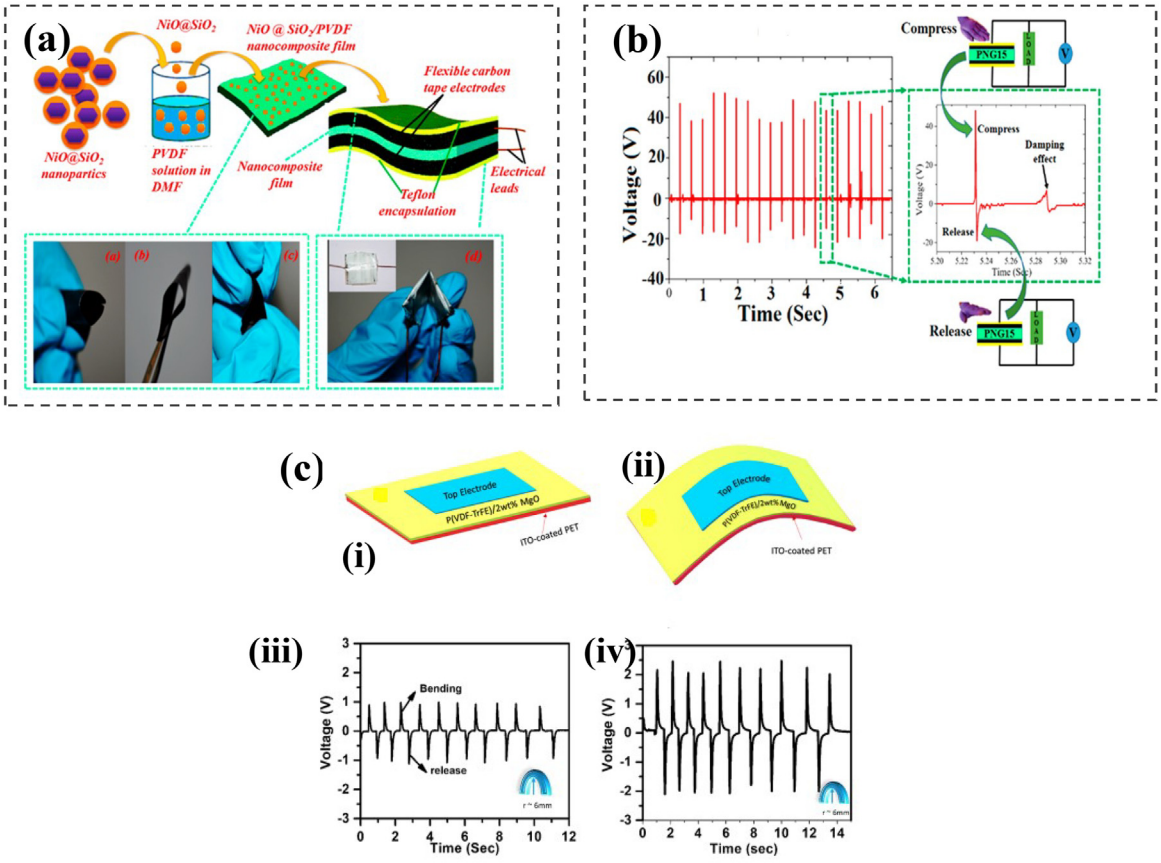

Fig. 7. PENGs based on organic piezoelectric materials (piezopolymers). (a) Schematic of fabrication process of PVDF-NiO/SiO_2 based PENG. (b) Voltage output variation with time during compression by finger imparts in PVDF-NiO/SiO_2 based PENG. Reproduced with permission from [107]. Copyright 2018, American Chemical Society. (c) Schematic illustration of the PVDF-MgO based PENG in (i) release and (ii) bend state. Output voltage and current response during bending and release states of (iii) Pure P(VDF-TrFE) based PENG and (iv) P(VDF-TrFE)-MgO based PENG at a bending radius of 6 mm and frequency of 1 Hz. Reproduced with permission from [120]. Copyright 2018, American Chemical Society.

applications. Thin film was produced using PAN powder, dissolved in dimethylformamide (DMF), followed by casting it on glass substrate. The developed thin film was electrically poled at 5 kV/cm for 6 h. The device produced the maximum voltage of ~ 0.9 V under a compressive force of 15 N when the film was poled at a temperature of 80°C (5 kV/cm, 6 h). Wu et al. [124] suggested the potentiality of piezoelectric polypropylene for energy harvesting applications. A polypropylene film-based PENG was fabricated and proposed to generate energy from human body movements for monitoring physical health parameters. The device develops power density of ~ 52.8 mW/m^2.

4.3. Nature-inspired PENGs

Apart from inorganic (ceramics) and organic (polymers) piezoelectric materials, some naturally occurring piezoelectric materials (cellulose and collagen fibrils) can be used to develop PENG devices [125,126]. Zheng et al. [127] developed cellulose nanofibrils based PENG. PDMS layer was coated on freeze dried film of cellulose nanofibrils and the complete setup was enclosed in between two PDMS films to develop PENG device. The nanogenerator produces a voltage and current of 60.2 V and 10.1 μA, respectively. The PENG generates a power of 6.3 mW/cm^3. Maiti et al. [128] developed onion skin-based PENG device [Fig. 8 (a)]. Onion skin contains piezoelectric cellulose fibers. The fabricated onion skin-based PENG device produces a voltage and current output of 18 V and 166 nA, respectively [Fig. 8 (b)]. The device could generate a power of 1.7 μW/cm^2.

Kumar et al. [129] developed PVDF nanohybrid based PENG with bio-waste piezoelectric fish scale. The addition of fish scale into PVDF significantly increases the electroactive β-phase. The electrospun composite nanofibers-based PENG generated an open circuit voltage of 22 V under finger tapping motions with approximate pressure of 40 kPa. The device produced a power of 28.5 μW/cm^2. Similarly, Karan et al. [130] developed a PENG device, based on egg shell membrane, as illustrated in [Fig. 8 (c)]. The developed device produces the voltage and current of ~ 26.4 V and ~ 1.45 μA, respectively [Fig. 8 (d)]. The device generates a power of ~ 238.17 μW/cm^3. Likewise, fish swim bladder contains aligned piezoelectric collagen nanofibrils and therefore, can be used to develop PENG. A study was performed by Ghosh et al. [131], wherein a PENG was developed using fish swim bladder as the main constituent. The device produces a voltage of 10 V under normal stress of 10 N by finger tapping. The current and the power, generated by the device was 51 nA and ~ 4.15 μW/cm^2, respectively. The cellulose, hemicelluloses and pectin are responsible for piezoelectric effect in pomelo fruit membrane [132,133]. Bairagi et al. [134] developed a PENG device based on piezoelectric pomelo fruit membrane. The developed PENG device produces a voltage and current output of approximately 15 V and 130 μA, respectively. The device generates a power density of 487.5 μW/cm^2.

The M13 bacteriophage is a type of virus that contains single-stranded DNA and capsid proteins. Interestingly, the capsid protein of this virus has a dipole moment, which gives rise to piezoelectric properties i.e., virus generates an electric potential under mechan-

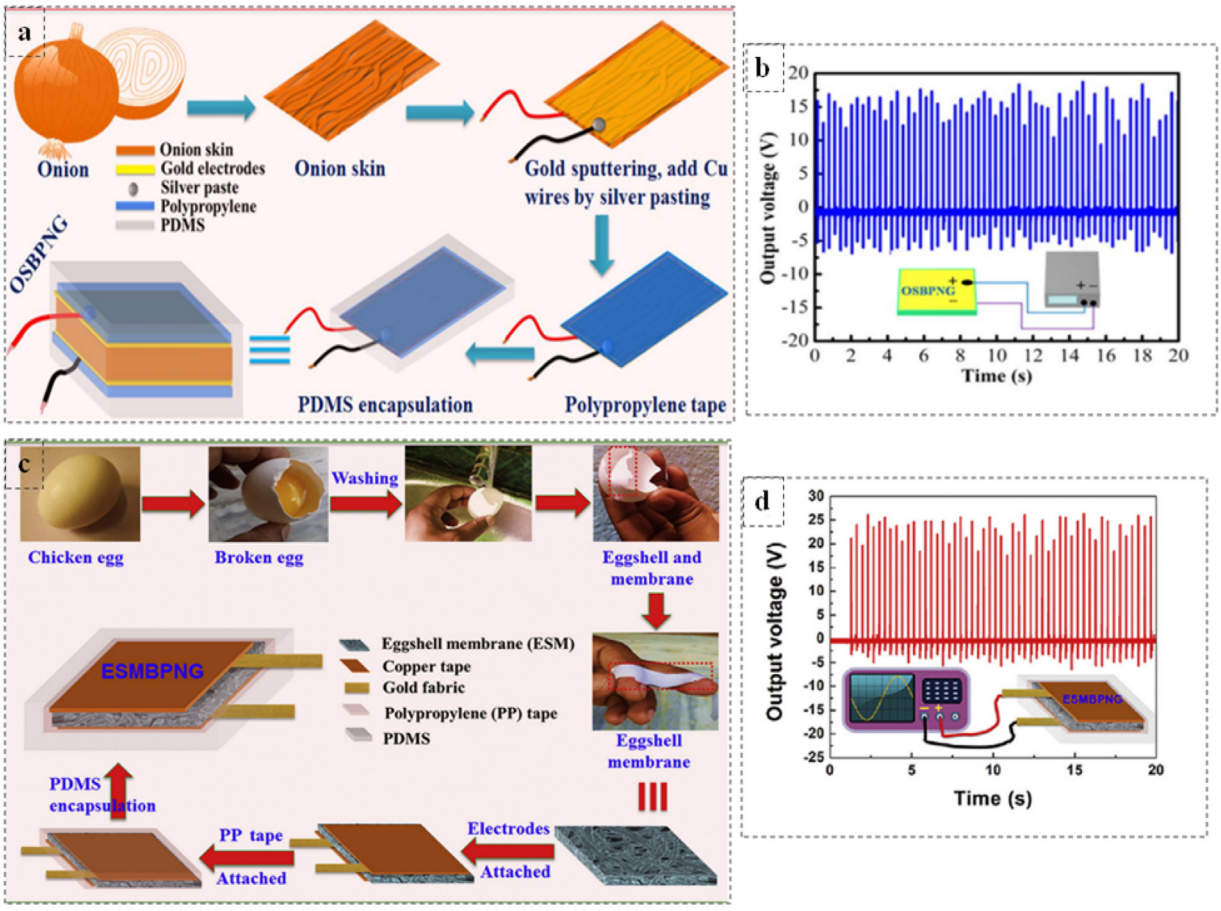

Fig. 8. Nature-inspired PENGs based on naturally occuring piezoelectric biomaterials. (a) Fabrication process of onion skin-based PENG. Extraction of onion skin, followed by electroding via gold sputtering and attachment of copper wires. Inclusion in polypropylene tape, followed by PDMS encapsulation. (b) Voltage response of onion skin-based PENG. Reproduced with permission from [128]. Copyright 2017, Elsevier. (c) Fabrication process of egg shell membrane-based PENG. Washing of the waste egg shells, followed by removal of egg shells, membrane. Electroding of top and bottom surface and attachment of polypropylene tape, followed by PDMS encapsulation. (d) Voltage response of egg shell membrane-based PENG. Reproduced with permission from [130]. Copyright 2018, Elsevier.

ical pressure or deformation [135]. Heo et al. [136] developed M13 bacteriophage based piezoelectric energy harvesting devices. M13 bacteriophage consists of a rod-shaped structure with length and diameter of 880 nm and 6.6 nm, respectively, covers 2700 copies of major coat proteins (pVIII) [Fig. 9 (a)]. The developed PENGs included 2D-dot, line and continuous bacteriophage film patterns-based devices. Bacteriophage based thin film of about 1 cm^2 area with micro-patterned structures were fabricated on gold coated SiO_2 substrate. The thin film patterns were sandwiched between two gold-coated electrodes, the entire assembly was then encapsulated in polydimethylsiloxane (PDMS), as shown in [Fig. 9 (b)]. The 2D-dot patterns-based device exhibited the highest piezoelectric performance with voltage and current of 0.95 V and 94 nA, respectively. It is able to power up LCD display [Fig. 9 (c)]. Spider silk containing protein fibers is another nature-inspired piezoelectric biomaterial. Spider silk exhibits electrical dipoles [137,138]. Karan et al. [139] developed spider silk-based PENG [Fig. 9 (d)], which produces voltage and current output of ~ 21.3 V and ~ 0.68 μA, respectively, under continuous finger tapping motions, with a power density of approximately 4.56 $\mu W/cm^2$. The device has been proposed to serve as a sensor for arterial pulse measurement. Chitin is a well-known piezoelectric biomaterial. Chitin nanofibers can be obtained from crab shells through mechanical processing after removing proteins and minerals [140]. Hoque et al. [141] developed crab shell derived chitin nanofibers-based PENG. Chitin nanofibers were extracted from bio-waste crab shell, thin film was developed by solvent casting method using chitin nanofibers and PVDF. The fabricated PENG device developed a voltage and current output of 49 V and 1.9 μA, respectively. Further, a nanogenerator was built up using extracted chitin which produced voltage and current output of 22 V and 0.12 μA, respectively. The device is able to charge a 2.2 μF capacitor to 3.6 V in 20 s and can light up 22 LEDs in series connection. Gaur et al. [142] used pomegranate peel as bio-waste filler material to induce electroactive phase in PVDF matrix and furthermore developed a nanogenerator device [Fig. 9 (e)]. The nanogenerator produces a voltage of 65 V and power density of 84 $\mu W/cm^2$. The generated power is sufficient to light up LEDs. Naturally available sugar containing sucrose is found to be piezoelectric in nature. Sucrose, a type of sugar, has a distinctive feature of center of symmetry. This symmetry can only be achieved through a binary rotation around the b-axis. This specific arrangement creates a piezoelectric effect, meaning that a potential is generated when sucrose is subjected to mechanical pressure or deformation. This property can have practical applications in diverse fields, including developing self-powered sensors or energy-harvesting devices [143]. Maity et al. [144] reported sugar encapsulated polyvinylidene fluoride (PVDF) nanofiberous web-based PENG device [Fig. 9 (f)]. The hybridization of sugar in PVDF resulted in excellent performance of the nanogenerator that resulted in voltage of ~100 V under continuous finger tapping which produced a force of 10 kPa. The power, produced by the PENG was 33 mW/m^2. The device could able to light several units of LEDs and a LCD

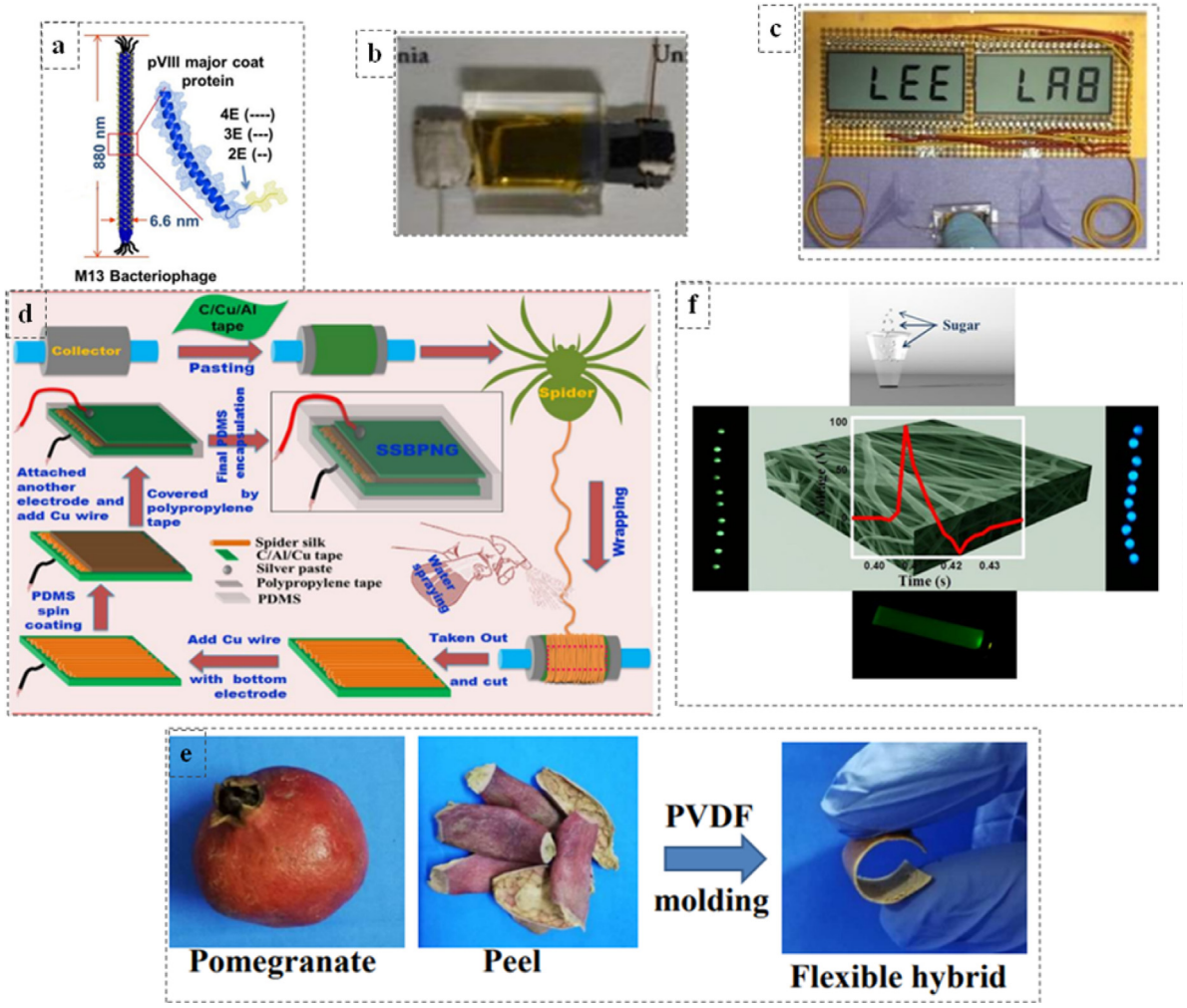

Fig. 9. Nature-inspired PENGs based on either living organisms (Bacteriophage) or natural materials (a) Schematics of M13 bacteriophage having length and thickness of 880 nm and 6.6 nm, respectively. (b) Photograph of M13 bacteriophage-based PENG device. (c) 'LEE LAB' letters visible on the LCD screen when powered by bacteriophage-based PENG device. Reproduced with permission from [136]. Copyright 2019, Elsevier. (d) Schematics depicting fabrication process of spider silk-based PENG device. Reproduced with permission from [139]. Copyright 2018, Elsevier. (e) Biowaste pomegranate peel based flexible hybrid PENG device. Waste peels of pomegranate are molded with PVDF to develop PENG. Reproduced with permission from [142]. Copyright 2020, American Chemical Society. (f) Addition of sugar crystals in PVDF-DMF solution to produce electrospun nanofibrous PENG, as illustrated. LCD screen and portable units of LED lights powered by a capacitor charged up by the PENG device. Reproduced with permission from [144]. Copyright 2018, American Chemical Society.

screen [Fig. 9 (f)]. DNA is found to be accountable for the initiation of the electroactive β-phase nucleation in PVDF [145]. A DNA-PVDF film based nanogenerator was fabricated that produced a power density of 11.5 μW/cm^2.

Table 1 presents a comprehensive summary of various categories of PENGs, including their specific material types, fabrication techniques, and electrical characteristics, relevant for energy harvesting applications in wearable and implantable bioelectronics. Such a summary indicates that PENGs based on PZT nanostructures exhibit superior electrical characteristics, especially in terms of voltage, which is a crucial parameter for bioelectronic devices. The highest voltage, recorded for a PENG based on electrospun PZT nanoarrays was 209 V, accompanied by a proportional current density of 23.5 μA/cm^2. The prominent fabrication techniques for producing high-performance nanogenerators are electrospinning, hydrothermal methods, and solvent casting. Considering the fact that lead-containing materials are prohibited due to toxicity and disposal issues, lead-free ceramics and polymer composites are suitable alternatives for developing high performance PENGs for various bioelectronics applications.

5. Healthcare-related applications of PENGs

5.1. Pulse sensor

It is widely recognized that human pulses play an essential role in diagnosing various diseases, majorly related to the cardiovascular system. Self-powered sensors, associated with real-time monitoring systems, can be very useful for prevention of these diseases by precise monitoring [146,147]. Park et al. [148] fabricated a self-powered pulse monitoring sensor, based on piezoelectric PZT thin film. The PZT thin film was applied and subsequently, annealed on a sapphire substrate, and a thermal release tape was affixed, as illustrated in Fig. 10 (a). The PENG device was attached on wrist top and middle of throat for pulse monitoring, as shown in Fig. 10 [(b), (c)]. The pulses on real-time basis were transferred to mobile phone via wireless communication system. The PENG produces a voltage of 65 mV in response to the pulses, generated by radial arteries, before and after exercise. The voltage, produced by the PENG is 81.5 mV. The voltage, generated by PENG for carotid artery pulses and for saliva swallowing is 400 mV and 1000 mV,

Table 1
Summary of piezoelectric nanogenerators (PENGs) for energy harvesting applications.

Nanogenerator Type	Fabrication technique	External stimuli/applied load/pressure/ Force	Voltage	Current/ Current density	Power/ Power density	Ref.
ZnO nanotubes/polycarbonate	Hydrothermal method	Bending	1.15 V	100 μA	287.5 μW/cm^3	43
Diphenylalanine nanotubes	Meniscus driven self-assembly process	42 N	2.8 V	37.4 nA	8.2 nW	44
$PbTiO_3$ nanotubes arrays	Self-assembly process	Bending	0.62 V	1 nA/cm^2	-	45
Diphenylalanine nanotubes/graphene oxide	Wettability assisted self-assembly process	Bending	6 V	60 nA	-	46
PZT nanotubes/PDMS	Template-assisted method	Bending	1.52 V	54.5 nA	37 nW/cm^2	47
ZnO nanorods	Chemical vapor deposition	Compression	0.7 V	0.000012 nA/cm^2	8.97 mW/cm^2	48
ZnO nanorod arrays	Hydrothermal method	Palm clapping	4 V	20 nA	-	49
ZnO nanorods	Hydrothermal method	Vibrator motions	0.16 V	11 nA	0.92 μW/cm^3	50
$0.65Pb(Mg_{1/3}Nb_{2/3})O_3$–$0.35PbTiO_3$ nanowire	Hydrothermal method	Bending	0.009 V	1.5 nA	175.4 W/cm^3	51
ZnO nanorod arrays	Chemical bath deposition	Ambient force from cam follower	0.968×10^{-3} V	92 nA	-	52
ZnO nanorod arrays	Chemical bath deposition	Cyclic force	0.62 V	-	-	53
$BaTiO_3$ nanotubes/Polydimethylsiloxane	Hydrothermal method	1 Mpa	5.5 V	350 nA	-	58
$BaTiO_3$ thin film	RF Magnetron sputtering	Bending	1 V	0.19 μA/cm^2	7 mW/cm^3	59
$BaTiO_3$/PDMS /3.2 % Carbon	Solid state route, spin coating	Periodic vibration	7.43 V	-	7.92 μW	60
$BaTiO_3$ nanowires	Hydrothermal method	Bending	7 V	360 nA	1.2 μW	61
$BaTiO_3$ nanotubes	Hydrothermal method	Bending	10.6 V	1.1 μA	-	62
$0.97(Na_{0.5}K_{0.5})NbO_3$–$0.03(Bi_{0.5}Na_{0.5})TiO_3$	Solid state route	650 N	10.8 V	-	24.6 nW/cm^2	65
$(K_{0.5}Na_{0.5})NbO_3$	Solid state route	0.1 MPa	3.5 V	0.3 μA	1.13 mW	67
$(K_{0.5}Na_{0.5})NbO_3$ / PVDF	Hydrothermal method	Compressive force	3.4 V	0.1 μA	0.053 W/cm^3	68
KNLN/Cu nanorods/PDMS	Solid state, Spin casting	Clapping	140 V	8 μA	0.5 mW	69
KNN/PDMS/STO	Hydrothermal method	Compressive force	10 V	50 nA	2.25 nW	70
PVDF/$0.915(Na_{0.5}K_{0.5})(Nb_{0.94}Sb_{0.06})O_3$-$0.045LiTaO_3$-$0.04BaZrO_3$ (NKNS-LT-BZ)	Solid state route, Solvent casting	50 N	18 V	2.6 μA	-	71
$0.91K_{0.48}Na_{0.52}NbO_3$–$0.04Bi_{0.5}Na_{0.5}ZrO_3$–$0.05AgSbO_3$–0.2% Fe_2O_3 (KNN–BNZ–AS–Fe)/PDMS	Solid state route, Spin casting	25 N	52 V	4.8 μA	-	72
PZT nanowires	Electrospinning	Bending	6 V	45 nA	200 μW/cm^3	74
PZT nanowires	Hydrothermal method	70 kPa	10 V	-	0.27 μW/cm^2	75
PZT nanorod arrays	Hydrothermal method	Finger tapping motions	8 V	-	5.92 μW/cm^2	76
PZT/PDMS	Sacrificial template method	30 N	29 V	116 nA	-	77
PZT-NH_2/ Maliec anhydride	Drop casting	Periodic bending	65 V	1.6 μA	26 μW	78
PZT nanofibers	Electrospinning	Periodic stress	1.63 V	-	0.03 μW	80
PZT nanowire arrays	Electrospinning	Impact force	209 V	53 μA	23.5 μA/cm^2	81
$Pb(Mg,Nb)O_3$-$PbTiO_3$ (PMN-PT) nanobelt arrays	RF sputtering, Top down approach	0.2 % strain agitation	6 V	102 μA	-	86
$0.7Pb(Mg_{1/3}Nb_{2/3})O_3$-$0.3PbTiO_3$(0.7PMN-0.3PT) nanorods	Hydrothermal method	Mechanical tapping	10.3 V	46 nA	-	87
ZnO nanorods/carbon paper/PDMS	Hydrothermal method, Spin coating	Vertical mechanical strain	6.8 V	1.45 μA	-	89
ZnO nanopraticles/PDMS	Hydrothermal method, Mechanical agitation	Finger tapping	20 V	20 μA	20 μW	90
Sulphur doped ZnO nanowires	Hydrothermal route,	Environmental vibrations	0.689 V	5.73×10^{-8} A	-	91
Y-doped ZnO nanorods	Co-precipitation method	0.01 kgf (gentle finger tapping)	20 V	-	-	92
Ag-doped ZnO nanowires	Hydrothermal method	Sound wave	5.9 V	1 μA	0.5 μW	94
Fe-doped ZnO nanoarray	Seed-assisted wet chemical method	Compressive force	0.85 V	-	-	95
Vanadium-doped ZnO nanosheets/PDMS	Hydrothermal method	Periodic bending	32 V	6.2 μA	-	96
Gallium-doped ZnO nanowires	Hydrothermal method	Deformation	0.56 V	-	-	97
Chlorine-doped ZnO nanowire films	Hydrothermal method	External force	4.9 V	1030 nA/cm^2	-	98
Lithium-doped ZnO nanowires	Hydrothermal method	Periodic bending	180 V	50 μA	-	99
Neodymium-doped ZnO nanorods	Co-precipitation method	0.3 N	31 V	-	-	100
AlN thin films	Sputtering technique	Periodical deformation	1.4 V	1.6 μA	1.57 μW	103

(*continued on next page*)

Table 1 (*continued*)

Nanogenerator Type	Fabrication technique	External stimuli/applied load/pressure/ Force	Voltage	Current/ Current density	Power/ Power density	Ref.
P(VDF-TrFE)/GeSe nanosheets	Solvent casting	50 N	17.58 V	1.14 μA/cm^2	9.76 μW/cm^2	105
ZnO/PVDF thin films	Solvent casting	Finger tapping	25.4 V	1.7 μA	32.5 mW/cm^3	106
SiO_2 coated NiO nanoparticles/PVDF	Hydrothermal method	Biomechanical force	53 V	0.3 μA/cm^2	685 W/cm^3	107
PVDF/$BaTiO_3$ nanoparticles	Solvent casting	Finger tapping	78 V	-	120 μW/cm^2	108
PVDF micro/nanofibers/PDMS	Electrospinning	0.5 % strain (cyclic stretching)	4.1 V	295 nA	-	112
P(VDF-TrFE) thin film	Spin coating	Mechanical strain	7 V	58 nA	-	114
P(VDF-TrFE) nanofibers	Electrospinning	Walking	5 V	1.2 μA	-	116
PLLA nanofibers	Electrospinning	Strain deformation angle 28.9 degree	0.55 V	230 pA	-	121
Cellulose microfibers/PDMS/MWCNTs	Solvent casting	Hand punching	30 V	500 nA	0.9 μW/cm^3	126
Cellulose nanofibrils/PDMS aerogel film	Freeze drying	Vibrations from oscillator	3.7 V	10.1 μA	6.3 mW/cm^3	127
Onion skin/PDMS	Homespun device fabrication	Finger tapping	18 V	166 nA	55 μW/cm^3	128
Fish Scale/PVDF	Solvent casting	Finger tapping	22 V	-	28.5 μW/cm^2	129
Egg shell membrane (ESM)/PDMS	Biowaste ESM	81.6 kPa	26.4 V	1.45 μA	238.17 μW/cm^3	130
Fish swim bladder (FSB) /PDMS	Biowaste FSB	Finger tapping	10 V	51 nA	4.15 μW/cm^3	131
Pomelo fruit membrane (PFM)	Biowaste PFM	Finger tapping	6.4 V	7.44 μA	12 μW/cm^3	134
M13 bacteriophage	Self-templating assembly process	Compressive load	0.95 V	94 nA	-	136
Spider silk fibers	Nature derived	Finger imparting	21.3 V	0.68 μA	4.56 μW/cm^3	139
Crab shell (Chitin nanofibers)	Nature derived	Finger impartating	49 V	1.9 μA	6600 μW/cm^3	141
Pomegranate peel/PVDF	Nature derived	Finger tapping	65 V	-	84 μW/cm^3	142
Sugar encapsulated PVDF	Electrospinning	10 kPa	100 V	-	33 mW/m^2	144
DNA/PVDF film	Solvent casting	63 Mpa	20 V	0.184 μA	-	145

respectively. The sensor showed good durability, biocompatibility and the measurements were non-invasive.

Similarly, Meng et al. [149] developed a polytetrafluoroethylene (PTFE) woven construction based self-powered pressure sensor. The device was attached on fingertip, wrist, ear and ankle for pulse measurements [Fig. 10 (d) ((a_1), (b_1), (c_1), (d_1))]. The variation of output voltage with time is shown in Fig. 10 (d) ((a_2), (b_2), (c_2), (d_2)), where, P_m, P_s and P_d are mean arterial pressure, systolic peak and diastolic valley point, respectively. It was reported that the health condition of cardiovascular system can be assessed based on the values of 'K', where K= [(P_m- P_d)/(P_s- P_d)]. The PENG device showed an ultra-sensitivity of 45.7 mV/Pa and low pressure (2.5 Pa) detection ability. The response time of the device is less than 5 ms with good durability, as it sustained 40,000 motion cycles.

5.2. Sensor for blood pressure monitoring

Hypertension due to high blood pressure can lead to many diseases such as heart problem, cerebrovascular disease, renal failure etc. [150,151]. Self-powered sensors, designed for measuring blood pressure can be highly beneficial in diagnosing diseases and evaluating the effectiveness of medical treatments for such conditions. Cheng et al. [152] developed 200 μm PVDF thin film-based PENG device for blood pressure monitoring. The film was covered with Al layer on both, top and the bottom. The entire assembly was engulfed on both sides (top and bottom) by polyimide films, as shown in Fig. 11 (a) (i). The flexible device exhibited the Young's modulus of 3500 MPa. For monitoring purposes, the PENG device was encased around the ascending aorta of a porcine model [Fig. 11 (a) (ii)]. Fig. 11 (b) presents the schematic illustration of the device wrapped around aorta, with a visual display unit for blood pressure monitoring, connected via an integrated circuit. The compressive and tensile stresses, generated in the aorta walls lead to voltage generation in PENG device. A linearity of $R^2 > 0.99$ was obtained between voltage output and the pressure of blood flow, *in vitro* and $R^2 = 0.971$, *in vivo*. The device exhibited good durability by sustaining more than 50,000 operation cycles. The sensitivity of the device is 173 mV/ mm Hg with a power of 2.3 μW, *in vitro*. However, obtained sensitivity was 14.32 mV/ mm Hg with the power of 40 nW, *in vivo*.

Tan et al. [153] developed a wristband for artificial intelligence driven blood pressure monitoring. The system contained a PENG based sensor with multilayered structure, as shown in Fig. 11 (c) (A) and a wireless communication system was adopted, based on bluetooth connectivity for transmission of signals. The system detects the wave pulses of blood flow, coming from the heart [Fig. 11 (c) (B)]. The wrist band contained rubber strap, polylactic acid shell, Li-ion battery, bluetooth and PENG based sensor [Fig. 11 (d) ((A)–(C))]. The system receives wave pulses from the wearer and these pulses are compared with an established deep learning model, based on which, the blood pressure was predicted [Fig. 11 (d) (D)].

5.3. Strain sensor

Strain sensors can be employed for tracking or observing physical activities in the body such as, small movements during speaking, large movements like finger motion, knee motion, wrist motion along with physical health parameters [154–157]. Song et al. [14] developed PbI_2 nanosheets based PENG device for strain sensing application [Fig. 12 (a)]. PbI_2 nanosheets were prepared using chemical vapour deposition method. During deformation of the PENG device, charges and the voltage output were observed to varied upon the generated strain. Thereby, the developed PENG acts as a strain sensor with a strain detection range of 0.339 %. The mechanism of generation of electricity is illustrated in Fig. 12 (b), under unstrained, strained and releasing conditions. When the PENG de-

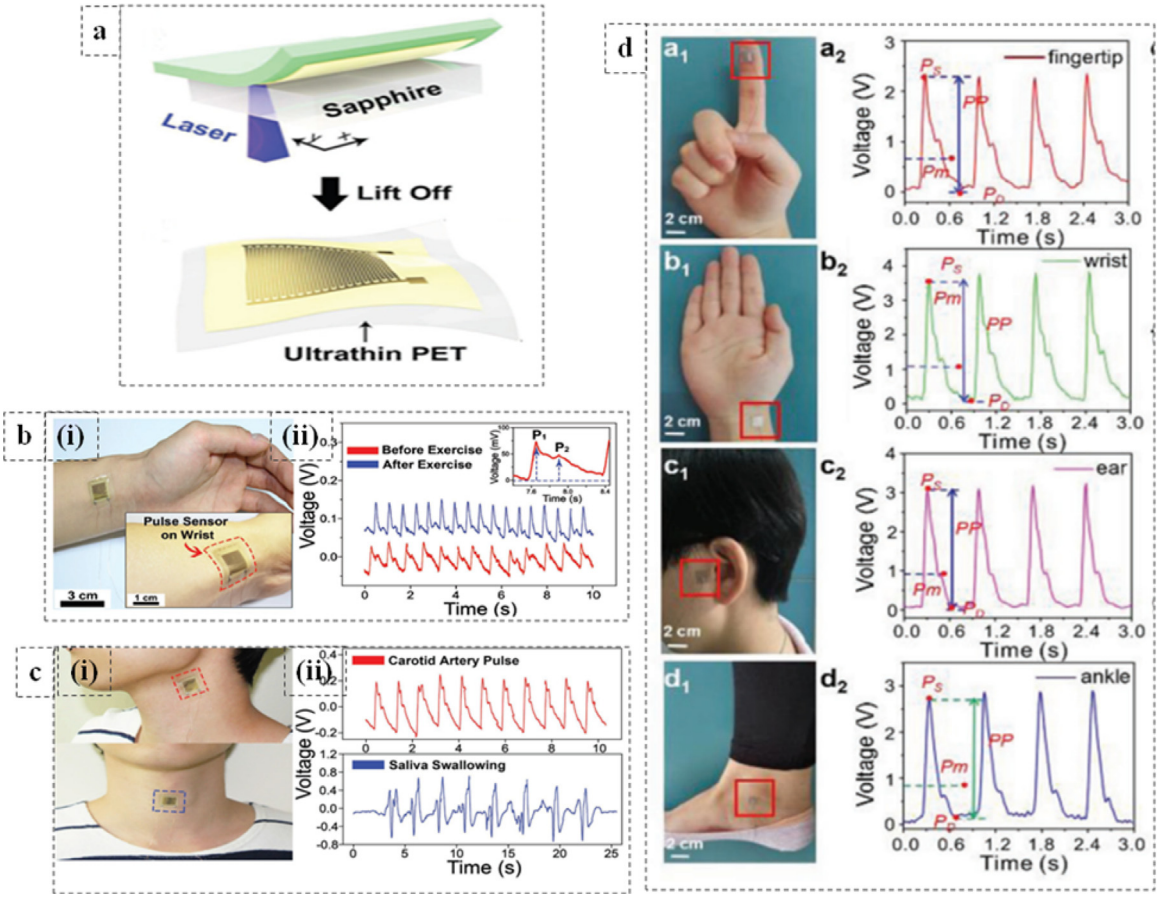

Fig. 10. PENG thin film-based sensor developed using conventional piezoelectric materials (PZT). (a) Schematics representing the fabrication of PZT thin film based self-powered pulse sensor. (b) (i) Photograph of pulse-sensor attached on wrist and (ii) Radial artery pulse readout based on the voltage response, before (red line) and after (blue line) exercise. P_1 and P_2 in the inset image denote the pulse pressure and late systolic pressure augmentation, respectively. (c) (i) Pulse-sensor attached on top and middle of throat, (ii) Carotid artery pulse variation and pulses during saliva swallowing readouts based on voltage variation. Reproduced with permission from [148]. Copyright 2017, John Wiley and Sons. (d) (a_1-d_1) Pulse sensor attached at finger tip, wrist, ear and ankle, (a_2-d_2) Voltage variation for four different places of sensor attachment. Reproduced with permission from [149]. Copyright 2019, John Wiley and Sons. [P_m = mean arterial pressure, P_s = systolic peak and P_d = diastolic valley point].

vice is compressed, it polarizes along the direction of tensile strain, which results in the generation of a piezoelectric potential and a positive flow of electric current. Nevertheless, once the force is released, the piezoelectric potential decreases, resulting in a negative flow of electric current. The PENG device produces a voltage of 29.4 mV and could generate power of 0.12 pW [Fig. 12 (c)]. The current, produced by the device is 20.9 pA [Fig. 12 (d)].

Agarwala et al. [156] conducted a study aimed at developing a cost-effective strain sensor with good combination of flexibility and stretchability for wearables and home health applications. Aerosol jet printing was utilized to create the strain sensor on a bandage substrate. To enhance its performance and stability, laser light was used to sinter the silver nanoparticle ink. The experimental results clearly indicated that the strain sensor maintained its functionality even after 700 repeated bending cycles, proving its stretchability, sensitivity, and stability. Similarly, Xiao et al. [158] developed ZnO nanowires and polystyrene-based PENG device for strain sensing. The strain sensor has the capability to withstand high strain of upto 50 %. Fig. 12 (e) presents I vs V characteristic curve for the PENG device under different strain conditions and at fixed bias voltage of 10 V. On the other hand, Fig. 12 (f) reports the current variation in the PENG device, attached on the index finger at different bending conditions and at a fixed biased voltage of 10 V. Based on the strain sensing capability, it has several applications for personalized healthcare.

5.4. Pressure sensor

A wide range of pressure (10-100 Pa) is induced all across the body, while executing our daily life activities. PENGs generate electrical charges in proportion to the applied pressure. For this pressure sensing applications, flexible materials are of greater interest [159,160]. Rafique et al. [161] developed Br-doped (0.02M) ZnO nanosheets based PENGs for pressure sensing applications. The operational mechanism of the PENG device is depicted in Fig. 13 (a). When an external force is applied on the top electrode, ZnO nanosheets deform along c-axis owing to which polarization of Zn^{2+} and O^{2-} takes place in the crystal structure. Electrons flow in the circuit and accumulate at the bottom electrode [Fig. 13 (a) (i)]. Once the force is eliminated, the electrons return to the top electrode [Fig. 13 (a) (ii)]. Such alternate flow of electron produces an AC signal. The sensitivity of undoped PENG was measured to be 0.0318 V/kPa and for doped, it was 0.0863 V/kPa. The doped PENG produces a voltage of 8.82 V at a frequency of 6 Hz, which is found to be 3 times higher than undoped PENG [Fig. 13 (b)] and the current is measured to be 4.41 μA. The device could able to produce power density of 38.90 $\mu W/cm^3$. The Br-doped PENG was used to extract energy from the pressure-based motions of wrist and fingers.

Waseem et al. [162] developed a PENG for gas pressure sensing application. The pressure sensor was based on coaxially aligned

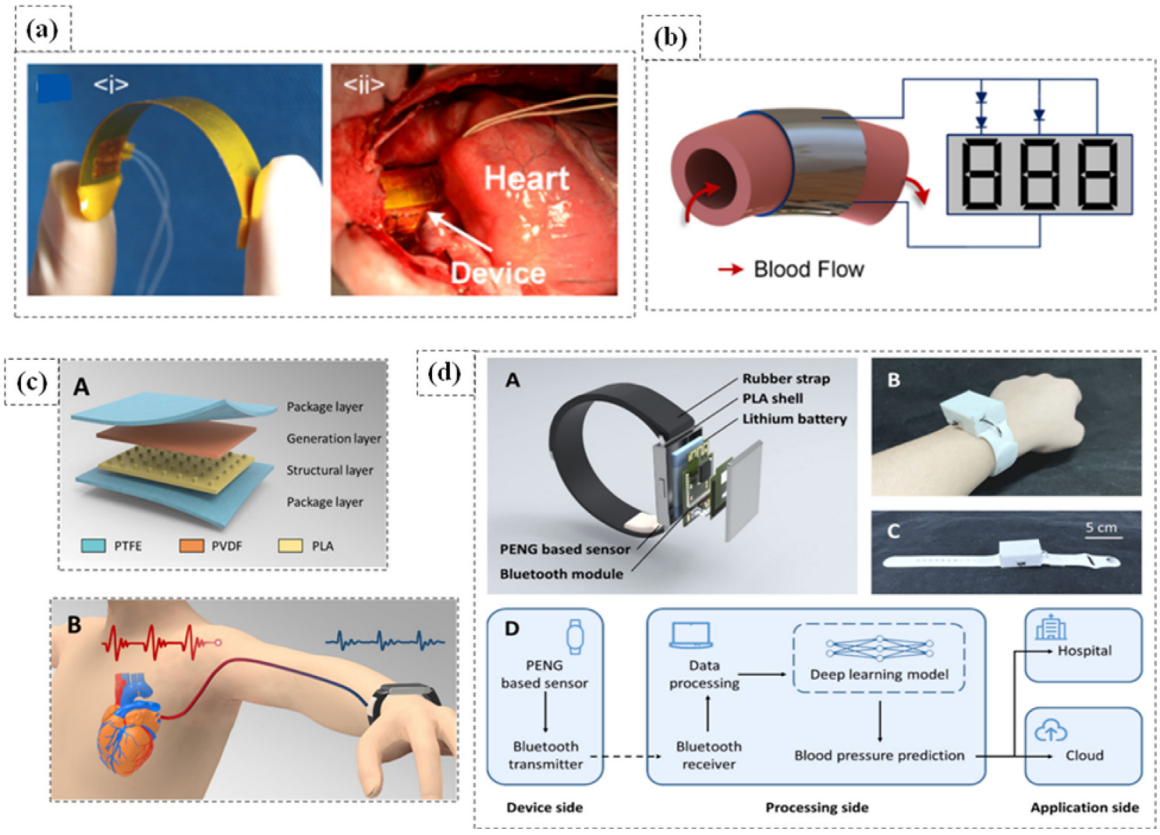

Fig. 11. Flexible PENGs have more appealing clinical applications. (a) (i) Photograph showing flexibility of PVDF based PENG device by bending it with fingers, (ii) PENG device wrapped around the ascending aorta of porcine heart. (b) Schematics of PENG device wrapped around aorta, wires and LCD display unit. Reproduced with permission from [152]. Copyright 2016, Elsevier. (c) A. Photograph showing multilayered PENG device-based sensor [packaging layer, generation layer, structural layer and packaging layer], B. Schematics showing flow of blood from heart to wrist via artery which is being measured by the PENG sensor present in the wrist watch attached on hand of the subject. (d) A. Photograph showing different components of wrist band-based blood pressure monitoring system, B. Photograph of subject's hand wearing the blood pressure monitoring system, C. Photograph of entire blood pressure monitoring system having a length of 26 cm, D. Schematic showing processing of the blood pressure monitoring system. [Open access] [153].

GaN nanowires. Fig. 13 (c) represents the actual images of a sensor housing with diaphragm with a sensor element both the states, unglued and glued. A simulation study was performed to evaluate sensing operation at different gas pressure conditions and corresponding voltage generation. For gas pressures of 50, 100, 150, 200 psi, corresponding potentials of 35, 71, 103, 132 mV were generated [Fig. 13 (d)]. The simulated potential results matched with the experimental results. The sensor exhibited very close linear response, i.e., $R^2 = 0.992$ and a very high sensitivity of 14.25 V/kPa. A fast time response of 55 ms was achieved with the power density of 66.3 μW/cm^2 under a load resistance of 6 MΩ. At a pressure of 2 kPa, the energy, stored by the pressure sensor was measured to be 53.8 μJ.

5.5. Sensor for biomimetic artificial hair cells

Approximately one-tenth of the global population has hearing difficulties [163]. Hearing losses occur due to several factors such as age, noise, illness, trauma etc. One of the attentions seeking hearing impairment is sensorineural hearing loss that occurs due to dysfunctioning of frequency discrimination and is primarily caused by the loss of hair cells from the organ of *Corti*, present in the cochlea [164,165]. Sometimes, sensorineural hearing loss is irreversible because of non-regenerative capacity of the hair cells. Hair cells in the basilar membrane converts the vibrations, induced due to sound waves into electricity to provide stimulation to the auditory nerves. Cochlear implants, which transform acoustic sound energy into electrical signals to stimulate the auditory nerves through an electrode array inserted into the cochlea, are utilized for treating hearing impairments [166–170]. However, discomfort, limited ability to detect low-frequency sounds due to the small number of electrodes, and the high-power consumption are the key issues, associated with cochlear implants. Towards this end, self-powered sensors, exhibiting high piezoelectric strain coefficients, can be used to mimic the functioning of the hair cells and can stimulate the auditory nerves [171,172]. Lee et al. [173] developed PZT thin film nanogenerator [inorganic based Piezoelectric Acoustic Nanosensor (iPANS)] for sensorineural hearing loss repair. Thin film nanogenerator was fabricated on a trapezoidal silicone membrane (SM) using laser lift-off technique. The generated piezoelectric potential based on amplitudes of sound vibration was theoretically predicted, in accordance with the experimental conditions, using finite element method. Fig. 14 (a) represents the schematic diagram of organ of *Corti* in a mammalian cochlea and a PZT thin film, placed below the basilar membrane under bent condition. The basilar membrane deflects by 600 nm as a reaction to sound waves and the PZT film generates a piezoelectric potential of 3 V. Such voltage is sufficient to stimulate the auditory nerves. Fig. 14 (b) demonstrates the PENG, fixed on the silicone membrane frequency separator [inset image of Fig. 14 (c)]. The frequency separator includes an acrylic plate with a trapezoidal slit, which is covered by a trapezoidal silicone membrane. The trapezoidal silicone-based membrane, over the slit, signifies the basilar membrane, which spatially separates the frequencies of incoming sound waves. When sound waves incident on the frequency separator, the silicone membrane vibrates due to resonance and as a

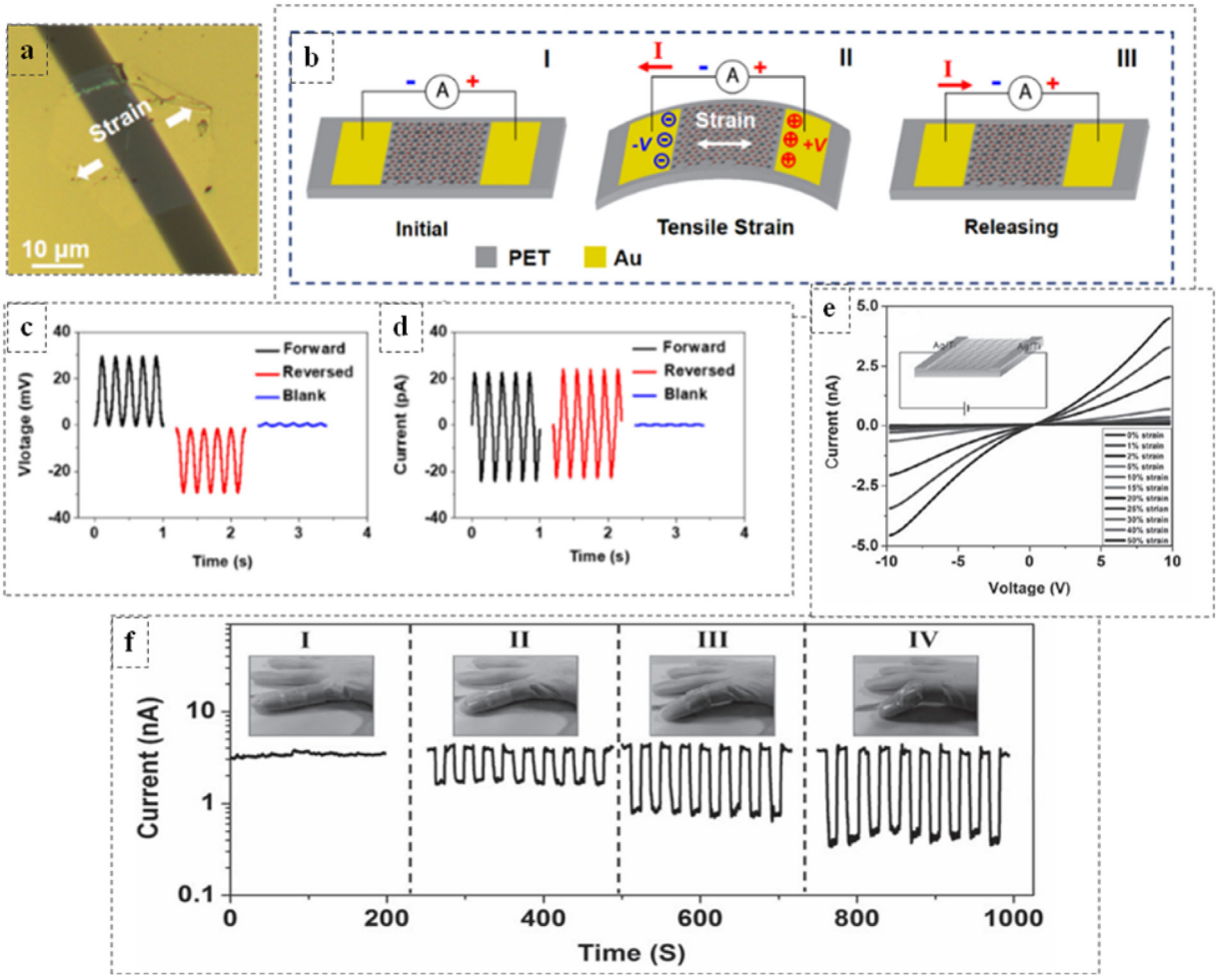

Fig. 12. Some of the newer piezoelectric ceramics, like PbI_2 are also used in developing PENGs. (a) Microscopic image of the PbI_2 based PENG device under strain with two Au contact pads. (b) (i) Schematics depicting the current generation process in PENG device under, I. Unstrained, II. Tensile strain condition, III. Released condition. (c) Voltage output of the PbI_2 based PENG device. (d) Current output of the PbI_2 based PENG device. Reproduced with permission from [14]. Copyright 2018, Elsevier. (e) Current vs Voltage curves for ZnO nanowires-based PENG under different strain conditions. The inset image represents the fabricated PENG device. (f) Current vs time curves for PENG device, fixed at the index finger at different bending motions under a fixed bias voltage of 10 V. Reproduced with permission from [158]. Copyright 2011, John Wiley and Sons.

result, the PENG gets deformed and produces electricity. Fig. 14 (c) shows silicone membrane (SM) frequency separator with a-iPANS, b-iPANS, c-iPANS, present in the apex, intermediate and base regions, respectively, of the frequency separator. PENGs are presented distantly to precisely detect the sound vibrations from the silicone membrane and further deform to produce electricity and the inset depicts the flexibility and mechanical stability of the PENG. The PENG was able to detect displacements of SM by approximately 15 nm and produce voltage output of ~ 55 μV.

5.6. Sensor for human-machine interface (HMI)

Human-machine interface (HMI) enables individuals to interact with a device in various applications related to aviation, military, automotive etc. [174,175]. Deng et al. [176] developed PVDF-ZnO nanofibers-based PENG device for human gesture recognition and thereby, controlling robotic hand for human machine interface application [Fig. 15 (a) (i)]. The nanofibrous film was sandwiched between Mxene electrodes [Fig. 15 (a) ((ii), (iii))]. The nanofibers revealed cow-pea structured morphology [Fig. 15 (a) (iv)]. The PENG was developed to monitor both, bending motion and pressure sensing, and it exhibited both the operations with high sensitivity and exhibited good flexibility, as demonstrated in Fig. 15 (b) (i). The fibrous structure of the film is shown in Fig. 15 (b) (ii) and the cow-pea structure was confirmed through TEM image [Fig. 15 (b) (iii)]. To analyze the electrical parameters and stress distribution theoretically, finite element analyses was performed on this bending motion induced piezoelectric model [Fig. 15 (b) (iv)]. For bending mode, device sensitivity was obtained to be 4.4 mV/deg over a range of 44° to 122° and the response time of 76 ms. While in pressing mode, the device had a sensitivity of 0.33 V/kPa and the response time of 16 ms [Fig. 15 (b) (v)].

Zhou et al. [177] developed a tungsten disulfide nanosheets based PENG for HMI applications [Fig. 15 (c)]. WS_2 nanosheets were prepared by chemical vapor deposition method. It was reported that the device had good strain sensing ability and can be further used to develop gesture recognizing systems. The device produced a power of 6 mW/m^2 under 1.56 % strain condition. The device produces voltage and current of 65 mV and 325 pA, respectively [Fig. 15 ((d), (e))]. The variations in voltage and current output with time for different hand gestures are shown in Fig. 15 [(f) and (g)].

5.7. Cardiac sensor

Cardiac sensors play a vital role in early-stage diagnosis of heart condition [178]. PENGs have the potential to serve as sensors for low-powered bioelectronic devices [179]. Kim et al. [5] developed

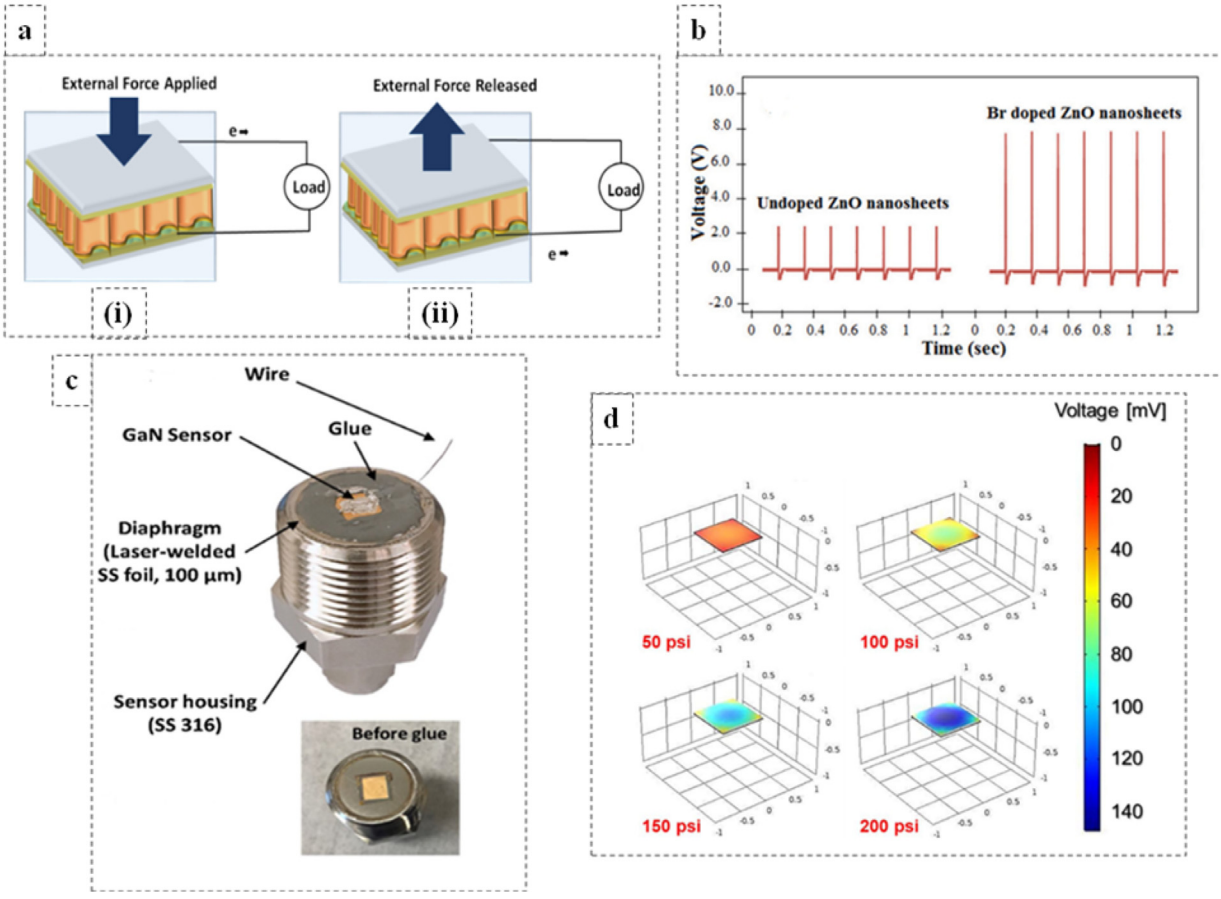

Fig. 13. Doped ZnO is also used in PENG. (a) Working mechanism of Br-doped ZnO PENG (i) during application of force, electrons move towards bottom electrode and (ii) When the applied force is released, electrons move back to positive electrode. (b) Voltage output in undoped ZnO and Br-doped ZnO PENG device. Reproduced with permission from [161]. Copyright 2021, Elsevier. (c) Schematic photograph of the sensor housing with diaphragm with a sensing element at the top before and after glue. (d) Simulated voltage output profiles at 50, 100, 150, 200 psi. Reproduced with permission from [162]. Copyright 2020, Elsevier.

0.5 mol% Mn-doped PMN-PZT PENG as a cardiac sensor with a bending stiffness of 9.95 × 10^{-5} Nm, good flexibility and durability [Fig. 16 (a)]. The inset of [Fig. 16 (a)] shows the SEM image of single crystalline PMN-PZT, which is transferred to the PET substrate without any cracks, fracture or waviness. Fig. 16 (b) schematically illustrates the cardiac sensing activity via wireless communication system. The sensor was implanted to the heart of porcine model with a stitch at each corner between right ventricle and left ventricular apex [Fig. 16 (c)]. The highest vibratory motion from the PENG was observed when it was placed in-between the apex of right and left ventricles. The PENG produces voltage and current outputs of 40 V and 4.5 µA, respectively, under mechanical unbending and bending at a bending radius of 2 cm and frequency of 0.4 Hz [Fig. 16 (d)]. During the heart's contraction and relaxation movements, the device produced a voltage and current of 17.8 V and 1.75 µA, respectively [Fig. 16 (d)]. As depicted in Fig. 16 (e), the voltage and current peaks are synchronized with the QRS peaks of the electrocardiogram (ECG) at different heart beating frequencies (i.e., 1.7, 2.7, and 5.3 Hz). This indicates that the produced (*in vivo*) voltage can control the frequency of the heartbeat.

5.8. Self-powered pacemakers

Cardiac pacemakers are used for the treatment of arrhythmia. These pacemakers use electrochemical batteries, which have short life span (6-7 years) and consequently, such replacements lead to repetitive surgeries and associated clinical complications, such as inflammation, infection etc [180–183]. PENGs have the potential to extract energy from heart's vibratory motions to develop self-powered pacemaker [184]. Hwang et al. [4] developed PMN-PT thin film-based PENG for self-powered pacemaker application. The developed PENG had good flexibility, required for energy conversion from the movements of soft organs [Fig. 17 (a)]. The PMN-PT based PENG was linked to the stimulation electrodes to provide electrical stimulation to the anesthetized rat's heart [Fig. 17 (b)]. The ECG amplitudes of rat, presented in Fig. 17 (c), along with the P wave, Q wave, and QRS complex with an inset, showing a heart rate of 6 beats per second. Fig. 17 (d) shows the spike peaks on a rat's normal heartbeat in the ECG via stimulation, produced by the periodic bending and unbending movements of the PENG. In this case, the PENG generates the voltage and current of 8.2 V and 145 µA, respectively.

Similarly, Azimi et al. [185] developed P(VDF-TrFE) thin films with ZnO nanofillers based PENG device for self-powered pacemaker. The PENG device was implanted in a large animal model (dog) [Fig. 17 ((e), (f))]. Evidently in Fig. 17 (g), the output electrical parameters of the implanted PENG did not interfere with the normal cardiophysiology, as a normal ECG was obtained after implantation. The *in vivo* voltage and current, generated by the PENG were 3.90 ± 0.65 V and 2.33 ± 0.62 µA, respectively. Xu et al. [186] incorporated ZnO nanoparticles and MWCNTs in P(VDF-TrFE) films to develop a PENG device for energy harvesting from heartbeat motions. The device produces a voltage output of 3.22±0.24 V. Furthermore, PDMS was introduced into the polymer matrix to fill the pores, which increased the voltage output by 105%.

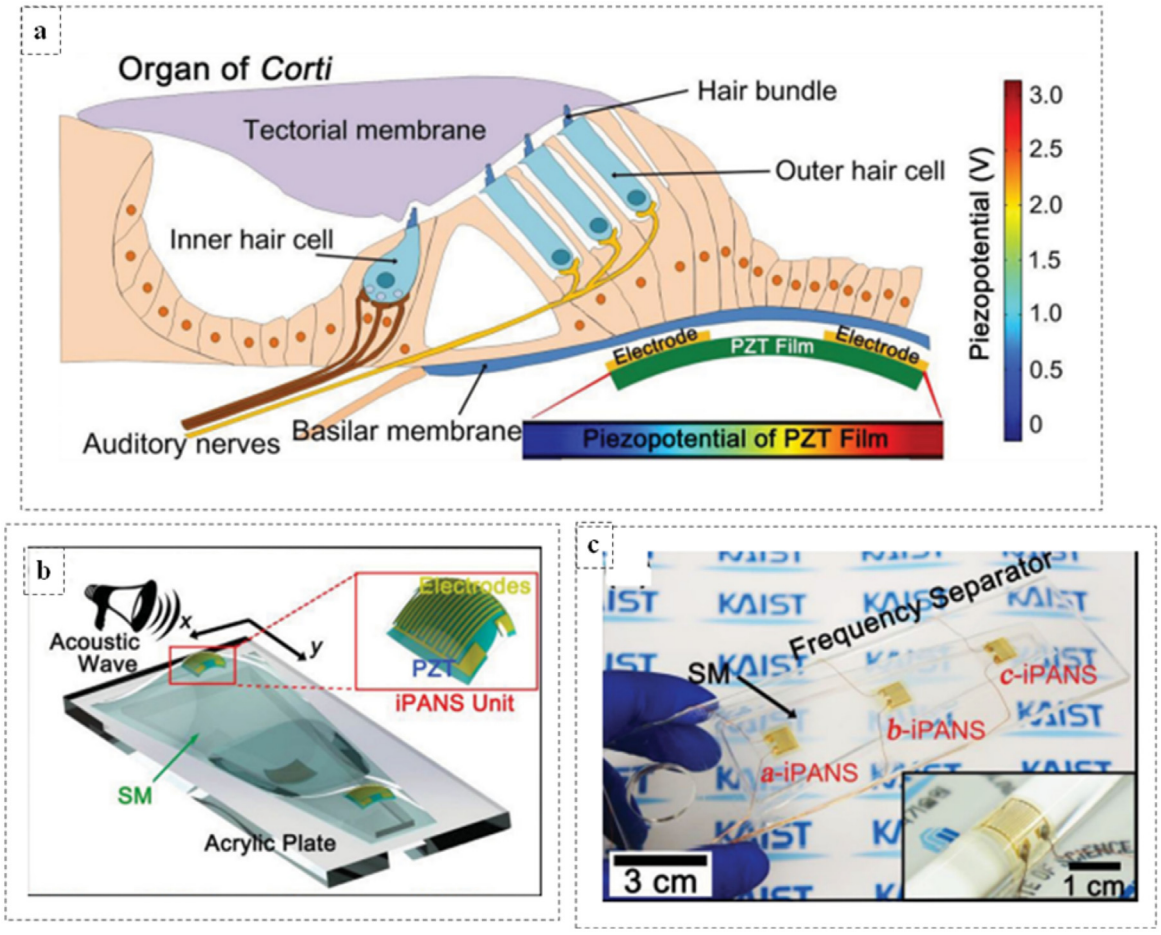

Fig. 14. PENG as acoustic sensor for biomimetic artificial hair cells. (a) Schematics of organ of *Corti* in mammalian cochlea. PZT based PENG placed below the basilar membrane which is bent upwards at a height of 600 nm and generated a potential of 3 V. (b) Acoustic waves falling on the frequency separator, containing silicone membrane (SM) covering an acrylic plate with a trapezoidal slit. The SM vibrates and causes the PENG to deform and produce electricity. The inset image shows the PZT thin film nanogenerator. (c) Photograph of the PENGs (a-iPANS, b-iPANS, c-iPANS) distantly placed on the frequency separator. The inset image represents the PENG, adhered to the glass rod having curvature radius of 1 cm, revealing the flexibility and mechanical stability. Reproduced with permission from [173]. Copyright 2014, John Wiley and Sons. [iPANS- inorganic based Piezoelectric Acoustic Nanosensor, SM- Silicone Membrane].

5.9. Deep brain stimulation (DBS)

Many patients worldwide suffer from certain brain disorders such as parkinson, psychiatric disorders, epilepsy, depression, tremor etc. [187,188]. The application of properly tuned electrical stimulation in the affected regions of the brain can heal the disorders [189]. Commercially available neurostimulators require battery replacements at regular intervals (3-5 years), which results in repetitive surgeries that may cause post-operative complications. In order to address such concern, the development of self-powered deep brain stimulators gained remarkable attention. Hwang et al. [18] developed PIMNT thin film-based PENG for deep brain stimulation. The flexible thin film was developed on a plastic substrate, as shown in Fig. 18 (a). The energy harvesting ability was measured by bending the device [Fig. 18 (b) ((i)–(iii))]. The deep brain stimulation (DBS) electrode was placed at M1 cortex of mouse's brain. Stimulation of left motor cortex, which control the movements of contralateral body, resulted in paw movements which were tracked and recorded [Fig. 18 (c)]. The energy was supplied by the PENG under cyclic bending and unbending motions. The PENG device produces the maximum voltage output and current to be 11 V and 283 μA, respectively [Fig. 18 ((d), (e))]. The developed PENG exhibited good piezoelectric characteristics along with flexibility and durability.

5.10. Drug delivery

The advancement in drug delivery methodologies is in continuous thrust to enhance effectiveness and efficiency in targeted as well as controlled release of therapeutics. Recently, PENG devices are recognized for their potentiality in effective and efficient drug delivery systems. Yang et al. [19] developed a transdermal drug delivery system, based on self-powered PENG and microneedles patch, for the treatment of psoriasis [Fig. 19 (a)]. Microneedles are used for delivery of drugs into the epidermis. The system was designed such that the release of drugs can be controlled by the patient and it can be applied anywhere on the skin [Fig. 19 (b)]. The controlled release of drug is based on the fact that by slapping or bending the drug delivery device, electrical signals are generated, and the microneedles patch releases the drug into the dermis. The PENG was based on piezoelectric PVDF and microneedles patch containing two layers. One was polylactic acid-gold-polypyrrole (PLA-Au-PPy) microneedle array loaded Dex (working electrode) and another PLA-Au microneedle array loaded dex (counter electrode). The voltage and current produced by PENG were ~ 100 V and 2 μA, respectively, and charge storing capability of the device was 300 nC [Fig. 19 ((c), (d))].

Jariwala et al. [190] developed P(VDF-TrFE) and PVDF based PENGs for drug delivery system. The PENG was composed of

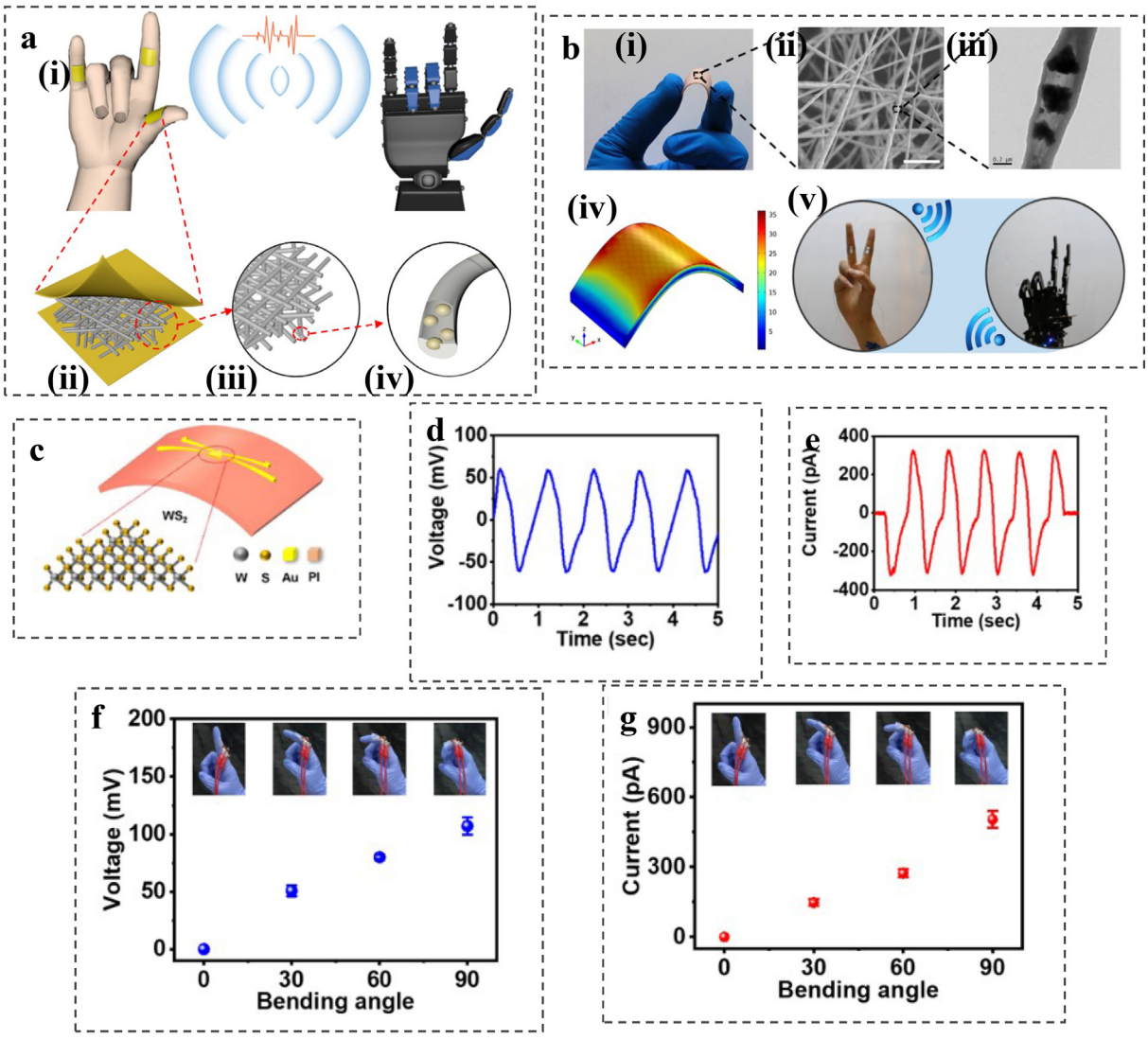

Fig. 15. Organic-inorganic hybrid composites, like PVDF-ZnO are also used in developing PENGs. Application of PENGs in HMI. (a) (i-ii) PVDF-ZnO PENG, (iii) Nanofibrous film, (iv) Single nanofiber. (b) (i) PENG under bending, (ii) SEM micrograph of the nanofibers, (iii) TEM image of single nanofiber, (iv) Finite element simulation of the piezoelectric film under bending, (v) PENG worn on human finger to control gestures of robotic hand. Reproduced with permission from [176]. Copyright 2019, Elsevier. (c) Tungsten nanosheet based PENG. (d) Output voltage of tungsten nanosheet based PENG. (e) Output current for tungsten-based PENG. (f) Output voltage corresponding to different bending angles. (g) Output current corresponding to different bending angles. Reproduced with permission from [177]. Copyright 2022, Elsevier.

nanofibrous membranes, developed using electrospinning. For the *in vitro* test, the membranes of size 1×1 cm^2 were loaded with 750 µg of crystal violet and were enclosed between two layers of drug capturing films, i.e., nitrocellulose and were pre-wetted with phosphate buffer saline (PBS). They were further enclosed inside two layers of PDMS, acting as buffer pads under applied perturbations. Shockwaves were further given to these pads to generate the effect of piezoelectricity and thereby, the drug release was ensured. The mechanical stimulations change the surface polarity of nanofibers (negative to positive), which induce the release of drugs, adhered on the surface [Fig. 19 (e)]. The release of drug was optically quantified and tested in 3D, by encapsulating the individually loaded membranes inside hydrogel and shockwaves were given [Fig. 19 (f) ((i), (ii))]. The drug release was also quantified on skin of porcine model, *ex-vivo* [Fig. 19 (g)].

5.11. Tissue regeneration/wound healing

Electrical stimulation can be a useful tool in promoting the healing and regeneration of injured tissue. The cellular activity can be modulated by electrical stimulation in a way to support the repair process. The applied electrical stimulation accelerates cell proliferation and differentiation that leads to development of new tissues [191–197]. Scaffolds, based on piezoelectric materials, can generate surface charges upon mechanical deformation which can actively transform as a tissue construct [198].

When bone tissue is deformed under stress, it generates bioelectrical signals, which are responsible for its remodeling. As the piezoelectricity is an inherent property of bone and therefore, piezoelectric materials have the potential to act as apt grafts for bone tissue engineering [199–202]. Szewczyk et al. [203] developed PVDF nanofibers-based PENG for bone tissue construct. Two types of scaffolds were designated to use as a construct, one with positive charges on surface and another with negative charges. The bone mineralization and cellular response was found to be maximum for negatively charged surfaces with a potential of - 95 mV. Zhang et al. [204] reported PVDF film-based PENG and fixation splint for fracture repair of bone [Fig. 20 (a) (i)]. The PENG device produces a voltage and current output of 78 V and 20 µA, respectively. The current, from the PENG, induced proliferation of

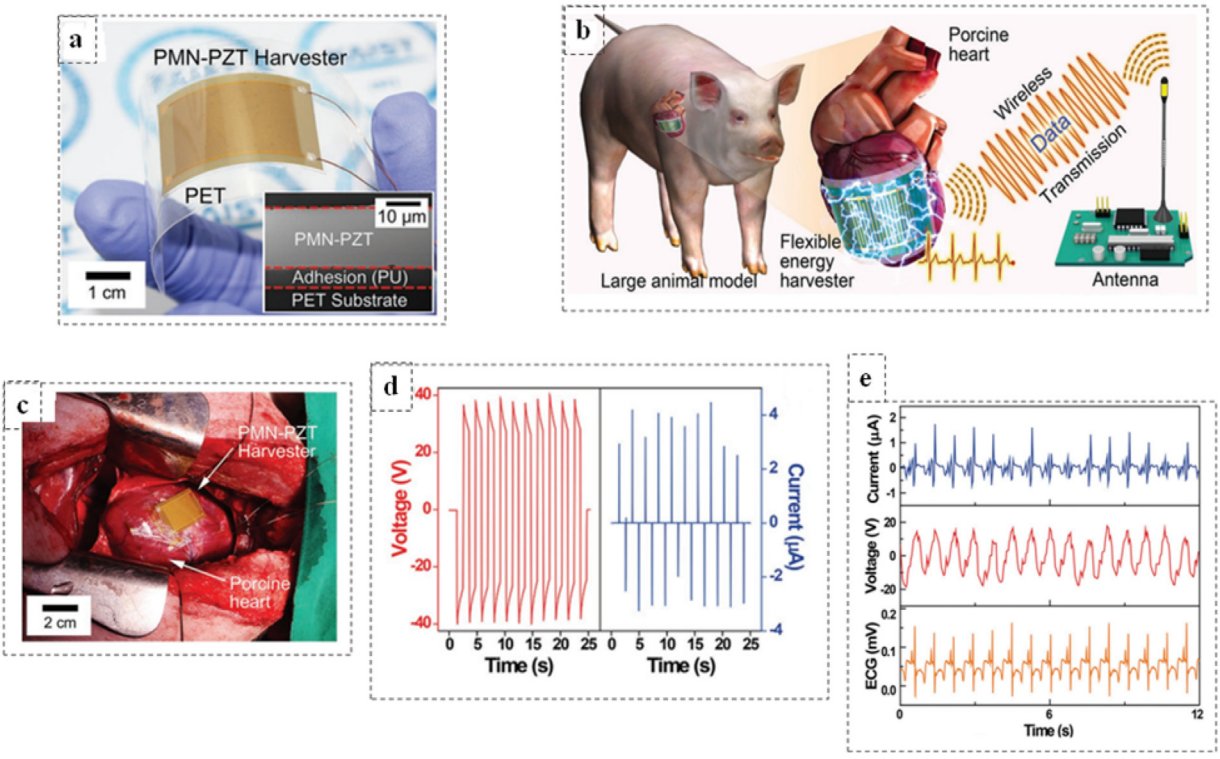

Fig. 16. PENGs are also used in flexible bioelectronic medicine applications. (a) Photograph showing flexibility of PMN-PZT-Mn based PENG device. The inset shows the SEM image of PMN-PZT-Mn thin film on PET substrate. (b) Schematic of self-powered cardiac sensor. The data, generated (piezoelectric potentials) from gradual contraction and relaxation activities of heart can be transferred via wireless communication system for cardiovascular system monitoring. (c) Photograph of PENG device attached to the heart of a porcine model between right ventricle and left ventricular apex. (d) Output voltage and current variation with time of the PENG device. (e) *In vivo* output voltage and current variation with time of PENG device attached to the porcine heart along with the simultaneously recorded ECG. Reproduced with permission from [5]. Copyright 2017, John Wiley and Sons.

pre-osteoblasts (MC3T3-E1) and increased the intracellular calcium ions [Fig. 20 (a) (ii)]. Alongside, the alkaline phosphatase activity was also increased under the pulsed DC stimulation. Overall, the PVDF film-based PENG device served as a pulsed DC stimulator to repair bone fracture, that induced significant osteogenesis. Surface-charge induced biodegradable nanofibers are quite popular to restore intracellular activities by providing electrical stimulations, while self-degrading themselves over time, till complete restoration. Das et al. [205] developed ultrasound driven PLLA nanofibers-based PENG to serve as a bone scaffold. Non-invasive ultrasound was used to generate surface charges on the implanted piezoelectric scaffold to provide electrical stimulation to regenerate defect in calvarial bone tissue.

In cardiovascular tissues, cardiomyocytes are electrically conductive. The contraction and relaxation behavior of the heart is controlled by bio-electrical signals. The electrical activities of cardiomyocytes are controlled by action potentials. Myocardial infarction, or injured heart muscles, causes the remodeling of tissues, which produces new tissues that are not only non-conductive but also non-functional, as a result of which, nutrients and oxygen supply reduces [206–209]. Piezoelectric materials can be active substitutes towards cardiac tissue engineering by generating functional implant [210–214]. Wang et al. [215] developed cell-laden polyaniline (PANI) blended PLLA nanofibrous sheets-based PENG for cardiac tissue engineering. The fabricated scaffold was observed to be conductive in nature and showed H9c2 cardiomyoblasts differentiation with improved cell viability. The piezoelectric nanosheets allowed cell to cell interaction, improved maturation and fusion index. Moreover, these PLLA/PANI electrospun nanofibrous sheets mimic the extracellular matrix of myocardium. Arumugam et al. [216] developed PVDF/HAp/TiO_2 electrospun nanofibrous patch-based PENG for the treatment of damaged tissue of heart muscles. Cardiomyocytes, seeded on nanofiber scaffold adhered, differentiated and enabled vascularization. β-phase of PVDF based scaffolds has been suggested to replace damaged/scar tissues of the heart [Fig. 20 (b)]. Similarly, Adadi et al. [217] developed P(VDF-TrFE) electrospun nanofibers-based PENG for cardiac tissue engineering and those scaffolds supported the differentiation of stem cells into cardiomyocytes.

Peripheral nerve injuries occur due to trauma, genetic factors and immune diseases etc. The damaged peripheral nerves can result in defects that disrupt the connectivity of neurons and tissues. To address this issue, tubular nerve guidance conduits are used to provide electrical stimulation and structural and biochemical support. These conduits are typically connected to the injured ends of neurons to treat the defects [218–221]. Electric field stimulations allow the motor and axon growth across the injured sites. During regeneration of the injured nerve system, the electrical stimulations induce the Schwann cells, which allow fast nerve reinnervation [222–224]. PENGs are more suitable for providing these electrical stimulations and therefore, PENGs are suggested as potential device for peripheral nerve regeneration. Mao et al. [225] developed polycaprolactone (PCL) based PENG for peripheral nerve tissue regeneration. The nanofibrous mat based PENG was implanted at the sciatic nerve defect in a rat model. It has been reported that the electrical stimulations, provided by the implant regenerated the nerve defects within just 4 weeks. The PENG produces the highest voltage of upto 120 mV, as shown in Fig. 20 (c).

Similarly, Evans et al. [226] developed PLLA nerve guidance conduit-based PENG for peripheral nerve regeneration. The conduit-based PENG was fabricated using extrusion technique with inner and outer diameters of 1.6 and 3.2 mm, respectively, which

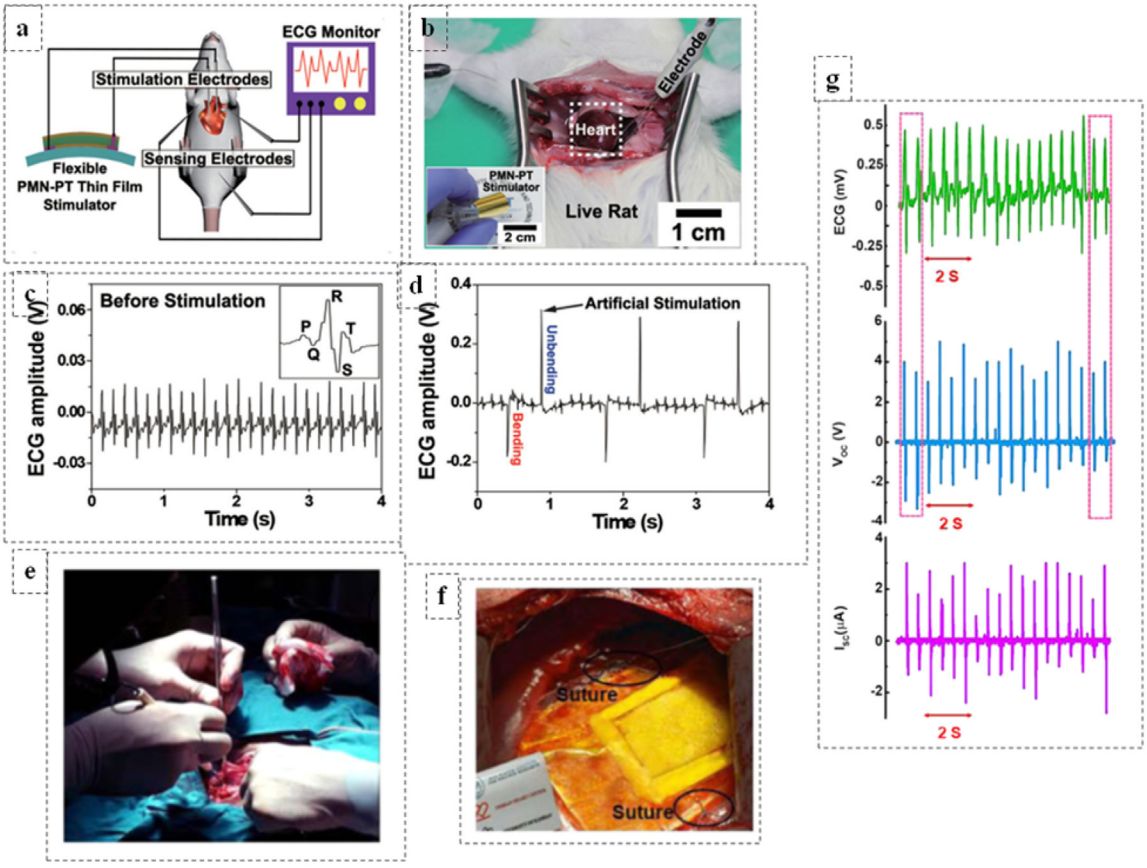

Fig. 17. One of the potential clinical applications of PENG in cardiac pacemaker. (a) Schematic of self-powered cardiac pacemaker based on PMN-PT PENG. (b) Photograph showing an experiment conducted on a living rat model, demonstrating the stimulation of the heart using PENG (PMN-PT Stimulator). The inset shows the PMN-PT based PENG device. (c) ECG of the living rat before stimulation. The inset shows the magnified image of heartbeats of rat containing P wave, T wave and QRS complex (ECG). (d) Artificial peaks in the ECG from the stimulation of rat's heart by periodic bending and unbending of the PENG device. Reproduced with permission from [4]. Copyright 2014, John Wiley and Sons. (e) Surgical process of implantation of PENG in a dog model. (f) PENG sutured to the lateral wall of left ventricle of heart in a dog model. (g) *In vivo* output voltage and current of P(VDF-TrFE)-ZnO based PENG in synchronous with ECG. Reproduced with permission from [185]. Copyright 2021, Elsevier.

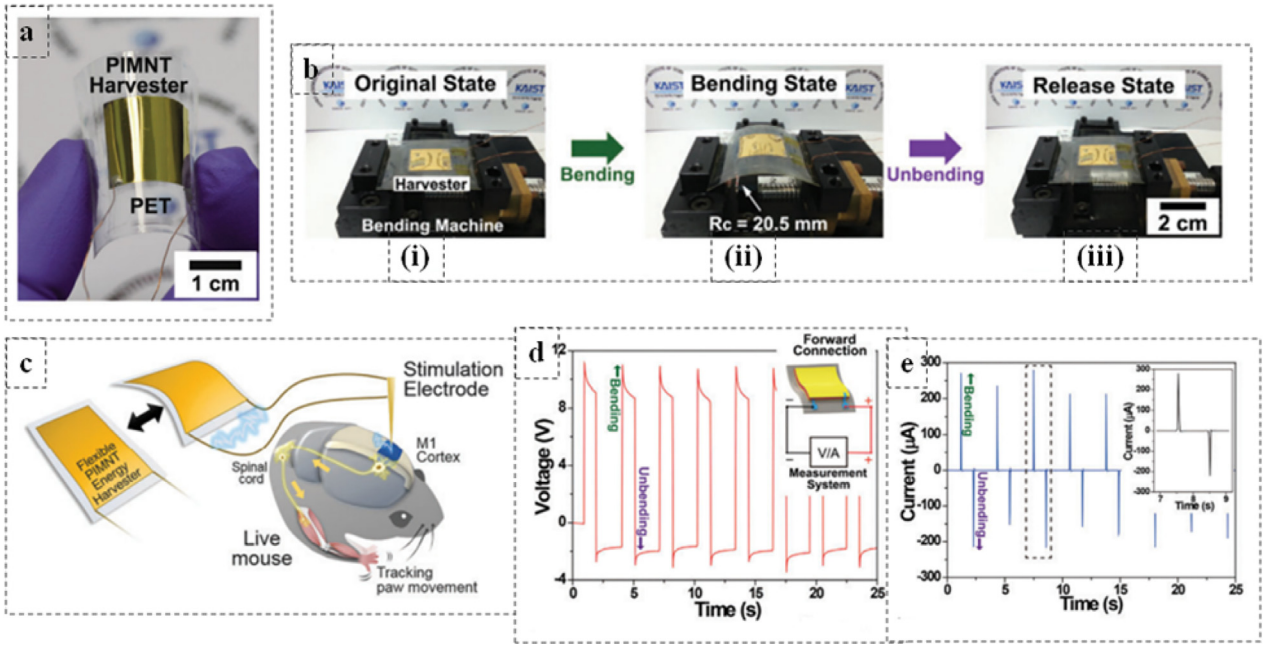

Fig. 18. Another potential clinical application of PENG is Deep Brain Stimulation (DBS). (a) Photograph of PIMNT based PENG device bent by human fingers. (b) PENG device under (i) Original, (ii) Bending and (iii) Released states. (c) Schematic illustration of deep brain stimulation in a mouse model using a stimulation electrode, attached at the M1 cortex. The PENG provides electrical currents to the electrode to stimulate the brain. (d) Voltage output during bending and unbending. (e) Output current during bending and unbending. Reproduced with permission from [18]. Copyright 2015, Royal Society of Chemistry.

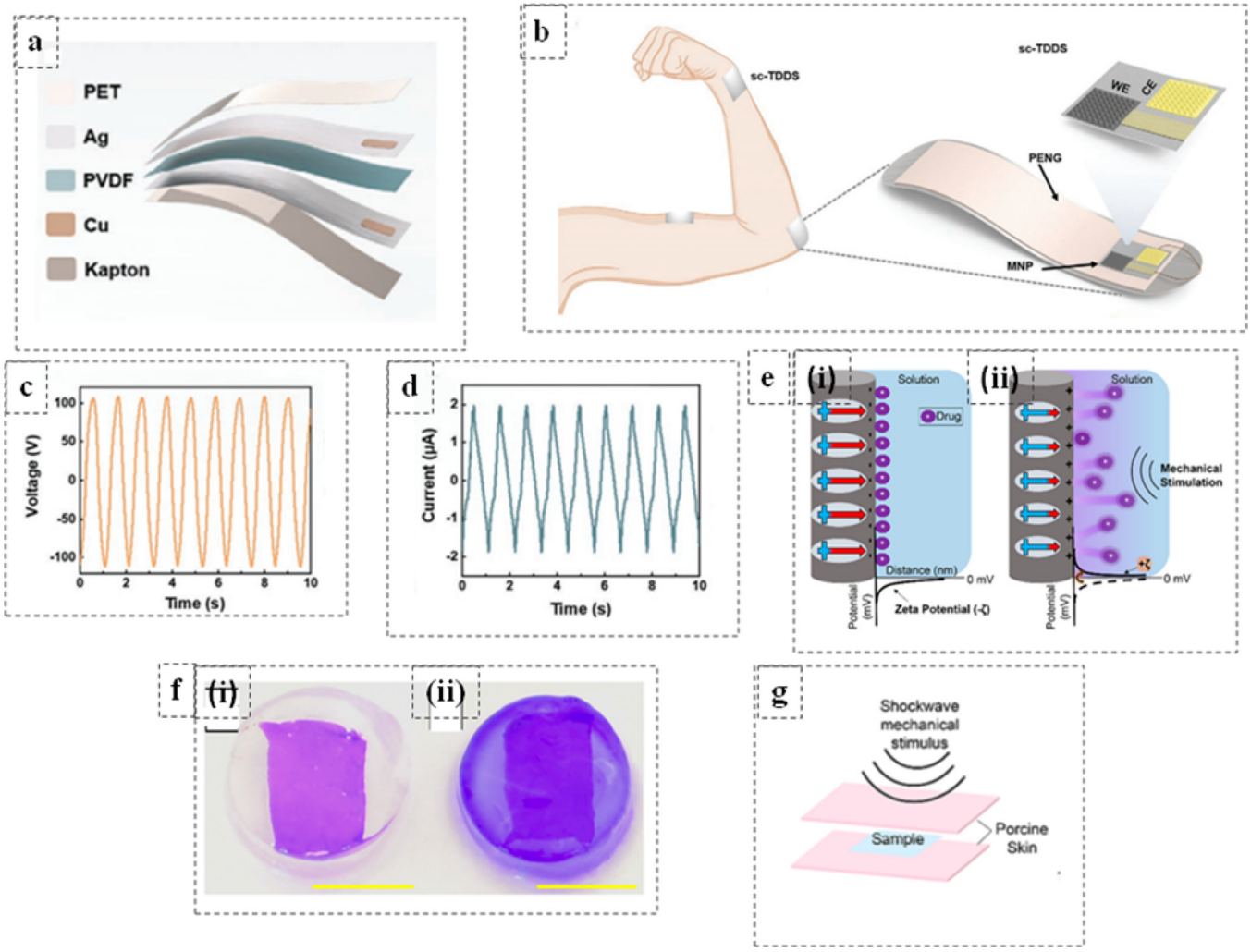

Fig. 19. PENGs can be used for targeted drug delivery applications. (a) PVDF based PENG containing multiple layers along with encapsulation layers. (b) Transdermal drug delivery system containing PENG and microneedles patch (MNP). (c) Voltage output of the PVDF based PENG. (d) Current output of the PENG. (e) Drug delivery based on mechanical stimuli response. (i) The piezoelectric dipoles of P(VDF-TrFE) in static state and in association with the negative zeta potential at the surface of nanofibers, attracting the cationic molecules of drug. (ii) There is change in the polarity of the dipoles towards positive values due to mechanical stimulation that overcomes the negative zeta potential which subsequently, repel the drug molecules away from the surface. Reproduced with permission from [19]. Copyright 2021, John Wiley and Sons. (f) Optical images of hydrogel plug having drug loaded P(VDF-TrFE) membrane (i) Prior to application of mechanical stimulation by shockwaves, (ii) After application of mechanical stimulation by shockwaves. (g) Schematic illustration of *ex-vivo* setup for simulation and quantification of release of drugs into soft tissues upon application of mechanical stimulation by shockwaves. Reproduced with permission from [190]. Copyright 2021, American Chemical Society. [sc-TDDS: self-powered Controllable Drug Delivery System, WE: Working Electrode, CE- Counter Electrode].

has a length of 12 mm. It had a porous structure with a porosity of 83.5% and mean pore size of 12.1 μm. The conduits were implanted at the right sciatic nerve defect in a rat model via microsurgery. For 16 weeks, walking track analysis was done. It has been revealed that PLLA based conduits served as suitable scaffold for peripheral nerve tissue regeneration.

6. Summary and future scope

A critical review of working mechanisms of piezoelectric energy harvesting, piezoelectric materials and applications of piezoelectric nanogenerators has been presented in this article. The concept of piezoelectricity has made a significant impact on the energy sector based on the energy conversion mechanism. This review article is mainly focused on development of PENGs for wearable and implantable bioelectronics for numerous biomedical applications. Piezoelectric organic polymers provide flexibility and stretchability in flexible bioelectronics, but their limited electro-mechanical energy conversion factor often restricts their performance. To overcome such limitation, piezoceramics are incorporated as fillers in the polymer matrix, thereby creating a biocompatible polymer-ceramic composite with enhanced piezoelectric properties. Such composites have good potential for applications in flexible bioelectronics, such as wearable and implantable devices for healthcare monitoring, human-machine interfaces, and energy harvesting. The combination of polymer flexibility and the improved piezoelectric behavior opens up new possibilities to advance bioelectronic systems. PVDF and its copolymers with their moderate piezoelectric characters and extensive flexibility portray the requirement for their use in piezoelectric energy harvesting. They are often incorporated with high piezoelectric constant ceramics such as KNN, BT etc. Apart from the artificially synthesized piezoelectric materials, some of the naturally occurring piezoelectric materials like the bio-wastes (onion skin, egg shell membrane, fish swim bladder etc.) can be of greater interests to develop cost-effective energy harvesting technology. Also, sensors, used for various applications like, tactile sensing, pressure sensing, pulse sensing etc. can also be made self-powered.

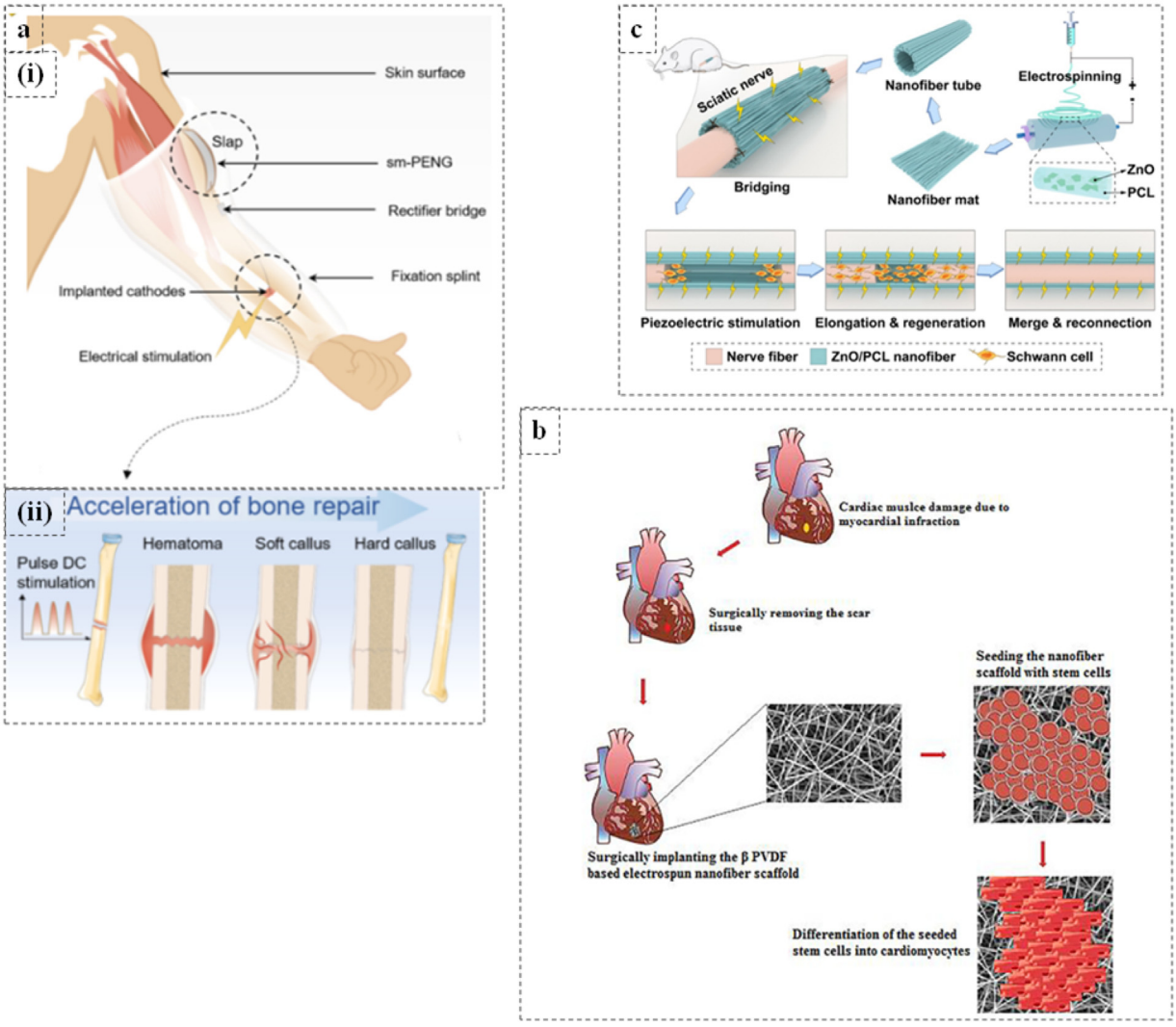

Fig. 20. Another clinically relevant application domain for PENGs is the tissue engineering. (a) (i) PVDF based PENG for bone tissue regeneration along with fixation splint, (ii) Pulse electric stimulation assisted accelerated bone growth. Reproduced with permission from [204]. Copyright 2021, Elsevier. (b) Schematic illustration of cardiac tissue regeneration using PVDF/HAp/TiO_2 based PENG. Removal of the scar, followed by implantation of cardiac patch. The stem cells being seeded on the implanted cardiac patch. Differentiation of the stem cells into cardiomyocytes. Reproduced with permission from [216]. Copyright 2019, Elsevier. (c) Schematic illustration of peripheral nerve tissue regeneration using PCL/ZnO based tubular PENG. Formation of electrospun nanofiberous mat, rolling of the mat to form a tubular structure PENG, bridging the sciatic nerve for providing electrical stimulations for nerve tissue regeneration. Reproduced with permission from [225]. Copyright 2022, Elsevier.

The development of PENGs necessitates critical consideration of a combination of several factors. These include the careful selection of ceramic and polymeric materials to achieve the desired combination of electro-mechanical response, flexibility, stability, and durability for sustainable energy harvesting. Understanding the correlation is crucial between the device structure and its properties to optimize output characteristics. To this end, the utilization of density functional theory (DFT) and biomolecular simulations can provide theoretical insights for device fabrication and performance optimization [227]. Additionally, special attention must be provided to the interfaces among different materials within the nanogenerator to ensure that the output of device aligns with the specific requirements of biomedical applications. It is essential to achieve the optimal contact between the PENGs and the tissues or organs at the implantation site for harnessing maximum mechanical deformation. This ensures that the PENGs can efficiently utilize the mechanical energy and convert it into electricity. By establishing right interface, the PENGs can effectively capture and transform mechanical deformations into usable electrical power, enhancing their overall functionality and capacity for energy harvesting. Efficient and reliable piezoelectric energy harvesting technology faces challenges in power output, recording sensitivity, motion detection, breakdown strength, manufacturing complexity, electrical polarization, energy conversion efficiency, stability, durability, and heat/moisture management. Such challenges should be appropriately addressed for the successful development of PENGs [228].

The fabrication of piezoelectric nanogenerators through additive manufacturing processes (inkjet printing, screen printing, or 3D printing) involving layer-by-layer deposition has been pursued in last one decade, to achieve precise and scalable production. This approach allows the controlled and customizable fabrication of these devices [22,79,156]. The additive nature of printing enables the creation of intricate and customized shapes, facilitating the integration of sensors, electrodes, and other components into a single device. This adaptability allows the development of wearable bioelectronics that conform to the human body for comfortable usage.

At the close, it needs to be reiterated that the PENGs to be used for wearable bioelectronics does not need to go through

the assessment of the entire biocompatibility spectrum. However, PENGs to be used as implanted biomedical devices need to critically pass through all the biocompatibility profile testing and regulatory clearances. As mentioned in this review, most of the hybrid PENGs, developed using organic and inorganic materials have been tested at the lab-scale with miniature prototypes and in most of the cases, they have either not been tested or their foreign body response has not been investigated using animal models. There are also few examples where, self-powered pacemakers have been investigated in dog model [185]. However, such studies in the large animal models need to be conducted in future before realizing the clinical potential of PENGs for specific applications. Such study should also focus on the analysis of the functional outcomes of the PENGs in those targeted applications. For example, if PENGs are to be used for cardiovascular applications then cardiac response functions or electrocardiogram (ECG) is to be recorded. If it is for neuro-surgical applications, then several neurological functionalities are to be evaluated using animal model studies. After obtaining necessary regulatory clearances, these devices are to be further tested in human clinical studies [229]. The final hurdle to overcome would be to obtain FDA clearances for many of these PENGs which are being developed globally.

It is perceived that the nature-inspired PENGs perhaps would have better biocompatibility than synthetic materials based PENGs. Also, the regulatory clearances would be perhaps easier for nature-inspired PENGs than for synthetic materials based PENGs.

Data science has emerged as one of the important research themes across several engineering disciplines in last one decade [230]. In the context of PENGs, it would be interesting to apply machine learning and deep learning-based algorithms to develop predictive capability of output current and voltage by varying the material compositions, used in PENG devices. Moreover, the integration of PENGs with Internet of Things (IoT), machine learning, and artificial intelligence (AI) technologies enables real-time monitoring and comprehensive analysis of device usage. This data can be shared with healthcare agencies, doctors, and hospitals, facilitating a more informed and collaborative approach to patient care. The combination of PENGs, IoT, machine learning, and AI holds immense potential for transforming healthcare. These advancements can revolutionize diagnostics and improve patient care, thereby contributing to public healthcare. To substantiate further, this review has extensively emphasized the design of several new hybrid material compositions, used in a number of PENG devices. This requires the optimization of the combination of the organic and inorganic phases with specific piezoelectric properties. The idea to adapt data science approaches to see, based on the input parameters (material compositions or piezoelectric strain coefficients), whether, one can predict that what would be the output voltage or current for a given PENG device. This would accelerate the discovery of PENG device and also reduce the time, research cost in terms of reduced number of experiments to be conducted to develop PENGs for clinical applications.

At the closure, the discussion in this review paper indicates the futuristic growth of the field of PENGs clearly needs the large collaboration among the biomaterials scientists, physicists, chemists, data scientists, biologists and clinicians. More quantitative approaches are needed to develop mechanistic insights into the correlation among the functional properties of the materials and the device performance. This together with the predictive capability using AI/ML approaches will certainly accelerate the discovery of the next generation of PENGs.

Declaration of Competing Interest

This is to confirm that there is no conflict of interest to declare.

Acknowledgements

One of the authors, BB acknowledges the financial support received from the Abdul Kalam technology Innovation Fellowship of the Indian National Academy of Engineering-Department of Science and Technology, Government of India. Both BB and AKD thank the Scheme for Promotion of Academic and Research Collaboration (SPARC), an initiative of Ministry of Human Resource Development, Government of India for financial support through the project 'Electrical stimulation with electroactive biomaterials as therapeutic strategy for intractable bone and neurodegenerative diseases'. AKD also acknowledges the financial support from CST, Govt. of Uttar Pradesh.

References

[1] N. Sezer, M. Koç, A comprehensive review on the state-of-the-art of piezoelectric energy harvesting, Nano Energy 80 (2021) 105567.
[2] F. Ali, W. Raza, X. Li, H. Gul, K.H. Kim, Piezoelectric energy harvesters for biomedical applications, Nano Energy 57 (2019) 879–902.
[3] M.A. Wood, K.A. Ellenbogen, Cardiology patient pages. Cardiac pacemakers from the patient's perspective, Circulation 105 (18) (2002) 2136–2138.
[4] G.T. Hwang, H. Park, J.H. Lee, S. Oh, K.I. Park, M. Byun, H. Park, G. Ahn, C.K. Jeong, K. No, H. Kwon, S.G. Lee, B. Joung, K.J. Lee, Self-powered cardiac pacemaker enabled by flexible single crystalline PMN-PT piezoelectric energy harvester, Adv. Mater. 26 (28) (2014) 4880–4887.
[5] D.H. Kim, H.J. Shin, H. Lee, C.K. Jeong, H. Park, G.T. Hwang, H.Y. Lee, D.J. Joe, J.H. Han, S.H. Lee, J. Kim, B. Joung, K.J. Lee, *In vivo* self-powered wireless transmission using biocompatible flexible energy harvesters, Adv. Funct. Mater. 27 (25) (2017) 1700341.
[6] M.J. Wilhelm, C. Schmid, D. Hammel, S. Kerber, H.M. Loick, M. Herrmann, H.H. Scheld, Cardiac pacemaker infection: surgical management with and without extracorporeal circulation, Ann. Thorac. Surg. 64 (6) (1997) 1707–1712.
[7] M.H. Kabir, E. Marquez, G. Djokoto, M. Parker, T. Weinstein, W. Ghann, J. Uddin, M.M. Ali, M.M. Alam, M. Thompson, A.S. Poyraz, H.Z. Msimanga, M.M. Rahman, M. Rulison, J. Cramer, Energy harvesting by mesoporous reduced graphene oxide enhanced the mediator-free glucose-powered enzymatic biofuel cell for biomedical applications, ACS Appl. Mater. Interfaces 14 (21) (2022) 24229–24244.
[8] P.P. Mercier, A.C. Lysaght, S. Bandyopadhyay, A.P. Chandrakasan, K.M. Stankovic, Energy extraction from the biologic battery in the inner ear, Nat. Biotechnol. 30 (12) (2012) 1240–1243.
[9] J. Selvarathinam, A. Anpalagan, Energy harvesting from the human body for biomedical applications, IEEE Potentials 35 (6) (2016) 6–12.
[10] Z. Yang, S. Zhou, J. Zu, D. Inman, High-performance piezoelectric energy harvesters and their applications, Joule 2 (4) (2018) 642–697.
[11] J. Chen, Z.L. Wang, Reviving vibration energy harvesting and self-powered sensing by a triboelectric nanogenerator, Joule 1 (3) (2017) 480–521.
[12] Z. Wen, H. Guo, Y. Zi, M.H. Yeh, X. Wang, J. Deng, J. Wang, S. Li, C. Hu, L. Zhu, Z.L. Wang, Harvesting broad frequency band blue energy by a triboelectric–electromagnetic hybrid nanogenerator, ACS Nano 10 (7) (2016) 6526–6534.
[13] X. Zhao, Y. Zhou, J. Xu, G. Chen, Y. Fang, T. Tat, X. Xiao, Y. Song, S. Li, J. Chen, Soft fibers with magnetoelasticity for wearable electronics, Nat. Commun. 12 (1) (2021) 6755.
[14] H. Song, I. Karakurt, M. Wei, N. Liu, Y. Chu, J. Zhong, L. Lin, Lead iodide nanosheets for piezoelectric energy conversion and strain sensing, Nano Energy 49 (2018) 7–13.
[15] H. Ouyang, Z. Liu, N. Li, B. Shi, Y. Zou, F. Xie, Y. Ma, Z. Li, H. Li, Q. Zheng, X. Qu, Y. Fan, Z.L. Wang, H. Zhang, Z. Li, Symbiotic cardiac pacemaker, Nat. Commun. 10 (1) (2019) 1821.
[16] M. Jakobs, A. Fomenko, A. Lozano, K. Kiening, Cellular, molecular and clinical mechanisms of action of deep brain stimulation-a systematic review on established indications and outlook on future developments, EMBO Mol. Med. 11 (4) (2019) 1–18.
[17] S.H. Park, H.B. Lee, S.M. Yeon, J. Park, N.K. Lee, Flexible and stretchable piezoelectric sensor with thickness-tunable configuration of electrospun nanofiber mat and elastomeric substrates, ACS Appl. Mater. Interfaces 8 (37) (2016) 24773–24781.
[18] G. Hwang, Y. Kim, J.H. Lee, S. Oh, C.K. Jeong, D.Y. Park, J. Ryu, S.G. Lee, B. Joung, D. Kim, J. Lee, Self-powered deep brain stimulation via a flexible PIMNT energy harvester, Energy Environ. Sci. 8 (2015) 2677–2684.
[19] Y. Yang, L. Xu, D. Jiang, B.Z. Chen, R. Luo, Z. Liu, X. Qu, C. Wang, Y. Shan, Y. Cui, H. Zheng, Z. Wang, Z.L. Wang, X.D. Guo, Z. Li, Self-powered controllable transdermal drug delivery system, Adv. Funct. Mater. 31 (36) (2021) 2104092.
[20] F.C. Kao, H.H. Ho, P.Y. Chiu, M.K. Hsieh, J.C. Liao, P.L. Lai, Y.F. Huang, M.Y. Dong, T.T. Tsai, Z.H. Lin, Self-assisted wound healing using piezoelectric and triboelectric nanogenerators, Sci. Technol. Adv. Mater. 23 (1) (2022) 1–16.
[21] A. Bagchi, S.R. Meka, B.N. Rao, K. Chatterjee, Perovskite ceramic nanoparticles in polymer composites for augmenting bone tissue regeneration, Nanotechnology 25 (48) (2014) 485101.

[22] X. Zhou, K. Parida, O. Halevi, Y. Liu, J. Xiong, S. Magdassi, P.S. Lee, All 3D-printed stretchable piezoelectric nanogenerator with non-protruding kirigami structure, Nano Energy 72 (2020) 104676.
[23] H. Madinei, H.H. Khodaparast, S. Adhikari, M.I. Friswell, Design of MEMS piezoelectric harvesters with electrostatically adjustable resonance frequency, Mech. Syst. Signal Process. 81 (2016) 360–374.
[24] H. Li, Y. Hao, Z. Lin, X. He, J. Cai, X. Gong, Y. Gu, R. Zhang, H. Cheng, B. Zhang, (K, Na)NbO_3 lead-free piezoceramics prepared by microwave sintering and solvothermal powder synthesis, Solid State Commun. 353 (2022) 114871.
[25] M. Acosta, N. Novak, V. Rojas, S. Patel, R. Vaish, J. Koruza, G.A. Rossetti Jr., J. Rödel, $BaTiO_3$-based piezoelectrics: fundamentals, current status, and perspectives, Appl. Phys. Rev. 4 (4) (2017) 041305.
[26] X. Chen, H. Tian, X. Li, J. Shao, Y.H. Ding, N. An, Y. Zhou, High performance P(VDF-TrFE) nanogenerator with self-connected and vertically integrated fibers by patterned EHD pulling, Nanoscale 7 (2015) 11536–11544.
[27] R. Lay, G. Deijs, J. Malmstrom, The intrinsic piezoelectric properties of materials - a review with a focus on biological materials, RSC Adv. 11 (2021) 30657.
[28] A. Toprak, O. Tigli, Piezoelectric energy harvesting: state-of-the-art and challenges, Appl. Phys. Rev. 1 (3) (2014) 031104.
[29] S. Mishra, L. Unnikrishnan, S.K. Nayak, S. Mohanty, Advances in piezoelectric polymer composites for energy harvesting applications: a systematic review, Macromol. Mater. Eng. 304 (1) (2019) 1800463.
[30] G. Ciofani, A. Menciassi, Piezoelectric Nanomaterials for Biomedical Applications [Electronic Resource], Springer Berlin Heidelberg, Berlin, Heidelberg, 2012 edited by G. Ciofani, A. Menciassi, 1st 2012. ed..
[31] T. Stevenson, D.G. Martin, P.I. Cowin, A. Blumfield, A.J. Bell, T.P. Comyn, P.M. Weaver, Piezoelectric materials for high temperature transducers and actuators, J. Mater. Sci. Mater. Electron. 26 (12) (2015) 9256–9267.
[32] D.M. Shin, S.W. Hong, Y.H. Hwang, Recent advances in organic piezoelectric biomaterials for energy and biomedical applications, Nanomaterials 10 (1) (2020) 123.
[33] B. Zhao, F. Qian, A. Hatfield, L. Zuo, T.B. Xu, A review of piezoelectric footwear energy harvesters: principles, methods, and applications, Sensors 23 (13) (2023) 5841.
[34] R. Caliò, U.B. Rongala, D. Camboni, M. Milazzo, C. Stefanini, G. De Petris, C.M. Oddo, Piezoelectric energy harvesting solutions, Sensors 14 (3) (2014) 4755–4790.
[35] M.M. Yang, Z.D. Luo, Z. Mi, J. Zhao, E. Sharel Pei, M. Alexe, Piezoelectric and pyroelectric effects induced by interface polar symmetry, Nature 584 (7821) (2020) 377–381.
[36] Y. Liu, B. Zhang, W. Xu, A. Haibibu, Z. Han, W. Lu, J. Bernholc, Q. Wang, Chirality-induced relaxor properties in ferroelectric polymers, Nat. Mater. 19 (11) (2020) 1169–1174.
[37] I. Katsouras, K. Asadi, M. Li, T.B. van Driel, K.S. Kjær, D. Zhao, T. Lenz, Y. Gu, P.W.M. Blom, D. Damjanovic, M.M. Nielsen, D.M. de Leeuw, The negative piezoelectric effect of the ferroelectric polymer poly(vinylidene fluoride), Nat. Mater. 15 (1) (2016) 78–84.
[38] Y.C. Liang, Growth and structural characteristics of perovskite–wurtzite oxide ceramics thin films, Ceram. Int. 37 (3) (2011) 791–796.
[39] C.B. Eom, S. Trolier-McKinstry, Thin-film piezoelectric MEMS, MRS Bull. 37 (11) (2012) 1007–1017.
[40] H.S. Kim, J.H. Kim, J. Kim, A review of piezoelectric energy harvesting based on vibration, Int. J. Precis. Eng. Manuf. 12 (6) (2011) 1129–1141.
[41] K.I. Park, C.K. Jeong, N.K. Kim, K.J. Lee, Stretchable piezoelectric nanocomposite generator, Nano Converg. 3 (1) (2016) 12.
[42] R.A. Surmenev, T. Orlova, R.V. Chernozem, A.A. Ivanova, A. Bartasyte, S. Mathur, M.A. Surmeneva, Hybrid lead-free polymer-based nanocomposites with improved piezoelectric response for biomedical energy-harvesting applications: a review, Nano Energy 62 (2019) 475–506.
[43] S. Stassi, V. Cauda, C. Ottone, A. Chiodoni, C.F. Pirri, G. Canavese, Flexible piezoelectric energy nanogenerator based on ZnO nanotubes hosted in a polycarbonate membrane, Nano Energy 13 (2015) 474–481.
[44] J.H. Lee, K. Heo, K. Schulz-Schönhagen, J.H. Lee, M.S. Desai, H.E. Jin, S.W. Lee, Diphenylalanine peptide nanotube energy harvesters, ACS Nano 12 (8) (2018) 8138–8144.
[45] Y.B. Lee, J.K. Han, S. Noothongkaew, S.K. Kim, W. Song, S. Myung, S.S. Lee, J. Lim, S.D. Bu, K.S. An, Toward arbitrary-direction energy harvesting through flexible piezoelectric nanogenerators using perovskite $PbTiO_3$ nanotube arrays, Adv. Mater. 29 (6) (2017) 1604500.
[46] S. Almohammed, A. Thampi, A. Bazaid, F. Zhang, S. Moreno, K. Keogh, M. Minary-Jolandan, J.H. Rice, B.J. Rodriguez, Energy harvesting with peptide nanotube–graphene oxide flexible substrates prepared with electric field and wettability assisted self-assembly, J. Appl. Phys. 128 (11) (2020) 115101.
[47] W.S. Jung, Y.H. Do, M.G. Kang, C.Y. Kang, Energy harvester using PZT nanotubes fabricated by template-assisted method, Curr. Appl. Phys. 13 (2013) S131–S134.
[48] M.S. Al-Ruqeishi, T. Mohiuddin, B. Al-Habsi, F. Al-Ruqeishi, A. Al-Fahdi, A. Al-Khusaibi, Piezoelectric nanogenerator based on ZnO nanorods, Arab. J. Chem. 12 (8) (2019) 5173–5179.
[49] Z. Zhang, Y. Chen, J. Guo, ZnO nanorods patterned-textile using a novel hydrothermal method for sandwich structured-piezoelectric nanogenerator for human energy harvesting, Phys. E Low Dimens. Syst. Nanostruct. 105 (2019) 212–218.
[50] W. Deng, L. Jin, Y. Chen, W. Chu, B. Zhang, H. Sun, D. Xiong, Z. Lv, M. Zhu, W. Yang, An enhanced low-frequency vibration ZnO nanorod-based tuning fork piezoelectric nanogenerator, Nanoscale 10 (2) (2018) 843–847.
[51] B. Moorthy, C. Baek, J.E. Wang, C.K. Jeong, S. Moon, K.I. Park, D.K. Kim, Piezoelectric energy harvesting from a PMN–PT single nanowire, RSC Adv. 7 (1) (2017) 260–265.
[52] D. Godfrey, D. Nirmal, L. Arivazhagan, R. Rathes Kannan, P. Issac Nelson, S. Rajesh, B. Vidhya, N. Mohankumar, A novel ZnPc nanorod derived piezoelectric nanogenerator for energy harvesting, Phys. E Low Dimens. Syst. Nanostruct. 118 (2020) 113931.
[53] M.F. Wasim, S. Tayyaba, M.W. Ashraf, Z. Ahmad, Modeling and piezoelectric analysis of nano energy harvesters, Sensors 20 (14) (2020) 3931.
[54] J. Hao, W. Li, J. Zhai, H. Chen, Progress in high-strain perovskite piezoelectric ceramics, Mater. Sci. Eng. R Rep. 135 (2019) 1–57.
[55] D.F.K. Hennings, C. Metzmacher, B.S. Schreinemacher, Defect chemistry and microstructure of hydrothermal barium titanate, J. Am. Ceram. Soc. 84 (1) (2001) 179–182.
[56] T. Karaki, K. Yan, T. Miyamoto, M. Adachi, Lead-free piezoelectric ceramics with large dielectric and piezoelectric constants manufactured from $BaTiO_3$ nano-powder, Jpn. J. Appl. Phys. 46 (2007) L97–L98.
[57] Y. Zhao, Q. Liao, G. Zhang, Z. Zhang, Q. Liang, X. Liao, Y. Zhang, High output piezoelectric nanocomposite generators composed of oriented BaTiO3 NPs@PVDF, Nano Energy 11 (2015) 719–727.
[58] Z.H. Lin, Y. Yang, J.M. Wu, Y. Liu, F. Zhang, Z.L. Wang, $BaTiO_3$ nanotubes-based flexible and transparent nanogenerators, J. Phys. Chem. Lett. 3 (23) (2012) 3599–3604.
[59] K.I. Park, S. Xu, Y. Liu, G.T. Hwang, S.J. Kang, Z.L. Wang, K.J. Lee, Piezoelectric $BaTiO_3$ thin film nanogenerator on plastic substrates, Nano Lett. 10 (12) (2010) 4939–4943.
[60] C. Luo, S. Hu, M. Xia, P. Li, J. Hu, G. Li, H. Jiang, W. Zhang, A flexible lead-free $BaTiO_3$/PDMS/C composite nanogenerator as a piezoelectric energy harvester, Energy Technol. 6 (5) (2018) 922–927.
[61] K.I. Park, S.B. Bae, S.H. Yang, H.I. Lee, K. Lee, S.J. Lee, Lead-free $BaTiO_3$ nanowires-based flexible nanocomposite generator, Nanoscale 6 (15) (2014) 8962–8968.
[62] E.L. Tsege, G.H. Kim, V. Annapureddy, B. Kim, H.K. Kim, Y.H. Hwang, A flexible lead-free piezoelectric nanogenerator based on vertically aligned $BaTiO_3$ nanotube arrays on a Ti-mesh substrate, RSC Adv. 6 (84) (2016) 81426–81435.
[63] A. Khan, Z. Abas, H.S. Kim, I.K. Oh, Piezoelectric thin films: an integrated review of transducers and energy harvesting, Smart Mater. Struct. 25 (2016) 053002.
[64] B. Ponraj, R. Bhimireddi, K.B.R. Varma, Effect of nano- and micron-sized $K_{0.5}Na_{0.5}NbO_3$ fillers on the dielectric and piezoelectric properties of PVDF composites, J. Adv. Ceram. 5 (4) (2016) 308–320.
[65] J. Kim, J.H. Koh, Na,K)NbO_3–(Bi,Na)TiO_3 piezoelectric ceramics for energy-harvesting applications, J. Eur. Ceram. Soc. 35 (14) (2015) 3819–3825.
[66] Z. Wang, Y. Hu, W. Wang, D. Zhou, Y. Wang, H. Gu, Electromechanical conversion behavior of $K_{0.5}Na_{0.5}NbO_3$ nanorods synthesized by hydrothermal method, Integr. Ferroelectr. 142 (1) (2013) 24–30.
[67] Y. Huan, X. Zhang, J. Song, Y. Zhao, T. Wei, G. Zhang, X. Wang, High-performance piezoelectric composite nanogenerator based on Ag/(K,Na)NbO_3 heterostructure, Nano Energy 50 (2018) 62–69.
[68] S. Bairagi, S.W. Ali, Poly (vinylidine fluoride) (PVDF)/Potassium Sodium Niobate (KNN) nanorods based flexible nanocomposite film: influence of KNN concentration in the performance of nanogenerator, Org. Electron. 78 (2020) 105547.
[69] C.K. Jeong, K.I. Park, J. Ryu, G.T. Hwang, K.J. Lee, Large-area and flexible lead-free nanocomposite generator using alkaline niobate particles and metal nanorod filler, Adv. Funct. Mater. 24 (18) (2014) 2620–2629.
[70] Y. He, Z. Wang, X. Hu, Y. Cai, L. Li, Y. Gao, X. Zhang, Z. Huang, Y. Hu, H. Gu, Orientation-dependent piezoresponse and high-performance energy harvesting of lead-free (K,Na)NbO_3 nanorod arrays, RSC Adv. 7 (28) (2017) 16908–16915.
[71] C. Zhang, Y. Fan, H. Li, Y. Li, L. Zhang, S. Cao, S. Kuang, Y. Zhao, A. Chen, G. Zhu, Z.L. Wang, Fully rollable lead-free poly(vinylidene fluoride)-niobate-based nanogenerator with ultra-flexible nano-network electrodes, ACS Nano 12 (5) (2018) 4803–4811.
[72] M. Wu, T. Zheng, H. Zheng, J. Li, W. Wang, M. Zhu, F. Li, G. Yue, Y. Gu, J. Wu, High-performance piezoelectric-energy-harvester and self-powered mechanosensing using lead-free potassium–sodium niobate flexible piezoelectric composites, J. Mater. Chem. A 6 (34) (2018) 16439–16449.
[73] B. Jaffe, R.S. Roth, S. Marzullo, Piezoelectric properties of lead zirconate-lead titanate solid-solution ceramics, J. Appl. Phys. 25 (6) (2004) 809–810.
[74] W. Wu, S. Bai, M. Yuan, Y. Qin, Z.L. Wang, T. Jing, Lead zirconate titanate nanowire textile nanogenerator for wearable energy-harvesting and self-powered devices, ACS Nano 6 (7) (2012) 6231–6235.
[75] Q.L. Zhao, G.P. He, J.J. Di, W.L. Song, Z.L. Hou, P.P. Tan, D.W. Wang, M.S. Cao, Flexible semitransparent energy harvester with high pressure sensitivity and power density based on laterally aligned PZT single-crystal nanowires, ACS Appl. Mater. Interfaces 9 (29) (2017) 24696–24703.
[76] W. Jin, Z. Wang, H. Huang, X. Hu, Y. He, M. Li, L. Li, Y. Gao, Y. Hu, H. Gu, High-performance piezoelectric energy harvesting of vertically aligned Pb(Zr,Ti)O_3 nanorod arrays, RSC Adv. 8 (14) (2018) 7422–7427.
[77] Z. Zhao, Y. Dai, S.X. Dou, J. Liang, Flexible nanogenerators for wearable electronic applications based on piezoelectric materials, Mater. Today Energy 20 (2021) 100690.

[78] E.J. Lee, T.Y. Kim, S.W. Kim, S. Jeong, Y. Choi, S.Y. Lee, High-performance piezoelectric nanogenerators based on chemically-reinforced composites, Energy Environ. Sci. 11 (6) (2018) 1425–1430.
[79] Y. Qi, N.T. Jafferis, K. Lyons Jr., C.M. Lee, H. Ahmad, M.C. McAlpine, Piezoelectric ribbons printed onto rubber for flexible energy conversion, Nano Lett. 10 (2) (2010) 524–528.
[80] X. Chen, S. Xu, N. Yao, Y. Shi, 1.6 V nanogenerator for mechanical energy harvesting using PZT nanofibers, Nano Lett. 10 (6) (2010) 2133–2137.
[81] L. Gu, N. Cui, L. Cheng, Q. Xu, S. Bai, M. Yuan, W. Wu, J. Liu, Y. Zhao, F. Ma, Y. Qin, Z.L. Wang, Flexible fiber nanogenerator with 209 V output voltage directly powers a light-emitting diode, Nano Lett. 13 (1) (2013) 91–94.
[82] M. Detalle, G. Wang, D. Rémiens, P. Ruterana, P. Roussel, B. Dkhil, Comparison of structural and electrical properties of PMN-PT films deposited on Si with different bottom electrodes, J. Cryst. Growth 305 (1) (2007) 137–143.
[83] Z. Yang, J. Zu, Comparison of PZN-PT, PMN-PT single crystals and PZT ceramic for vibration energy harvesting, Energy Convers. Manag. 122 (2016) 321–329.
[84] S.E. Park, T.R. Shrout, Ultrahigh strain and piezoelectric behavior in relaxor based ferroelectric single crystals, J. Appl. Phys. 82 (4) (1997) 1804–1811.
[85] K. Wasa, T. Matsushima, H. Adachi, I. Kanno, H. Kotera, Thin-film piezoelectric materials for a better energy harvesting MEMS, IEEE/ASME J. Microelectromech. Syst. 21 (2012) 451–457.
[86] Y. Chen, Y. Zhang, L. Zhang, F. Ding, O.G. Schmidt, Scalable single crystalline PMN-PT nanobelts sculpted from bulk for energy harvesting, Nano Energy 31 (2017) 239–246.
[87] C. Li, W. Luo, X. Liu, D. Xu, K. He, PMN-PT/PVDF Nanocomposite for high output nanogenerator applications, Nanomaterials 6 (4) (2016) 67.
[88] Z.L. Wang, Zinc oxide nanostructures: growth, properties and applications, J. Phys. Condens. Matter 16 (25) (2004) R829.
[89] G.M. Hasan Ul Banna, I.K. Park, Flexible ZnO nanorod-based piezoelectric nanogenerators on carbon papers, Nanotechnology 28 (44) (2017) 445402.
[90] W. Rahman, S. Garain, A. Sultana, T. Ranjan Middya, D. Mandal, Self-powered piezoelectric nanogenerator based on wurtzite ZnO nanoparticles for energy harvesting application, Mater. Today Proc. 5 (3, Part 3) (2018) 9826–9830.
[91] C.L. Hsu, I.L. Su, T.J. Hsueh, Sulfur-doped-ZnO-nanospire-based transparent flexible nanogenerator self-powered by environmental vibration, RSC Adv. 5 (43) (2015) 34019–34026.
[92] N. Sinha, S. Goel, A.J. Joseph, H. Yadav, K. Batra, M.K. Gupta, B. Kumar, Y–doped ZnO nanosheets: gigantic piezoelectric response for an ultra-sensitive flexible piezoelectric nanogenerator, Ceram. Int. 44 (7) (2018) 8582–8590.
[93] E.S. Nour, A. Echresh, X. Liu, E. Broitman, M. Willander, O. Nur, Piezoelectric and opto-electrical properties of silver-doped ZnO nanorods synthesized by low temperature aqueous chemical method, AIP Adv. 5 (7) (2015) 077163.
[94] S. Lee, J. Lee, W. Ko, S. Cha, J. Sohn, J. Kim, J. Park, Y. Park, J. Hong, Solution-processed Ag-doped ZnO nanowires grown on flexible polyester for nanogenerator applications, Nanoscale 5 (20) (2013) 9609–9614.
[95] D. Zhu, T. Hu, Y. Zhao, W. Zang, L. Xing, X. Xue, High-performance self--powered/active humidity sensing of Fe-doped ZnO nanoarray nanogenerator, Sens. Actuators B 213 (2015) 382–389.
[96] S.H. Shin, Y.H. Kwon, M.H. Lee, J.Y. Jung, J.H. Seol, J. Nah, A vanadium-doped ZnO nanosheets–polymer composite for flexible piezoelectric nanogenerators, Nanoscale 8 (3) (2016) 1314–1321.
[97] T. Zhao, Y. Fu, Y. Zhao, L. Xing, X. Xue, Ga-doped ZnO nanowire nanogenerator as self-powered/active humidity sensor with high sensitivity and fast response, J. Alloys Compd. 648 (2015) 571–576.
[98] C. Liu, A. Yu, M. Peng, M. Song, W. Liu, Y. Zhang, J. Zhai, Improvement in the piezoelectric performance of a ZnO nanogenerator by a combination of chemical doping and interfacial modification, J. Phys. Chem. C 120 (13) (2016) 6971–6977.
[99] S.H. Shin, Y.H. Kim, M.H. Lee, J.Y. Jung, J.H. Seol, J. Nah, Lithium-doped zinc oxide nanowires–polymer composite for high performance flexible piezoelectric nanogenerator, ACS Nano 8 (10) (2014) 10844–10850.
[100] K. Batra, N. Sinha, S. Goel, H. Yadav, A.J. Joseph, B. Kumar, Enhanced dielectric, ferroelectric and piezoelectric performance of Nd-ZnO nanorods and their application in flexible piezoelectric nanogenerator, J. Alloys Compd. 767 (2018) 1003–1011.
[101] W. Deng, Y. Zhou, A. Libanori, G. Chen, W. Yang, J. Chen, Piezoelectric nanogenerators for personalized healthcare, Chem. Soc. Rev. 51 (9) (2022) 3380–3435.
[102] K. Tonisch, V. Cimalla, C. Foerster, D. Dontsov, O. Ambacher, Piezoelectric properties of thin AlN layers for MEMS application determined by piezoresponse force microscopy, Phys. Status Solidi C 3 (6) (2006) 2274–2277.
[103] L. Algieri, M.T. Todaro, F. Guido, V. Mastronardi, D. Desmaële, A. Qualtieri, C. Giannini, T. Sibillano, M. De Vittorio, Flexible piezoelectric energy-harvesting exploiting biocompatible AlN thin films grown onto spin-coated polyimide layers, ACS Appl. Energy Mater. 1 (10) (2018) 5203–5210.
[104] G. Kalimuldina, N. Turdakyn, I. Abay, A. Medeubayev, A. Nurpeissova, D. Adair, Z. Bakenov, A review of piezoelectric PVDF film by electrospinning and its applications, Sensors 20 (2020) 5214.
[105] W. Zhai, L. Zhu, Q. Lai, L. Chen, Z. Wang, Flexible piezoelectric nanogenerators based on P(VDF–TrFE)/GeSe nanocomposite films, ACS Appl. Electron. Mater. 2 (8) (2020) 2369–2374.
[106] P. Thakur, A. Kool, N.A. Hoque, B. Bagchi, F. Khatun, P. Biswas, D. Brahma, S. Roy, S. Banerjee, S. Das, Superior performances of *in situ* synthesized ZnO/PVDF thin film based self-poled piezoelectric nanogenerator and self--charged photo-power bank with high durability, Nano Energy 44 (2018) 456–467.
[107] B. Dutta, E. Kar, N. Bose, S. Mukherjee, NiO@SiO_2/PVDF: a flexible polymer nanocomposite for a high performance human body motion-based energy harvester and tactile e-skin mechanosensor, ACS Sustain. Chem. Eng. 6 (8) (2018) 10505–10516.
[108] A. Gaur, S. Tiwari, C. Kumar, P. Maiti, Flexible, lead-free nanogenerators using poly(vinylidene fluoride) nanocomposites, Energy Fuels 34 (5) (2020) 6239–6244.
[109] H. Gade, S. Nikam, G.G. Chase, D.H. Reneker, Effect of electrospinning conditions on β-phase and surface charge potential of PVDF fibers, Polymer 228 (2021) 123902.
[110] T. Sharma, S. Naik, J. Langevine, B. Gill, J.X. Zhang, Aligned PVDF-TrFE nanofibers with high-density PVDF nanofibers and PVDF core–shell structures for endovascular pressure sensing, IEEE Trans. Biomed. Eng. 62 (1) (2015) 188–195.
[111] M. Baniasadi, J. Huang, Z. Xu, S. Moreno, X. Yang, J. Chang, M.A. Quevedo-Lopez, M. Naraghi, M. Minary-Jolandan, High-performance coils and yarns of polymeric piezoelectric nanofibers, ACS Appl. Mater. Interfaces 7 (9) (2015) 5358–5366.
[112] Y.K. Fuh, H.C. Ho, B.S. Wang, S.C. Li, All-fiber transparent piezoelectric harvester with a cooperatively enhanced structure, Nanotechnology 27 (43) (2016) 435403.
[113] Z.H. Liu, C.T. Pan, C.Y. Su, L.W. Lin, Y.J. Chen, J.S. Tsai, A flexible sensing device based on a PVDF/MWCNT composite nanofiber array with an interdigital electrode, Sens. Actuators A 211 (2014) 78–88.
[114] Z. Pi, J. Zhang, C. Wen, Z.B. Zhang, D. Wu, Flexible piezoelectric nanogenerator made of poly(vinylidenefluoride-co-trifluoroethylene) (PVDF-TrFE) thin film, Nano Energy 7 (2014) 33–41.
[115] C. Li, P.M. Wu, L.A. Shutter, R.K. Narayan, Dual-mode operation of flexible piezoelectric polymer diaphragm for intracranial pressure measurement, Appl. Phys. Lett. 96 (5) (2010) 053502.
[116] J. Gui, Y. Zhu, L. Zhang, X. Shu, W. Liu, S. Guo, X. Zhao, Enhanced output-performance of piezoelectric poly(vinylidene fluoride trifluoroethylene) fibers-based nanogenerator with interdigital electrodes and well-ordered cylindrical cavities, Appl. Phys. Lett. 112 (7) (2018) 072902.
[117] R.M. Habibur, U. Yaqoob, S. Muhammad, A.S.M.I. Uddin, H.C. Kim, The effect of RGO on dielectric and energy harvesting properties of P(VDF-TrFE) matrix by optimizing electroactive β phase without traditional polling process, Mater. Chem. Phys. 215 (2018) 46–55.
[118] S. Ju, H. Zhang, M. Chen, C. Zhang, X. Chen, Z. Zhang, Improved electrical insulating properties of LDPE based nanocomposite: effect of surface modification of magnesia nanoparticles, Compos. Part A 66 (2014) 183–192.
[119] Y. Zhou, J. He, J. Hu, B. Dang, Surface-modified MgO nanoparticle enhances the mechanical and direct-current electrical characteristics of polypropylene/polyolefin elastomer nanodielectrics, J. Appl. Polym. Sci. 133 (1) (2016) 42863.
[120] D. Singh, A. Choudhary, A. Garg, Flexible and robust piezoelectric polymer nanocomposites based energy harvesters, ACS Appl. Mater. Interfaces 10 (3) (2018) 2793–2800.
[121] J. Zhu, L. Jia, R. Huang, Electrospinning poly(l-lactic acid) piezoelectric ordered porous nanofibers for strain sensing and energy harvesting, J. Mater. Sci. Mater. Electron. 28 (16) (2017) 12080–12085.
[122] M. Smith, Y. Calahorra, Q. Jing, S. Kar-Narayan, Direct observation of shear piezoelectricity in poly-l-lactic acid nanowires, APL Mater. 5 (7) (2017) 074105.
[123] T. Cai, Y. Yang, E. Bi, RETRACTED: preparation of high-performance polyacrylonitrile piezoelectric thin film by temperature control, React. Funct. Polym. 154 (2020) 104638.
[124] N. Wu, X. Cheng, Q. Zhong, J. Zhong, W. Li, B. Wang, B. Hu, J. Zhou, Cellular polypropylene piezoelectret for human body energy harvesting and health monitoring, Adv. Funct. Mater. 25 (30) (2015) 4788–4794.
[125] H. Yuan, P. Han, K. Tao, S. Liu, E. Gazit, R. Yang, Piezoelectric peptide and metabolite materials, Research 2019 (2019) 9025939 (Wash D C).
[126] M.M. Alam, D. Mandal, Native cellulose microfiber-based hybrid piezoelectric generator for mechanical energy harvesting utility, ACS Appl. Mater. Interfaces 8 (3) (2016) 1555–1558.
[127] Q. Zheng, H. Zhang, H. Mi, Z. Cai, Z. Ma, S. Gong, High-performance flexible piezoelectric nanogenerators consisting of porous cellulose nanofibril (CNF)/poly(dimethylsiloxane) (PDMS) aerogel films, Nano Energy 26 (2016) 504–512.
[128] S. Maiti, S. Kumar Karan, J. Lee, A. Kumar Mishra, B. Bhusan Khatua, J. Kon Kim, Bio-waste onion skin as an innovative nature-driven piezoelectric material with high energy conversion efficiency, Nano Energy 42 (2017) 282–293.
[129] C. Kumar, A. Gaur, S. Tiwari, A. Biswas, S.K. Rai, P. Maiti, Bio-waste polymer hybrid as induced piezoelectric material with high energy harvesting efficiency, Compos. Commun. 11 (2019) 56–61.
[130] S.K. Karan, S. Maiti, S. Paria, A. Maitra, S.K. Si, J.K. Kim, B.B. Khatua, A new insight towards eggshell membrane as high energy conversion efficient bio-piezoelectric energy harvester, Mater. Today Energy 9 (2018) 114–125.
[131] S.K. Ghosh, D. Mandal, Efficient natural piezoelectric nanogenerator: electricity generation from fish swim bladder, Nano Energy 28 (2016) 356–365.
[132] B. Hassan, S.A.S. Chatha, A.I. Hussain, K.M. Zia, N. Akhtar, Recent advances on polysaccharides, lipids and protein based edible films and coatings: a review, Int. J. Biol. Macromol. 109 (2018) 1095–1107.

[133] B.J. Savary, A. Nuñez, Gas chromatography-mass spectrometry method for determining the methanol and acetic acid contents of pectin using headspace solid-phase microextraction and stable isotope dilution, J. Chromatogr. A 1017 (1-2) (2003) 151–159.
[134] S. Bairagi, S. Ghosh, S.W. Ali, A fully sustainable, self-poled, bio-waste based piezoelectric nanogenerator: electricity generation from pomelo fruit membrane, Sci. Rep. 10 (1) (2020) 12121.
[135] I.W. Park, K.W. Kim, Y. Hong, H.J. Yoon, Y. Lee, D. Gwak, K. Heo, Recent developments and prospects of M13- bacteriophage based piezoelectric energy harvesting devices, Nanomaterials 10 (1) (2020) 93.
[136] K. Heo, H.E. Jin, H. Kim, J.H. Lee, E. Wang, S.W. Lee, Transient self-templating assembly of M13 bacteriophage for enhanced biopiezoelectric devices, Nano Energy 56 (2019) 716–723.
[137] J.A. Kluge, O. Rabotyagova, G.G. Leisk, D.L. Kaplan, Spider silks and their applications, Trends Biotechnol. 26 (5) (2008) 244–251.
[138] T. Yucel, P. Cebe, D.L. Kaplan, Structural origins of silk piezoelectricity, Adv. Funct. Mater. 21 (4) (2011) 779–785.
[139] S.K. Karan, S. Maiti, O. Kwon, S. Paria, A. Maitra, S.K. Si, Y. Kim, J.K. Kim, B.B. Khatua, Nature driven spider silk as high energy conversion efficient bio-piezoelectric nanogenerator, Nano Energy 49 (2018) 655–666.
[140] S. Ifuku, H. Saimoto, Chitin nanofibers: preparations, modifications, and applications, Nanoscale 4 (11) (2012) 3308–3318.
[141] N.A. Hoque, P. Thakur, P. Biswas, M.M. Saikh, S. Roy, B. Bagchi, S. Das, P.P. Ray, Biowaste crab shell-extracted chitin nanofiber-based superior piezoelectric nanogenerator, J. Mater. Chem. A 6 (28) (2018) 13848–13858.
[142] A. Gaur, S. Tiwari, C. Kumar, P. Maiti, Polymer biowaste hybrid for enhanced piezoelectric energy harvesting, ACS Appl. Electron. Mater. 2 (5) (2020) 1426–1432.
[143] C. Peng, A.H.L. Chow, C.K. Chan, Hygroscopic study of glucose, citric acid, and sorbitol using an electrodynamic balance: comparison with UNIFAC predictions, Aerosol Sci. Technol. 35 (3) (2001) 753–758.
[144] K. Maity, S. Garain, K. Henkel, D. Schmeißer, D. Mandal, Natural sugar-assisted, chemically reinforced, highly durable piezoorganic nanogenerator with superior power density for self-powered wearable electronics, ACS Appl. Mater. Interfaces 10 (50) (2018) 44018–44032.
[145] A. Tamang, S.K. Ghosh, S. Garain, M.M. Alam, J. Haeberle, K. Henkel, D. Schmeisser, D. Mandal, DNA-assisted β-phase nucleation and alignment of molecular dipoles in PVDF film: a realization of self-poled bioinspired flexible polymer nanogenerator for portable electronic devices, ACS Appl. Mater. Interfaces 7 (30) (2015) 16143–16147.
[146] J. Yang, J. Chen, Y. Su, Q. Jing, Z. Li, F. Yi, X. Wen, Z. Wang, Z.L. Wang, Eardrum-inspired active sensors for self-powered cardiovascular system characterization and throat-attached anti-interference voice recognition, Adv. Mater. 27 (8) (2015) 1316–1326.
[147] C.M. Boutry, A. Nguyen, Q.O. Lawal, A. Chortos, S. Rondeau-Gagné, Z. Bao, A sensitive and biodegradable pressure sensor array for cardiovascular monitoring, Adv. Mater. 27 (43) (2015) 6954–6961.
[148] D.Y. Park, D.J. Joe, D.H. Kim, H. Park, J.H. Han, C.K. Jeong, H. Park, J.G. Park, B. Joung, K.J. Lee, Self-powered real-time arterial pulse monitoring using ultrathin epidermal piezoelectric sensors, Adv. Mater. 29 (37) (2017) 1702308.
[149] K. Meng, J. Chen, X. Li, Y. Wu, W. Fan, Z. Zhou, Q. He, X. Wang, X. Fan, Y. Zhang, J. Yang, Z.L. Wang, Flexible weaving constructed self-powered pressure sensor enabling continuous diagnosis of cardiovascular disease and measurement of cuffless blood pressure, Adv. Funct. Mater. 29 (5) (2019) 1806388.
[150] P.A. Heidenreich, J.G. Trogdon, O.A. Khavjou, J. Butler, K. Dracup, M.D. Ezekowitz, E.A. Finkelstein, Y. Hong, S.C. Johnston, A. Khera, D.M. Lloyd-Jones, S.A. Nelson, G. Nichol, D. Orenstein, P.W.F. Wilson, Y.J. Woo, Forecasting the future of cardiovascular disease in the United States, Circulation 123 (8) (2011) 933–944.
[151] L.Y. Chen, B.C.K. Tee, A.L. Chortos, G. Schwartz, V. Tse, D.J. Lipomi, H.S.P. Wong, M.V. McConnell, Z. Bao, Continuous wireless pressure monitoring and mapping with ultra-small passive sensors for health monitoring and critical care, Nat. Commun. 5 (1) (2014) 5028.
[152] X. Cheng, X. Xue, Y. Ma, M. Han, W. Zhang, Z. Xu, H. Zhang, H. Zhang, Implantable and self-powered blood pressure monitoring based on a piezoelectric thinfilm: simulated, *in vitro* and *in vivo* studies, Nano Energy 22 (2016) 453–460.
[153] P. Tan, Y. Xi, S. Chao, D. Jiang, Z. Liu, Y. Fan, Z. Li, An artificial intelligence-enhanced blood pressure monitor wristband based on piezoelectric nanogenerator, Biosensors (2022).
[154] W. Pan, W. Xia, F.S. Jiang, X.X. Wang, Z.G. Zhang, X.G. Li, P. Li, Y.C. Jiang, Y.Z. Long, G.F. Yu, Stretchable strain sensor for human motion monitoring based on an intertwined-coil configuration, Nanomaterials 10 (10) (2020) 1980.
[155] Z. Yang, Y. Pang, X.L. Han, Y. Yang, J. Ling, M. Jian, Y. Zhang, Y. Yang, T.L. Ren, Graphene textile strain sensor with negative resistance variation for human motion detection, ACS Nano 12 (9) (2018) 9134–9141.
[156] S. Agarwala, G.L. Goh, T.S.Dinh Le, J. An, Z.K. Peh, W.Y. Yeong, Y.J. Kim, Wearable bandage-based strain sensor for home healthcare: combining 3D aerosol jet printing and laser sintering, ACS Sens. 4 (1) (2019) 218–226.
[157] H. Liu, Q. Li, S. Zhang, R. Yin, X. Liu, Y. He, K. Dai, C. Shan, J. Guo, C. Liu, C. Shen, X. Wang, N. Wang, Z. Wang, R. Wei, Z. Guo, Electrically conductive polymer composites for smart flexible strain sensors: a critical review, J. Mater. Chem. C 6 (45) (2018) 12121–12141.
[158] X. Xiao, L. Yuan, J. Zhong, T. Ding, Y. Liu, Z. Cai, Y. Rong, H. Han, J. Zhou, Z.L. Wang, High-strain sensors based on ZnO nanowire/polystyrene hybridized flexible films, Adv. Mater. 23 (45) (2011) 5440–5444.
[159] D.I. Kim, T. Quang Trung, B.U. Hwang, J.S. Kim, S. Jeon, J. Bae, J.J. Park, N.E. Lee, A sensor array using multi-functional field-effect transistors with ultrahigh sensitivity and precision for bio-monitoring, Sci. Rep. 5 (1) (2015) 12705.
[160] N.T. Tien, T.Q. Trung, Y.G. Seoul, D.I. Kim, N.E. Lee, Physically responsive field-effect transistors with giant electromechanical coupling induced by nanocomposite gate dielectrics, ACS Nano 5 (9) (2011) 7069–7076.
[161] S. Rafique, A.K. Kasi, Aminullah, J.K. Kasi, M. Bokhari, S. Zafar, Fabrication of Br doped ZnO nanosheets piezoelectric nanogenerator for pressure and position sensing applications, Curr. Appl. Phys. 21 (2021) 72–79.
[162] N.I. Kim, Y.L. Chang, J. Chen, T. Barbee, W. Wang, J.Y. Kim, M.K. Kwon, S. Shervin, M. Moradnia, S. Pouladi, D. Khatiwada, V. Selvamanickam, J.H. Ryou, Piezoelectric pressure sensor based on flexible gallium nitride thin film for harsh-environment and high-temperature applications, Sens. Actuators A 305 (2020) 111940.
[163] N. Oishi, J. Schacht, Emerging treatments for noise-induced hearing loss, Expert Opin. Emerg. Drugs 16 (2) (2011) 235–245.
[164] A.S. Nordmann, B.A. Bohne, G.W. Harding, Histopathological differences between temporary and permanent threshold shift, Hear. Res. 139 (1-2) (2000) 13–30.
[165] T. Endo, T. Nakagawa, T. Kita, F. Iguchi, T.S. Kim, T. Tamura, K. Iwai, Y. Tabata, J. Ito, Novel strategy for treatment of inner ears using a biodegradable gel, Laryngoscope 115 (11) (2005) 2016–2020.
[166] K. Mizutari, M. Fujioka, M. Hosoya, N. Bramhall, H.J. Okano, H. Okano, A.S. Edge, Notch inhibition induces cochlear hair cell regeneration and recovery of hearing after acoustic trauma, Neuron 77 (1) (2013) 58–69.
[167] M. Izumikawa, R. Minoda, K. Kawamoto, K.A. Abrashkin, D.L. Swiderski, D.F. Dolan, D.E. Brough, Y. Raphael, Auditory hair cell replacement and hearing improvement by Atoh1 gene therapy in deaf mammals, Nat. Med. 11 (3) (2005) 271–276.
[168] Z. He, Y. Ding, Y. Mu, X. Xu, W. Kong, R. Chai, X. Chen, Stem cell-based therapies in hearing loss, Front. Cell Dev. Biol. 9 (2021) 730042.
[169] S.B. Waltzman, Cochlear implants: current status, Expert Rev. Med. Devices 3 (5) (2006) 647–655.
[170] M.K. Cosetti, S.B. Waltzman, Cochlear implants: current status and future potential, Expert Rev. Med. Devices 8 (3) (2011) 389–401.
[171] J.H. Han, J.H. Kwak, D.J. Joe, S.K. Hong, H.S. Wang, J.H. Park, S. Hur, K.J. Lee, Basilar membrane-inspired self-powered acoustic sensor enabled by highly sensitive multi tunable frequency band, Nano Energy 53 (2018) 198–205.
[172] T. Inaoka, H. Shintaku, T. Nakagawa, S. Kawano, H. Ogita, T. Sakamoto, S. Hamanishi, H. Wada, J. Ito, Piezoelectric materials mimic the function of the cochlear sensory epithelium, Proc. Natl. Acad. Sci. USA 108 (45) (2011) 18390–18395.
[173] H.S. Lee, J. Chung, G.T. Hwang, C.K. Jeong, Y. Jung, J.H. Kwak, H. Kang, M. Byun, W.D. Kim, S. Hur, S.H. Oh, K.J. Lee, Flexible inorganic piezoelectric acoustic nanosensors for biomimetic artificial hair cells, Adv. Funct. Mater. 24 (44) (2014) 6914–6921.
[174] D. Esposito, J. Centracchio, E. Andreozzi, G.D. Gargiulo, G.R. Naik, P. Bifulco, Biosignal-based human-machine interfaces for assistance and rehabilitation: a survey, Sensors 21 (20) (2021) 6863.
[175] H. Singh, P. Kumar, Developments in the human machine interface technologies and their applications: a review, J. Med. Eng. Technol. 45 (2021) 1–22.
[176] W. Deng, T. Yang, L. Jin, C. Yan, H. Huang, X. Chu, Z. Wang, D. Xiong, G. Tian, Y. Gao, H. Zhang, W. Yang, Cowpea-structured PVDF/ZnO nanofibers based flexible self-powered piezoelectric bending motion sensor towards remote control of gestures, Nano Energy 55 (2019) 516–525.
[177] Y.X. Zhou, Y.T. Lin, S.M. Huang, G.T. Chen, S.W. Chen, H.S. Wu, I.C. Ni, W.P. Pan, M.L. Tsai, C.I. Wu, P.K. Yang, Tungsten disulfide nanosheets for piezoelectric nanogenerator and human-machine interface applications, Nano Energy 97 (2022) 107172.
[178] A.D. Krahn, R.A. Pickett, S. Sakaguchi, N. Shaik, J. Cao, H.S. Norman, P. Guerrero, R-wave sensing in an implantable cardiac monitor without ECG-based preimplant mapping: results from a multicenter clinical trial, Pacing Clin. Electrophysiol. 37 (4) (2014) 505–511.
[179] H. Park, Y. Kim, Y. Kim, C. Lee, H. Park, H. Joo, J. Hun Lee, J.H. Lee, Self-assembly of unidirectionally polarized piezoelectric peptide nanotubes using environmentally friendly solvents, Appl. Surf. Sci. 618 (2023) 156588.
[180] M. Madhavan, S.K. Mulpuru, C.J. McLeod, Y.M. Cha, P.A. Friedman, Advances and future directions in cardiac pacemakers: part 2 of a 2-part series, J. Am. Coll. Cardiol. 69 (2) (2017) 211–235.
[181] Y. Kim, H. Park, Y. Kim, C. Lee, H. Park, J.H. Lee, Control of the biodegradability of piezoelectric peptide nanotubes integrated with hydrophobic porphyrin, ACS Appl. Mater. Interfaces 14 (34) (2022) 38778–38785.
[182] Q. Zheng, H. Zhang, B. Shi, X. Xue, Z. Liu, Y. Jin, Y. Ma, Y. Zou, X. Wang, Z. An, W. Tang, W. Zhang, F. Yang, Y. Liu, X. Lang, Z. Xu, Z. Li, Z.L. Wang, *In vivo* self-powered wireless cardiac monitoring via implantable triboelectric nanogenerator, ACS Nano 10 (7) (2016) 6510–6518.
[183] G.T. Hwang, M. Byun, C.K. Jeong, K.J. Lee, Flexible piezoelectric thin-film energy harvesters and nanosensors for biomedical applications, Adv. Healthc. Mater. 4 (5) (2015) 646–658.
[184] H. Guo, D.M. Lee, P. Zhao, S.H. Kim, I. Hyun, B.J. Park, J.H. Lee, H. Sun, S.W. Kim, Cell activity manipulation through optimizing piezoelectricity and polarization of diphenylalanine peptide nanotube-based nanocomposite, Chem. Eng. J. 468 (2023) 143597.

[185] S. Azimi, A. Golabchi, A. Nekookar, S. Rabbani, M.H. Amiri, K. Asadi, M.M. Abolhasani, Self-powered cardiac pacemaker by piezoelectric polymer nanogenerator implant, Nano Energy 83 (2021) 105781.
[186] Z. Xu, C. Jin, A. Cabe, D. Escobedo, N. Hao, I. Trase, A.B. Closson, L. Dong, Y. Nie, J. Elliott, M.D. Feldman, Z. Chen, J.X.J. Zhang, Flexible energy harvester on a pacemaker lead using multibeam piezoelectric composite thin films, ACS Appl. Mater. Interfaces 12 (30) (2020) 34170–34179.
[187] H.S. Mayberg, A.M. Lozano, V. Voon, H.E. McNeely, D. Seminowicz, C. Hamani, J.M. Schwalb, S.H. Kennedy, Deep brain stimulation for treatment-resistant depression, Neuron 45 (5) (2005) 651–660.
[188] G. Deuschl, C. Schade-Brittinger, P. Krack, J. Volkmann, H. Schäfer, K. Bötzel, C. Daniels, A. Deutschländer, U. Dillmann, W. Eisner, D. Gruber, W. Hamel, J. Herzog, R. Hilker, S. Klebe, M. Kloss, J. Koy, M. Krause, A. Kupsch, D. Lorenz, S. Lorenzl, H.M. Mehdorn, J.R. Moringlane, W. Oertel, M.O. Pinsker, H. Reichmann, A. Reuss, G.H. Schneider, A. Schnitzler, U. Steude, V. Sturm, L. Timmermann, V. Tronnier, T. Trottenberg, L. Wojtecki, E. Wolf, W. Poewe, J. Voges, A randomized trial of deep-brain stimulation for Parkinson's disease, N. Engl. J. Med. 355 (9) (2006) 896–908.
[189] C. Dagdeviren, Y. Shi, P. Joe, R. Ghaffari, G. Balooch, K. Usgaonkar, O. Gur, P.L. Tran, J.R. Crosby, M. Meyer, Y. Su, R. Chad Webb, A.S. Tedesco, M.J. Slepian, Y. Huang, J.A. Rogers, Conformal piezoelectric systems for clinical and experimental characterization of soft tissue biomechanics, Nat. Mater. 14 (7) (2015) 728–736.
[190] T. Jariwala, G. Ico, Y. Tai, H. Park, N.V. Myung, J. Nam, Mechano-responsive piezoelectric nanofiber as an on-demand drug delivery vehicle, ACS Appl. Bio Mater. 4 (4) (2021) 3706–3715.
[191] G. Thrivikraman, S.K. Boda, B. Basu, Unraveling the mechanistic effects of electric field stimulation towards directing stem cell fate and function: a tissue engineering perspective, Biomaterials 150 (2018) 60–86.
[192] A.K. Dubey, A. Mukhopadhyay, B. Basu, Interdisciplinary engineering sciences: concepts and applications to materials science (2020).
[193] B. Basu, Biomaterials Science and Tissue Engineering: Principles and Methods, Cambridge University Press, 2017.
[194] P.J. Gouveia, S. Rosa, L. Ricotti, B. Abecasis, H.V. Almeida, L. Monteiro, J. Nunes, F.S. Carvalho, M. Serra, S. Luchkin, A.L. Kholkin, P.M. Alves, P.J. Oliveira, R. Carvalho, A. Menciassi, R.P. das Neves, L.S. Ferreira, Flexible nanofilms coated with aligned piezoelectric microfibers preserve the contractility of cardiomyocytes, Biomaterials 139 (2017) 213–228.
[195] A. Zaszczynska, P. Sajkiewicz, A. Gradys, Piezoelectric scaffolds as smart materials for neural tissue engineering, Polymers 12 (1) (2020) 161.
[196] M.R. Gomes, F. Castelo Ferreira, P. Sanjuan-Alberte, Electrospun piezoelectric scaffolds for cardiac tissue engineering, Biomater. Adv. 137 (2022) 212808.
[197] D. Khare, B. Basu, A.K. Dubey, Electrical stimulation and piezoelectric biomaterials for bone tissue engineering applications, Biomaterials 258 (2020) 120280.
[198] N. Weber, Y.S. Lee, S. Shanmugasundaram, M. Jaffe, T.L. Arinzeh, Characterization and *in vitro* cytocompatibility of piezoelectric electrospun scaffolds, Acta Biomater. 6 (9) (2010) 3550–3556.
[199] Y. Tai, A. Banerjee, R. Goodrich, L. Jin, J. Nam, Development and utilization of multifunctional polymeric scaffolds for the regulation of physical cellular microenvironments, Polymers 13 (22) (2021) 3880.
[200] A.H. Rajabi, M. Jaffe, T.L. Arinzeh, Piezoelectric materials for tissue regeneration: a review, Acta Biomater. 24 (2015) 12–23.
[201] A.K. Dubey, S.D. Gupta, B. Basu, Optimization of electrical stimulation parameters for enhanced cell proliferation on biomaterial surfaces, J. Biomed. Mater. Res. B Appl. Biomater. 98 (1) (2011) 18–29.
[202] P. Singh, X. Yu, A. Kumar, A.K. Dubey, Recent advances in silicate-based crystalline bioceramics for orthopedic applications: a review, J. Mater. Sci. 57 (28) (2022) 13109–13151.
[203] P.K. Szewczyk, S. Metwally, J.E. Karbowniczek, M.M. Marzec, E. Stodolak-Zych, A. Gruszczyński, A. Bernasik, U. Stachewicz, Surface-potential-controlled cell proliferation and collagen mineralization on electrospun polyvinylidene fluoride (PVDF) Fiber scaffolds for bone regeneration, ACS Biomater. Sci. Eng. 5 (2) (2019) 582–593.
[204] Y. Zhang, L. Xu, Z. Liu, X. Cui, Z. Xiang, J. Bai, D. Jiang, J. Xue, C. Wang, Y. Lin, Z. Li, Y. Shan, Y. Yang, L. Bo, Z. Li, X. Zhou, Self-powered pulsed direct current stimulation system for enhancing osteogenesis in MC3T3-E1, Nano Energy 85 (2021) 106009.
[205] R. Das, E.J. Curry, T.T. Le, G. Awale, Y. Liu, S. Li, J. Contreras, C. Bednarz, J. Millender, X. Xin, D. Rowe, S. Emadi, K.W.H. Lo, T.D. Nguyen, Biodegradable nanofiber bone-tissue scaffold as remotely-controlled and self-powering electrical stimulator, Nano Energy 76 (2020) 105028.
[206] B.G. Bruneau, Signaling and transcriptional networks in heart development and regeneration, Cold Spring Harb. Perspect. Biol. 5 (3) (2013) a008292.
[207] S.L. Paige, K. Plonowska, A. Xu, S.M. Wu, Molecular regulation of cardiomyocyte differentiation, Circ. Res. 116 (2) (2015) 341–353.
[208] A. Clerk, T.E. Cullingford, S.J. Fuller, A. Giraldo, T. Markou, S. Pikkarainen, P.H. Sugden, Signaling pathways mediating cardiac myocyte gene expression in physiological and stress responses, J. Cell. Physiol. 212 (2) (2007) 311–322.
[209] V. Talman, H. Ruskoaho, Cardiac fibrosis in myocardial infarction-from repair and remodeling to regeneration, Cell Tissue Res. 365 (3) (2016) 563–581.
[210] K. Kapat, Q.T.H. Shubhra, M. Zhou, S. Leeuwenburgh, Piezoelectric nano-biomaterials for biomedicine and tissue regeneration, Adv. Funct. Mater. 30 (44) (2020) 1909045.
[211] M. Solazzo, F.J. O'Brien, V. Nicolosi, M.G. Monaghan, The rationale and emergence of electroconductive biomaterial scaffolds in cardiac tissue engineering, APL Bioeng. 3 (4) (2019) 041501.
[212] M.J. Lab, Mechanoelectric feedback (transduction) in heart: concepts and implications, Cardiovasc. Res. 32 (1) (1996) 3–14.
[213] E.R. Pfeiffer, J.R. Tangney, J.H. Omens, A.D. McCulloch, Biomechanics of cardiac electromechanical coupling and mechanoelectric feedback, J. Biomech. Eng. 136 (2) (2014) 021007.
[214] L.P. da Silva, S.C. Kundu, R.L. Reis, V.M. Correlo, Electric phenomenon: a disregarded tool in tissue engineering and regenerative medicine, Trends Biotechnol. (2019).
[215] L. Wang, Y. Wu, T. Hu, B. Guo, P.X. Ma, Electrospun conductive nanofibrous scaffolds for engineering cardiac tissue and 3D bioactuators, Acta Biomater. 59 (2017) 68–81.
[216] R. Arumugam, E.S. Srinadhu, B. Subramanian, S. Nallani, β-PVDF based electrospun nanofibers – a promising material for developing cardiac patches, Med. Hypotheses 122 (2019) 31–34.
[217] N. Adadi, M. Yadid, I. Gal, M. Asulin, R. Feiner, R. Edri, T. Dvir, Electrospun fibrous PVDF-TrFe scaffolds for cardiac tissue engineering, differentiation, and maturation, Adv. Mater. Technol. 5 (3) (2020) 1900820.
[218] N.U. Kang, S.J. Lee, S.J. Gwak, Fabrication techniques of nerve guidance conduits for nerve regeneration, Yonsei Med. J. 63 (2) (2022) 114–123.
[219] A. Muheremu, Q. Ao, Past, present, and future of nerve conduits in the treatment of peripheral nerve injury, Biomed. Res. Int. 2015 (2015) 237507.
[220] S. Vijayavenkataraman, Nerve guide conduits for peripheral nerve injury repair: a review on design, materials and fabrication methods, Acta Biomater. 106 (2020) 54–69.
[221] C.A. Taylor, D. Braza, J.B. Rice, T. Dillingham, The incidence of peripheral nerve injury in extremity trauma, Am. J. Phys. Med. Rehabil. 87 (5) (2008) 381–385.
[222] T. Gordon, Electrical stimulation to enhance axon regeneration after peripheral nerve injuries in animal models and humans, Neurotherapeutics 13 (2) (2016) 295–310.
[223] Y. Shapira, V. Sammons, J. Forden, G.F. Guo, A. Kipp, J. Girgulis, T. Mishra, J.D. de Villers Alant, R. Midha, Brief electrical stimulation promotes nerve regeneration following experimental in-continuity nerve injury, Neurosurgery 85 (1) (2019) 156–163.
[224] M.P. Willand, M.A. Nguyen, G.H. Borschel, T. Gordon, Electrical stimulation to promote peripheral nerve regeneration, Neurorehabil. Neural Repair 30 (5) (2016) 490–496.
[225] R. Mao, B. Yu, J. Cui, Z. Wang, X. Huang, H. Yu, K. Lin, S.G.F. Shen, Piezoelectric stimulation from electrospun composite nanofibers for rapid peripheral nerve regeneration, Nano Energy 98 (2022) 107322.
[226] G.R. Evans, K. Brandt, M.S. Widmer, L. Lu, R.K. Meszlenyi, P.K. Gupta, A.G. Mikos, J. Hodges, J. Williams, A. Gürlek, A. Nabawi, R. Lohman, C.W. Patrick Jr., *In vivo* evaluation of poly(L-lactic acid) porous conduits for peripheral nerve regeneration, Biomaterials 20 (12) (1999) 1109–1115.
[227] L. Duggen, M. Willatzen, Z.L. Wang, Mechanically bent graphene as an effective piezoelectric nanogenerator, J. Phys. Chem. C 122 (36) (2018) 20581–20588.
[228] J. Zhang, Y. He, C. Boyer, K. Kalantar-Zadeh, S. Peng, D. Chu, C.H. Wang, Recent developments of hybrid piezo–triboelectric nanogenerators for flexible sensors and energy harvesters, Nanoscale Adv. 3 (19) (2021) 5465–5486.
[229] Y.S. Choi, H. Jeong, R.T. Yin, R. Avila, A. Pfenniger, J. Yoo, J.Y. Lee, A. Tzavelis, Y.J. Lee, S.W. Chen, H.S. Knight, S. Kim, H.Y. Ahn, G. Wickerson, A. Vázquez–Guardado, E. Higbee-Dempsey, B.A. Russo, M.A. Napolitano, T.J. Holleran, L.A. Razzak, A.N. Miniovich, G. Lee, B. Geist, B. Kim, S. Han, J.A. Brennan, K. Aras, S.S. Kwak, J. Kim, E.A. Waters, X. Yang, A. Burrell, K. San Chun, C. Liu, C. Wu, A.Y. Rwei, A.N. Spann, A. Banks, D. Johnson, Z.J. Zhang, C.R. Haney, S.H. Jin, A.V. Sahakian, Y. Huang, G.D. Trachiotis, B.P. Knight, R.K. Arora, I.R. Efimov, J.A. Rogers, A transient, closed-loop network of wireless, body-integrated devices for autonomous electrotherapy, Science 376 (6596) (2022) 1006–1012.
[230] B. Basu, N.H. Gowtham, Y. Xiao, S.R. Kalidindi, K.W. Leong, Biomaterialomics: data science-driven pathways to develop fourth-generation biomaterials, Acta Biomater. 143 (2022) 1–25.